**UNIVERSITÀ DEGLI STUDI DI TRIESTE**
Sede Amministrativa del Dottorato di Ricerca
**UNIVERSITÀ DEGLI STUDI DI UDINE**
Sede Convenzionata
XXIV CICLO DEL DOTTORATO DI RICERCA IN
**NANOTECNOLOGIE**

# EVOLVING BIOSENSORS: INTELLIGENT DEVICES AT THE NANOSCALE

Settore disciplinare: AGR/12

DOTTORANDA
Monica Marini

COORDINATORE DEL COLLEGIO DEI DOCENTI
Chiar.mo Prof. Maurizio Fermeglia
Università degli Studi di Trieste

RELATORE
Chiar.mo Prof. Giuseppe Firrao
Università degli Studi di Udine

CORRELATORE
Dott. Marco Lazzarino
IOM-CNR-Laboratorio TASC, Area Science Park

-2010/2011-

Alla mia famiglia

# Abstract

In this work I present a novel approach to the use of biomolecules as constructive material for an autonomous DNAbased platform on which is possible to do sensing consequently actuating the object after the transduction of an environmental signal.
The new approach is based on a DNA origami obtained by folding a long polynucleotide with hundreds of shorter oligonucleotides and resulting in a well defined and ordered disks of a diameter of about 100nm. Each disk is composed of two main parts, an external ring and an internal disk, connected each other in only two diametrically opposite points. A linear single stranded DNA molecule, the probe, is inserted on the upper face of the internal moving disk, perpendicularly to the connections and to the axis of constrain; as far as the probe remains single stranded, the DNA-object appears planar, but when it gets in contact with its complementary ssDNA called "target", forming a double stranded DNA, it opens the origami's structure.
The realization of such autonomous organic structure is preliminary to its application in many contests. The actuation principle was first applied for the development of a revertable biosensing platform, where the addition of a third single stranded molecule, displaces the target from the probe restoring the initial state of the origami.
The same principle was also improved with real samples such as viral RNAs.
In this thesis, I report the setting up of the single components of the device: complex DNA based objects, the switching mechanism, the validation with real samples and the possible applications of the whole system.

# Contents

# Chapter 1

# Introduction

## 1.1 Detection of molecular interactions

### 1.1.1 Biosensors and nanosensors

A biosensor is an analytical device consisting of a biological sensitive element such as enzymes, cells, DNA, microorganism and antibodies in contact with a transducer, the reading element (Turner, 2000). The sensitive element is the active part of the system, interacting with the sample to be analyzed, and due to this interaction provides a signal. The transducer can be coupled to an appropriate read out device, so a electrochemical, thermal, optical or acoustic signal transducer that, with the sensitive element, permits to analyze either the quantities or properties of the analyte.
Due to the specificity of the interactions between the target molecule and the biological part of the biosensor, they were seen as a solution to a number of problems in many research fields. The main advantages are the specificity and sensitivity of the techniques, associated to the low costs and the speed of the response. A commercially available example, is the blood glucose biosensor, which uses the enzyme glucose oxidase, that oxidizes glucose and uses two electrons to reduce a component of the enzyme. This in turn is oxidized by the electrode and the resulting current is a measure of the concentration of glucose (Clark and Lyons 1962). In this case, the electrode is the transducer and the enzyme is the biologically active element.
The biosensor technology has a great potential as analytical method in a variety of applications, ranging from medical diagnostics to the monitoring of the environment pollution. The development of an efficient biosensor has

to be supported by a deep comprehension of the biological parts and a fine set up of the working conditions, in order to have the best environment that provides high quality response. To be competitive, a biosensor has to fulfil some requirements such as a very short or even absent preparation of the sample; the reaction of the active element has to be highly specific; it should be stable under normal storage conditions; it has to show good reliability; the response should be accurate, precise, reproducible; it should have low background noise; should be cheap, small, portable and capable of being used by operators without specific training. The miniaturization of the biosensors devices is highly desirable in order to decrease the production costs, the quantity of the reagents used and of the target molecules to be analyzed. DNA is well suited for biosensing applications, due the specificity and robustness of base-pairing interactions between complementary sequences.
In a typical DNA biosensor, a single stranded DNA (ssDNA) is immobilized in the recognition layer, the place where the base pairing proprieties permits the recognition of the complementary DNA target molecules and the consequent direct immobilization of the targets on the surface. The hybridization event can be detected in many ways, applying different principles such as fluorescence, electrochemiluminescence, electrochemical and enzymatic methods (e.g. Kricka, 2002), choosing the appropriated one on the basis of the sensitivity of the molecules to be detected.
With the introduction of nanotechnology biosensors can be produced at the nanoscale dimension, allowing the insertion of more than one technology on the same platform and the determination of more than one element with high sensitivity and specificity.

### 1.1.2 Single molecule sensing

Over the last decades of the twentieth century, Feynman's suggestion that "Is plenty of room at the botto"' inspired the research for techniques based on the reaction of single, isolated molecules. The first analytical study of single molecules was the one in 1961 observing single $\mu$-galactosidase molecules trapped in microdroplets and acting on a fluorogenic substrate (Rotman, 1961). In the 1980s, successful near-field approaches were developed, including Scanning Tunneling Microscopy (STM) and Atomic Force Micorscopy (AFM). Modern STM techniques allow chemical synthesis at the

single molecule level, while AFM has been developed into a tool to image and change the conformational states of single nucleic acid and protein biopolymers. Perhaps the most immediate impact on bioanalytical technology may be expected from the miniaturization and multiple analysis of biological assays enabled by single molecule approaches such as those applied in DNA sequencing (Thompson *et al*, 2011). A separate set of approaches for single molecule detection is based on confocal microscopy. Confocal Fluorescence Correlation Spectroscopy (FCS) was developed in the 1970s as a way to measure the kinetics of chemical reactions (Magde *et al.*, 1972). In combination with fluorescence resonance energy transfer (FRET) as a molecular ruler (Förster, 1959), confocal fluorescence microscopy of freely diffusing molecules has also been used to report biological polymers folding (Walter, 2008). Furthermore, FCS in combination with FRET has been applied to single immobilized molecules to evaluate conformational changes (Walter, 2008). Starting in the early 1970s, optical tweezers were developed as a noninvasive tool to manipulate polarizable objects such as glass and plastic beads with refractive indices distinct from their environment (Ashkin, 1970). AFM has been applied with success to study unfolding in a number of proteins, but extensive investigations have been carried out for a filamentous protein molecule from muscle sarcomeres that carries multiple tandem repeat domains of several distinct types and is believed to furnish passive elasticity to muscle tissues. Several groups characterized the nanomechanical properties of single titin molecules (Rief *et al.*, 1997, Williams *et al.*, 2003).

Optical tweezers have been used, among the others, to investigate the elastic properties of nucleic acids (Smith *et al.*, 1996; Seol *et al.*, 2004), to measure protein-DNA interactions (Kotch *et al.* 2002), and to characterize the folding of nucleic acids (Liphardt *et al.* 2001, Woodside *et al.*, 2006).

### 1.1.3 "Top-down" and "bottom-up" approach

The progress of diagnostics has always been related to the construction of novel strategies of detection and the outstanding development of information technology in the last few decades has been strictly related to the progressive miniaturization of the components employed for making novel devices.

*Top-down approach*

The miniaturization of components for the construction of useful devices and machines has been and still is pursued by the top-down approach (Balzani, 2008). This approach, which leads physicists, biologists and engineers to manipulate progressively smaller pieces of matter in example by photolithography and related techniques, has operated in an outstanding way up until now. However, it is is becoming increasingly apparent, for example, that miniaturization in computer technology, which relies on silicon-based chips, is rapidly approaching the upper limits of its capabilities. Therefore the top-down approach does not seem capable of exploiting such an opportunity.

The most common top-down approach to fabrication involves lithographic patterning techniques using short-wavelength optical sources with the advantage that the parts constructed are patterned and built in place and consequently no assembly step is required. Optical lithography is a well known field due to the high degree of refinement in microelectronic chip manufacturing, with current short-wavelength optical lithography techniques reaching dimensions of 100 nanometre scale. Shorter-wavelength sources, such as extreme ultraviolet and X-ray, are being developed to allow lithographic printing techniques to reach dimensions from 10 to 100 nanometres. Scanning beam techniques such as electron-beam lithography provide patterns down to about 20 nanometres. Smaller features are obtained by using scanning probes to deposit or remove thin layers. Mechanical printing techniques-nanoscale imprinting, stamping, and molding have been extended to 20–40 nanometres. These techniques are based on making a master "stamp' obtained by a high-resolution technique such as electron-beam lithography and then applying this stamp to a surface to create the pattern. In example, the controlled patterning of a molecular monolayer on a surface can be achieved by stamping an ink of thiol groups onto gold-coated surfaces. In another approach the stamp is used mechanically to press the pattern into a thin layer of material. These nanoscale printing techniques offer several advantages beyond the ability to use a wider variety of materials with curved surfaces. In particular, such approaches can be carried out in ordinary laboratories with far-less-expensive equipment than that needed for conventional submicron lithography. The challenge for all top-down techniques is that, while they

work well at the microscale, it becomes difficult to apply them at nanoscale dimensions. A second disadvantage is that they involve planar techniques, which means that structures are created by the addition and subtraction of patterned layers (deposition and etching), so arbitrary three-dimensional objects are difficult to construct.

*Bottom-up approach*

An alternative and promising strategy to exploit science and technology at the nanometer scale is offered by the bottom-up approach, which starts from objects at the nano- or subnanometre scale (such as atoms or molecules) to build up nanostructures. The bottom-up approach is largely the realm of nanoscience and nanotechnology (Balzani, 2008). In this way chemists and physics able to manipulate atoms and molecules, and biologists able to manipulate organic biopolymers and their correspondent monomers, are in the ideal position to contribute to the development of nanoscience and nanotechnology. Bottom-up, or self-assembly, approaches to nanofabrication use chemical or physical forces operating at the nanoscale to assemble basic units into larger structures. Inspiration for bottom-up approaches comes from biological systems, where nature has harnessed chemical forces to create essentially all the structures needed by life. Researchers aim is to replicate nature's ability to produce small clusters of specific atoms, which can then self-assemble into more-elaborate structures. In the bottom-up approach to miniaturization can be distininguished two limiting cases (Balzani, 2008):

1. Nanoscale objects are chemically simple to characterize and have no specific intrinsic function (atoms, clusters of atoms, small molecules); the functionality arises from the ensemble of such objects. In example metal nanoparticles such gold can be used to cover surfaces; gold nanoparticles are made of gold atoms as are gold sheets, but in the nanoparticles most of the gold atoms are on or close to the surface, and, therefore, they are exposed to interactions with other species. Covering a macroscopic piece with gold sheets (technology) or with gold nanoparticles (nanotechnology) leads to materials characterized by quite different properties. This field of nanoscience and nanotechnology involving the study of nanoparticles, nanostructured materials, nanoporous materials, nanopigments, nanotubes, nanoimprinting,

quantum dots, etc. is of great interest, and has already originated many applications in materials science. For basic investigations, an important role is played by manipulation or imaging nanoscale techniques.

2. The nanoscale objects with complex chemical composition such as multicomponent systems, have characteristic structures with properties exploiting particular functions, as the natural molecular-level devices. The artificial molecular devices and machines need to go near this principle and must be synthesized starting from simpler components.

A number of bottom-up approaches have been developed for producing nanoparticles, ranging from condensation of atomic vapours on surfaces to coalescence of atoms in liquids. For example, liquid-phase techniques based on inverse micelles have been developed to produce size-selected nanoparticles of semiconductor, magnetic, and other materials (Jia *et al.*, 2011). An example of self-assembly that achieves a limited degree of control over both formation and organization is the growth of quantum dots. Indium gallium arsenide (InGaAs) dots can be formed by growing thin layers of InGaAs on GaAs in such a manner that repulsive forces caused by compressive strain in the InGaAs layer results in the formation of isolated quantum dots (Borri *et al.*, 2006). Another example of self-assembly of an intricate structure is the formation of carbon nanotubes under the right set of chemical and temperature conditions (Terranova *et al.*, 2006).
DNA-assisted assembly may provide a method to integrate heterogeneous parts into a single device. Biology combines naturally self-assembly and self-organization in fluidic environments where electrochemical forces play a significant role. By using DNA-like recognition, molecules on surfaces may be able to direct attachments between objects in fluids. Such assembly might be combined with electrical fields to assist in locating the attachment sites and then be followed by more-permanent attachment approaches, such as electrodeposition and metallization. The DNA-based approach has many advantages: DNA molecules can be sequenced and chemically sinthesized in large quantities at low cost, DNA sequences can be used to recognize complementary DNA strands, hybridized DNA strands form a number of hydrogen bonds to their complementary sequence giving great stability to the double stranded structure, and finally DNA strands can be modified with labels or other molecules or nanoparticles. These properties are being

explored as ways to self-assemble molecules into nanoscale units. For example, sequences of DNA have been attached only to pre-determined surfaces of compound, providing a basis for self-assembly. For example, thiol groups at the end of molecules cause them to bind to gold surfaces, while carboxyl groups can be used for attachment to silica surfaces. Directed assembly is an increasingly important variation of self-assembly where parts are moved mechanically, electrically, or magnetically and are placed precisely where they are planned.

## 1.2 DNA as a building material

Since the discovery by Watson and Crick in 1953, DNA was known mainly as the molecule for the storage of genetic information but nowadays it has also been shown to be very useful as material for the construction of micrometer and nanometer-scale objects with high feature resolution. In this context, nanostructures self-assembly offers great potential for nanofabrication of materials with applications in nanoelectronics, bionanosensors and autonomous machines.
In the last 20 years a number of constructs exploiting base pairing interactions were synthesized and fabricated; we can mention molecular transistors (Tans *et al.*, 2000), nanowires (Huang *et al.*, 2001, Klinov *et al.*, 2007) and single molecules simulating conventional electronic circuits (James *et al.*, 2005). In many cases nucleic acids are used as monomeric components of more complex structures (LaBean *et al.*, 2002) where DNA is only used in the double helix conformation without possibilities to branch the structure. After 1982, when Seeman and coworkers (Seeman *et al.*, 1982, Seeman *et al.*, 1983, Seeman *et al.*, 1999) started to construct artificial conjunctions with DNA (Figure 1.1Seeman junction. The motifs. e.g PX and its topoisomer JX, can result from reciprocal exchange of parallel double elices of DNA molecules, forming a crossover at every possible juxtaposition between them (from Yan, 2002).figure.caption.4), many research groups started realizing constructs such as DNA-based rigid triangles (Liu *et al.*, 2004), cubes (Fu *et al.*, 1993) and junctions for structures with three or four ramification points (Zhong *et al.*, 1992).

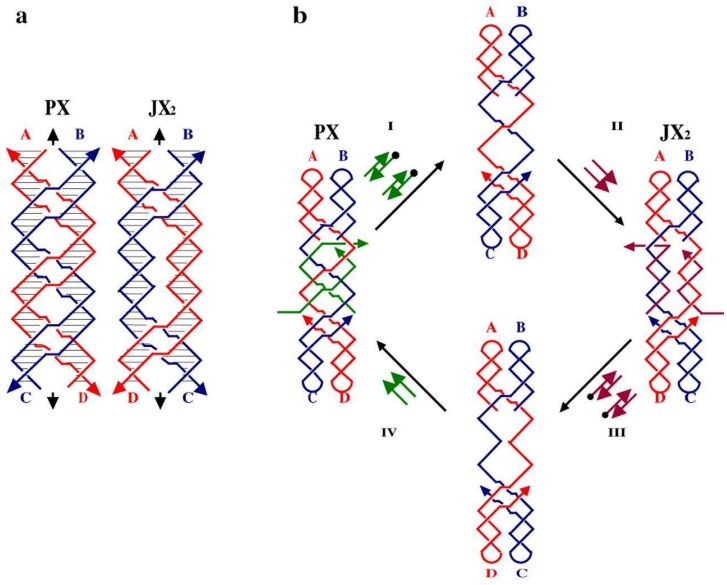


Figure 1.1: Seeman junction. The motifs. e.g PX and its topoisomer JX, can result from reciprocal exchange of parallel double elices of DNA molecules, forming a crossover at every possible juxtaposition between them (from Yan, 2002).

In 1996, the group of Mirkin and Alivisatos (Alivisatos *et al.*, 1996; Mirkin *et al.*, 1996) reported pioneering studies on the assembly ssDNA-mediated of gold nanoparticles (AuNPs) into aggregates, controlling the number and the site in the linear chain of the particles that have to be placed. Another interesting application of the autonomous self assembly of oligonucleotides in solution was reported in 2004 by the Dirk's group and called "Hybridization Chain Reaction" (HCR). This technique uses three synthetic ssDNAs able to hybridize each others in presence of a target DNA molecule at room temperature (Green, 2006). The result of the recognition is a cascade sequence of complementation events the formation of a polymer made of nucleic acids, triggered by the presence of the designed probe (Figure 1.2Hybridization Chain Reaction working principle. Two hairpin species, H1 and H2, are stable in solution but when a single stranded molecule called initiator (I) is added in solution, triggers the hybridization event between the hairpin species originating a DNA-based polymer (from Dirks *et al.*, 2004).figure.caption.5).

Linear ssDNAs can be designed also to arrange into branching structures

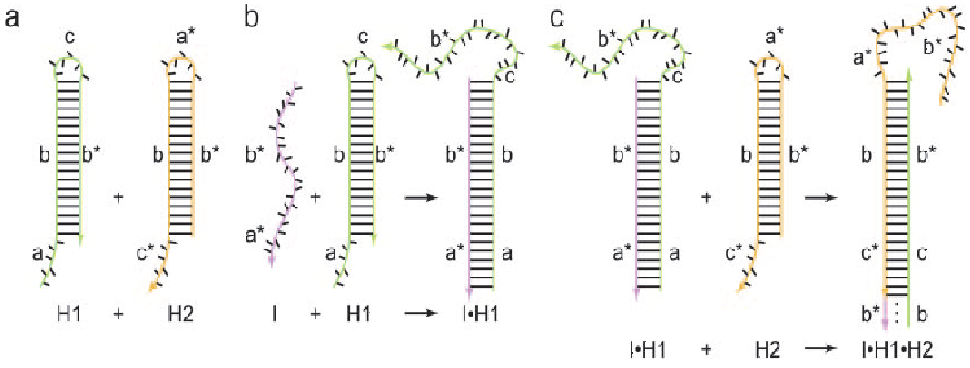


Figure 1.2: Hybridization Chain Reaction working principle. Two hairpin species, H1 and H2, are stable in solution but when a single stranded molecule called initiator (I) is added in solution, triggers the hybridization event between the hairpin species originating a DNA-based polymer (from Dirks *et al.*, 2004).

called "dendrimers", i.e. high ordered structures with a number of ramifications so that the reactive ends are exposed and functionalizable with endless possibilities. Starting from the pioneering works of '70s and '80s (Buhleier *et al.*, 1978, Denkewalter *et al.*, 1981, Newkome *et al.*, 1985, Tomalia *et al.*, 1985), in 2005 Li's group created DNA-based dendrimers interconnecting different branching subunits via sticky ends cohesion, choosing as constructive material DNAs among the other possibilities such as carbohydrates and proteins (Luo, 2003). The resulting polymer was monodispersed and controllable with a relatively high yeld and purity (Figure 1.3DNA dendrimers. As rapresented in the figure above, many oligonucleotides complement each other by hybridization forming an Y-shaped monomer. Due to the complementary of the monomers' sticky ends, ramificated comlpex structures made of the same monomer units can be obtained (from Li *et al.*, 2004).figure.caption.6).

### 1.2.1 The DNA-based origami method

DNA based nanotechnology, with its potential to address many challenges, has attracted a huge interest from a number of fields in research, such as chemistry, biology, physics, material and computer science. In the bionanotechnology field, DNA origami is a landmark invention and in a few years since its introduction has been exponentially widened. DNA origami is the technique introduced by Rothemund in 2006 in which a long single-stranded

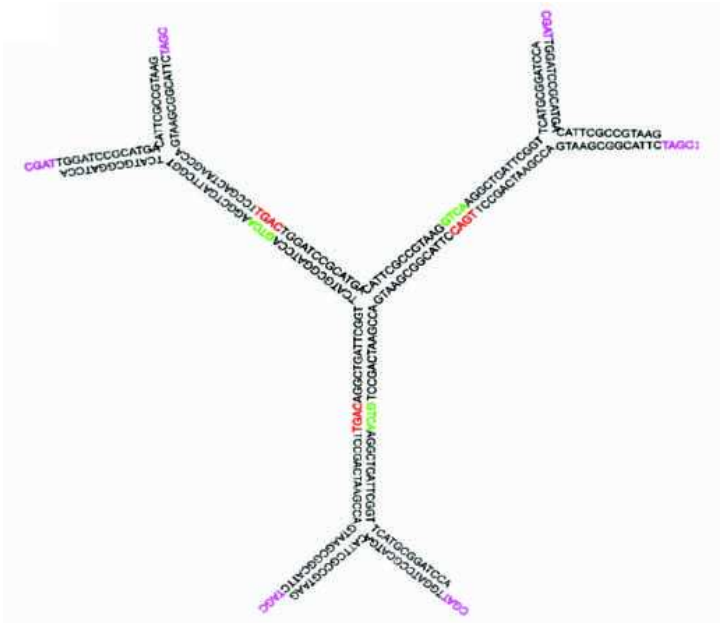

Figure 1.3: DNA dendrimers. As rapresented in the figure above, many oligonucleotides complement each other by hybridization forming an Y-shaped monomer. Due to the complementary of the monomers' sticky ends, ramificated comlpex structures made of the same monomer units can be obtained (from Li *et al.*, 2004).

polynucleotide, the "scaffold strand", is folded into arbitrary nanostructures with the help of many short oligonucleotides, named "staple strands". The DNA based objects yet created can be planar (smiles, squares, triangles, rectangles) as shown in Figure 1.4Two dimensional DNA-Origami. The DNA origami obtained by Rothemund in 2006 are stars, smiley faces and rectangles. With precise and localized modification of the surface of the origami, north and south america and other well defined shapes were obtained and visualized with AFM.figure.caption.7 but even three-dimensional (cubes, tooted gears) as in Figure 1.5Three dimensional DNA-Origami. The DNA origami obtained by Andersen in 2009 is a 3-D cube opening the lid after a hybridization event. The images were obtained with cryo-EM (Andersen *et al.*, 2009).figure.caption.8 and Figure1.6Three dimensional DNA-Origami. The toothed gear, spherical wireframe capsule resembling a beach ball and the concave and convex triangles obtained by Dietz' group, were visualized by negative-stain TEM. These objects are an example of how bending enables the design of intricate nonlinear shapes.figure.caption.9.

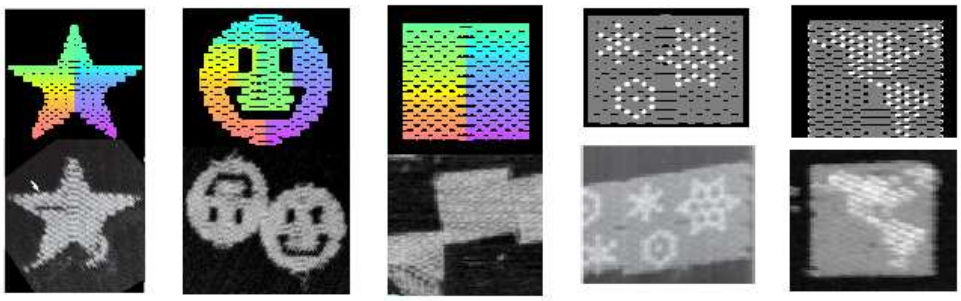

Figure 1.4: Two dimensional DNA-Origami. The DNA origami obtained by Rothemund in 2006 are stars, smiley faces and rectangles. With precise and localized modification of the surface of the origami, north and south america and other well defined shapes were obtained and visualized with AFM.

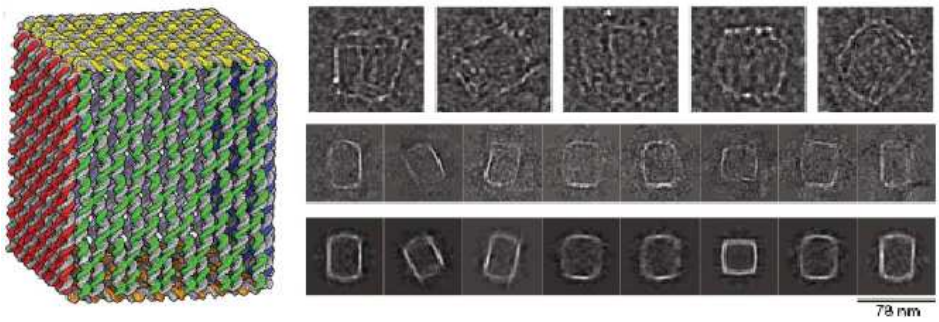


Figure 1.5: Three dimensional DNA-Origami. The DNA origami obtained by Andersen in 2009 is a 3-D cube opening the lid after a hybridization event. The images were obtained with cryo-EM (Andersen *et al.*, 2009).

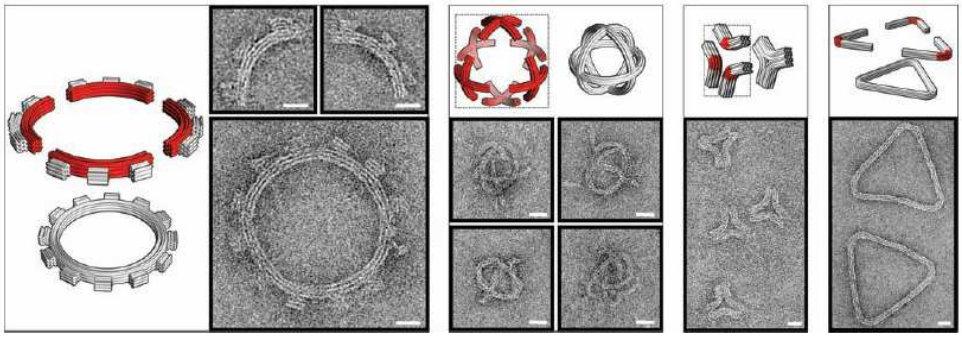

Figure 1.6: Three dimensional DNA-Origami. The toothed gear, spherical wireframe capsule resembling a beach ball and the concave and convex triangles obtained by Dietz' group, were visualized by negative-stain TEM. These objects are an example of how bending enables the design of intricate nonlinear shapes.

### 1.2.2 Preparation and design of a DNA origami

A DNA origami is a nanostructure composed by a long scaffold strand that runs back and forward to create a rigid building block or an autonomous structure and that is hold in place with the aid of many short single stranded DNA molecules complementary to the scaffold.
To design a DNA origami Paul Rothemund used a particular elaboration created with MatLab, in association with complex computational studies to calculate and predict the shape. At the moment there are several freeware open-source program packages, for the design of DNA origami nanostructures. These softwares are characterized by some differences making them more user-friendly and more compatible with the aim of the project in which are involved. In this work I took into consideration SARSE DNA origami package and caDNAno, two software packages.
The SARSE-DNA package was released by Kjems's group for the creation of 2D DNA origami structures. This software has a scientific data editor in which a bitmap picture can be imported to automatically generate a rough folding path through all the shape, representing the scaffold strand. The folding path has to be further modified and refined manually in the editor and then the staple strands with appropriate crossovers in the plane of the structure are added. A rough 3D model of the desired shape may also be generated. This software was used in the design of non-geometrical shapes such as dolphins (Andersen *et al.*, 2008) and in the construction of 3D DNA box (Andersen *et al.*, 2009), based on the hybridization between strands protruding from the edges of singular squares.
The software named caDNAno was released by Shih's group in 2009. Is specialized for design honeycomb or squared lattice DNA arrays, assuming for simplicity that the DNA double helix section is approximately a cylinder. This package is composed of three main panels: "Slice" to generate manually the number of helix of the scaffold strand, "Path" to manage scaffold and staples strands length, position and number of crossovers and the "Render" panel to see a rough 3D simulation of the structure. With this software a 3D model can be generated as demonstrated by Shih's group with the creation of innovative curved 3D DNA origami objects (Dietz *et al.*, 2009). As output, the operator obtains the sequences of the staple strands, reporting lengths, colours and positions. To create a DNA origami a geometric model has to be designed that approximates the desired shape. When the first

planar DNA nanostructures based on parallel double helical domains were made (Winfree *et al.*, 1998) a few points were focused about their structure. It was assumed that:

1. the helices would be lie close-packed
2. the helices would be be without bends
3. the length of the structures with parallel helices (measured perpendicular to the helices) was assumed to be given by the relation 2*h nanometers where h is the number of helices
4. the width of the structure was assumed to be 0.34nm*n (Brown, 1996) where n was the number of nucleotides in the structure.

By the observations of Rothemund (2006) imaging the structures by AFM the above assumptions were reviewed and, except the fourth, all of them turned out to be incorrect due to their approximation. The helices are not close packed, they reveal gaps between, tipically 1 or 2 nanometres wide whose position and length follow the pattern of crossovers in the underlying structure. Wherever two helices have a crossover, the gap is not observed at the crossovers but a few nanometers away. The source of the inter-helix gap may be electrostatic repulsion between helices of the crossovers. In Rothemund's work the width of the gap appears to depend on the spacing of crossovers: origami with 16 nucleotides spacing (about 1.5 turns) between crossovers have a 1 nm gap, origami with 26 nt spacing (about 2.5 turns) appear to have a 1.5 nm gap.
The interhelix gap appears to be an important aspect of DNA nanostructures constructed from parallel helices and this approximation was suggested: the length of the structure should be 2h+(h-1)g nm where h is the number of 2 nm wide helices and g is the inter-helix gap. Lengths measured by AFM are typically within 5% of the predicted length by this formula; for the width the error was tipically 10%.
Using caDNAno, the double helices are cut to fit the shape in pairs and to be an integer number of turns in length. To hold the adjacent helices together many crossovers have to be inserted in a periodic manner. These crossovers are possible only in certain points of the helices, more precisely in the sites where the strand switch position with the adjacent one. The crossovers have to be placed every 1.5 turns of the helix (10.5 nucleotides

or approximately 3.4 nm), but in the DNA origami designing process, one turn is approximated to be 3.5 nm in length and 10.7 nucleotides. In this way the software can consider an integer number of bases between periodic crossovers, in other words 16bp for 1.5 turns. The fundamental constraint, on a folding path, is that the scaffold can form a crossover only at those locations where the DNA twists; furthermore the parallel helices are not in a close contact between each other, influencing the y-resolution. Once this path is designed, a set of staple strands complementary to the scaffold strand are generated. Consequently the software is able to create the periodic crossovers. The asymmetric nature of the helix, due to the presence of the minor and major grooves and the non-integer number of base pairs per half turns in standard B-DNA, introduces some complications in the balancing of twist strain between crossovers. In order to avoid this problem, the crossovers are arranged with a symmetry that places, in alternating way, the minor groove at the top and at the bottom face of the shape. The last step of the design is the study of the length and the position of the staple strands, that must be comprised between 20 and 50 nucleotides; the length and temperature of hybridization have a crucial role to the final stability and well-formed success of the structure (Rothemund, 2006).

### 1.2.3 DNA origami nanoarrays and other nanostructures

A DNA origami is completely made of biological soft matter and can be used, as demonstrated, to create versatile structures with the possibility of modify few staple strands in order to add features necessary to create arbitrary active shapes. DNA origami has also been used as a substrate to integrate DNA nano-mechanical devices.
A work that showed how DNA origami can be complex was Kjems' group dolphin, designed with the SARSE software package. The DNA-based dolphin in Figure 1.7The dolphin structure imaged with AFM. In panels A and B are shown the possible tail flipping conformations and the correspondent AFM images (Andersen *et al.*, 2008).figure.caption.10 was composed of two main parts sew together by crossovers to form the dolphin eye. A particularity of this work was that the dolphin tail can flip up and down on the basis of the absence of crossovers in the tail seam. Kjems's group demonstrated that dimer interaction of the dolphin structure stabilizes tail conformation. The binding of two structure was provided by the insertion of extensions in

some specific points on the dolphin, providing sticky-end cohesion between the two structures. The flexibility is an interesting property of an active DNA structure that yields that may be a basis for creating new controllable dynamic nanostructures (Andersen *et al.* 2008).

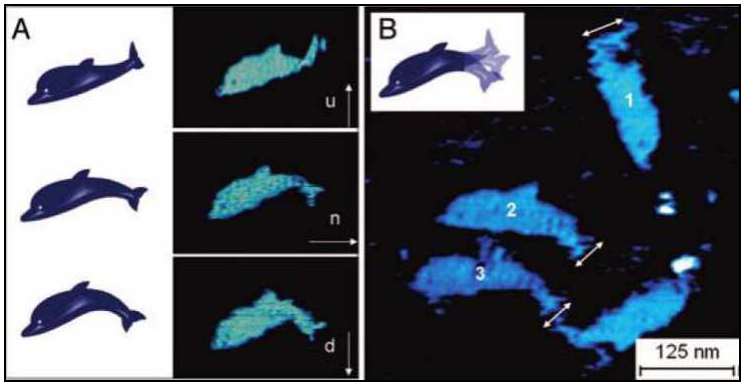


Figure 1.7: The dolphin structure imaged with AFM. In panels A and B are shown the possible tail flipping conformations and the correspondent AFM images (Andersen *et al.*, 2008).

### 1.2.4 DNA origami for nano-arraying

The DNA-based objects has been regarded as a promising platform for the precise arraying of nanomaterials. Functionalization of the DNA-origamis surface can be obtained by oligonucleotides modification during the chemical synthesis. The selective deposition of inorganic nanomaterials on the DNA origami is important for various applications based on the nanoarrays. An example of the selective deposition of gold nanoparticles (AuNP) addressed on a triangular-shaped DNA origami structure is reported on Ding's group work (Ding *et al.*, 2010): three different sizes of gold nanobeads were addressed with high precision on the origami surface (Figure 1.8Addressment of gold nanoparticles on DNA-origami surfaces. On the left, schematic drawing of the assembly of six AuNPs on a triangular DNA origami template through DNA hybridization. First, the scaffold strand (red) hybridizes with designed staple strands to form the DNA origami template with different binding sites on one side of the origami surface. Different AuNPs covered with corresponding DNA strands then bind to the designed locations through complementary strand hybridization. In panel a SEM image of six-AuNP linear structures organized by triangular DNA origami and

in panel b zoom-in image of one assembled origami-AuNP structure (from Ding *et al.*, 2010).figure.caption.11).

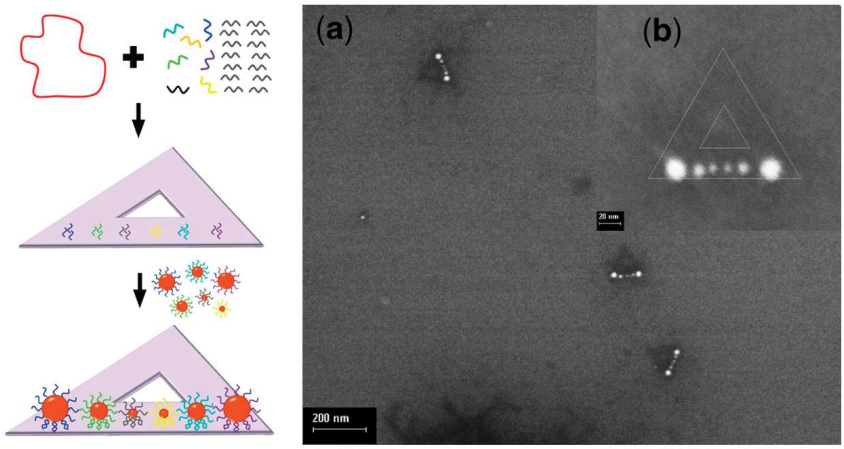


Figure 1.8: Addressment of gold nanoparticles on DNA-origami surfaces. On the left, schematic drawing of the assembly of six AuNPs on a triangular DNA origami template through DNA hybridization. First, the scaffold strand (red) hybridizes with designed staple strands to form the DNA origami template with different binding sites on one side of the origami surface. Different AuNPs covered with corresponding DNA strands then bind to the designed locations through complementary strand hybridization. In panel a SEM image of six-AuNP linear structures organized by triangular DNA origami and in panel b zoom-in image of one assembled origami-AuNP structure (from Ding *et al.*, 2010).

Other important biomolecules in biosensing are the proteins. One of the most used protein linked to DNA strands is biotin, ideal for the recognition by the streptavidin protein. The biotin-streptavidin bond is often used to link between the two parts and this principle was applied on the surface of the DNA origami, inserting staple strands modified with biotin. The strategy is to create binding sites on the DNA origami structure that might provide more stability and selectively than other techniques. The group of Yan in 2002 verified the specific placement of each biotinylated staple strand, for example the center tile, the corners, the diagonals and the center tiles at each edge. The arrays where than incubated with streptavidin, finding bound protein only at the predicted positions. In Figure 1.9Specific placement of streptavidin molecules on a biotin-modified DNA origami surface. The DNA-based arrays, incubated with streptavidin, revealed bright spots corresponding to the protein at the expected position (from Lund *et*

*al.*, 2005).figure.caption.12, panels on the left are schematic drawing showing the expected position of the streptavidin (green balls) on the array and panels on the right are corresponding AFM images where the bright spots reveals the the streptavidin. The work of Voigt and co-workers is another example how to use biotinylated staple strands in a rectangular shaped DNA-origami to address streptavidin molecules, demonstrating that it is possible to perform reactions on a DNA origami with a yield around 80-90% with high precision positioning (Voigt *et al.* 2010).

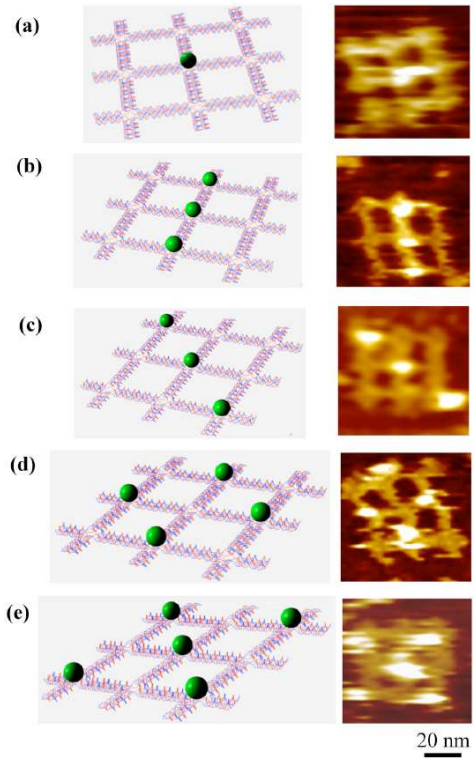


Figure 1.9: Specific placement of streptavidin molecules on a biotin-modified DNA origami surface. The DNA-based arrays, incubated with streptavidin, revealed bright spots corresponding to the protein at the expected position (from Lund *et al.*, 2005).

### 1.2.5 Selective deposition of DNA origami structures

In nanotechnology the recognition and hybridization of ordered pairs of molecules and substrates is attractive for building structures and devices on surfaces containing templates etched with lithography or other top-

down fabrication process. However the application of these techniques is not simple due to the size of the objects. An ideal strategy involves the spontaneous selection of the appropriate component for the surface sites, forming devices through a process of self-determined recognition and assembly. Using DNA-based building blocks, Kershner and coworkers described the shape-dependent templating of DNA origami objects onto lithographed solid supports (Kershner *et al.*, 2009). They first produce hollow triangular DNA origami tiles (Rothemund, 2006), with an approximate dimension of 120 nm; the tiles then find their allocation in the complementary sites in templates lithographically etched on a silicon oxide surface, to which they can bind with selectivity and correct orientation (Figure 1.10Specific placement of streptavidin molecules on a biotin-modified DNA origami surface. The DNA-based arrays, incubated with streptavidin, revealed bright spots corresponding to the protein at the expected position (from Kershner *et al.*, 2009).figure.caption.13).

On the basis of this self assembly strategy DNA-based tiles of the desired shape can be designed and functionalized; the surface templating dictated by tile-template shape and size cal allow specific surface placement. Technologies that could benefit from this hierarchical ability include molecular electronics, "lab-on-a-chip" applications, optical and logic devices, and a variety of biomedical applications with templated sites governing many biomolecules functions.

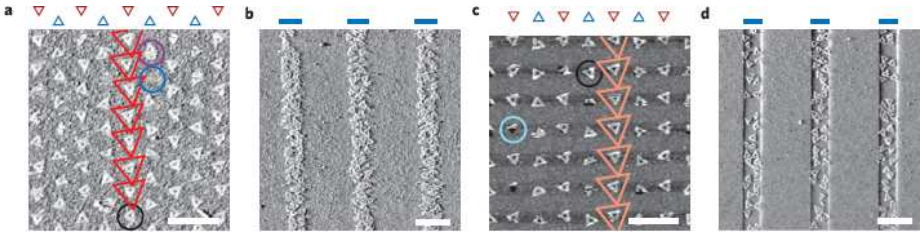


Figure 1.10: Specific placement of streptavidin molecules on a biotin-modified DNA origami surface. The DNA-based arrays, incubated with streptavidin, revealed bright spots corresponding to the protein at the expected position (from Kershner *et al.*, 2009).

### 1.2.6 3-D DNA origami structures

The DNA origami technology has no limitations for its use in the creation of 3D structures, field of increasing interest in the last years. In 2009, different cuboid shapes with various dimensions were designed and tested experimentally (Ke *et al.*, 2009) using the scaffolded- DNA-origami strategy with DNA helices packed on a square lattice geometry, as shown in Figure 1.11Schematics of the squared lattice DNA origami on the left and correspondent TEM images on the right (Ke *et al.*, 2009).figure.caption.14.

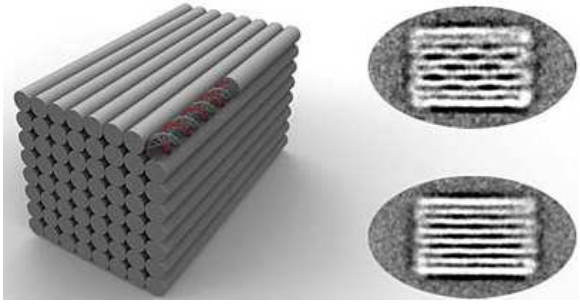

Figure 1.11: Schematics of the squared lattice DNA origami on the left and correspondent TEM images on the right (Ke *et al.*, 2009).

In the last years the Shih's group was able to create a 3D shape using a like six-helix bundle; a set of adjacent helices framed with an angle of 120 °instead of the planar angle of the 2D structures were designed. This angle can be obtained with a different spacing of the crossovers between the staple helices (Douglas *et al.*, 2007). This idea was further extended to 3D more complex structures like the honeycomb lattice structures with which twisted and bended structures may be introduced by adding or removing one or more bases at strategic positions (Dietz *et al.*, 2009). If just one base is deleted from the 7bp period, the result is an overwinding and tensile strain for the fragment, which causes a left-handed torque and a traction on its neighbors; on the contrary if a base is inserted, the result is a local underwinding and compressive strain that can be relieved by a compensatory global right-handed twist and bend away from the fragment (Figure 1.12Schematic models and TEM images of 3 by 6 helix bundles. As visible from the TEM images (scale bars 20 nm), combining site-directed insertions and deletions induces globally bent shapes, programmed to different degrees of bending (reproduced from Dietz *et al.*, 2009).figure.caption.15).

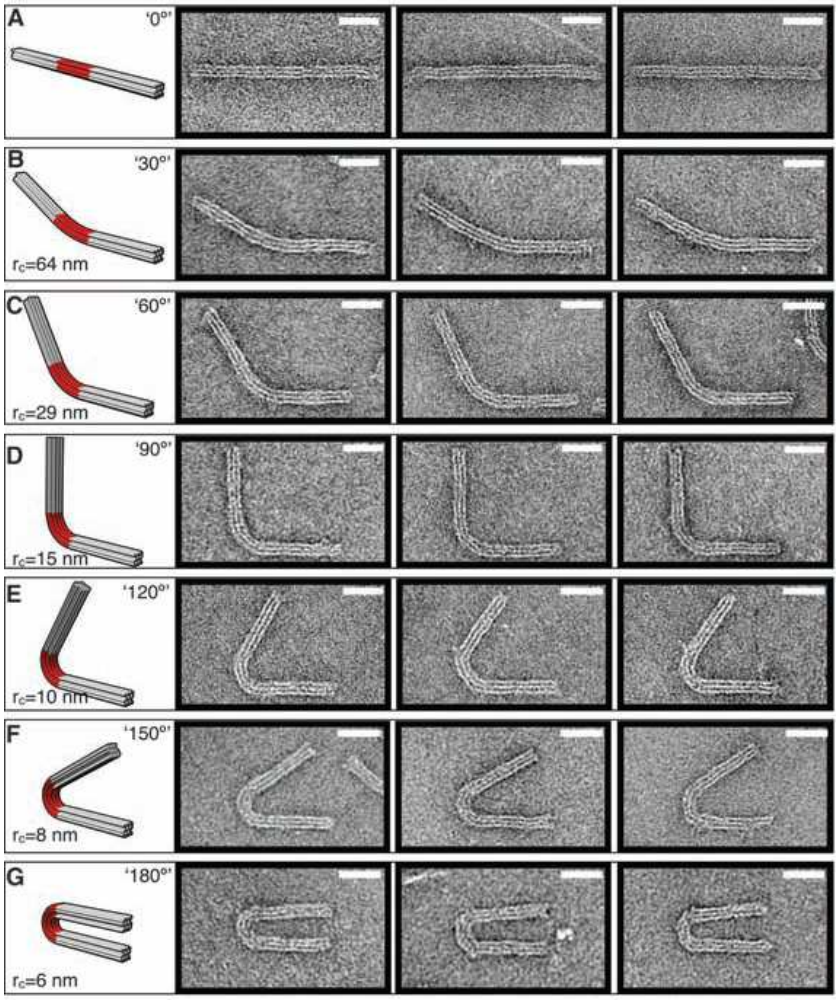


Figure 1.12: Schematic models and TEM images of 3 by 6 helix bundles. As visible from the TEM images (scale bars 20 nm), combining site-directed insertions and deletions induces globally bent shapes, programmed to different degrees of bending (reproduced from Dietz *et al.*, 2009).

This predictions where confirmed with the design and observation of the six and twelve teeth gears, the beach ball-like capsule, the convex and concave triangles and even spiral-like objects (Dietz *et al.*, 2009).
Another example is reported in the work of Kjem's group and its 3-D DNA-based box the M13mp18 scaffold strand was used to create the six squared domains, corresponding to the six cube's faces, connected each other by the continue scaffold. A key-lock system was also inserted: two protruding oligonucleotides with exposed sticky ends were inserted on the edge of two

adjacent faces of the box. The contact of the sticky ends with the target DNAs triggers the hybridization between the key-probe and the lock, opening the lid. The opening was qualitative detected with FRET technique and Atomic Force Microscopy. The closing process has not been considered (Andersen *et al.* 2009).

## 1.3 Nucleic acids visualization

In DNA nanotechnology, visualization of samples is crucial, in order to see whether or not the software elaborations and simulation correspond to the real features of the object synthesized. Different visualization techniques may be used depending on needs; electrophoresis and fluorescence techniques are mainly qualitative analysis, in contrary of microscopy techniques, that can give a precise information about shape and dimensions of what we are observing.

### 1.3.1 Gel electrophoresis

Standard agarose gel electrophoresis is the most used qualitative technique to check if the annealing process has performed well and if any constructs were formed. Electrophoresis allows the migration of a charged molecule in an electrical field; in example, DNA molecules with their negative charge can migrate in the electric field on the basis of their molecular weight and conformation. Generally, for double stranded DNAs, longer molecules migrate slower than smaller but for DNA origami, the conformation of the object affects migration. The information we can obtain is just if any constructs had formed in the annealing step by comparing the migration profile of the scaffold strand molecule with that of of the nano-object.

### 1.3.2 Fluorescence techniques

Fluorescence resonance energy transfer (FRET) is a mechanism describing the energy transfer from a donor fluorophore which transfers energy non-radiatively over long distances (10-100 Å), to an acceptor fluorophore. The relationship between fluorophore distance and energy transfer was first described by Förster in the 1940's (Förster, 1946; Förster, 1948) and was later verified by Stryer and colleagues, in the late 1970's. A number of advantages are inherent to the use of this technique, including the sensitivity of

fluorescence-based detection, the relatively short timescale of energy transfer, and the appreciable range of distances over which it can be applied. The processes underlying FRET have been reviewed extensively and are illustrated in Figure 1.13Schematic working principle of the FRET mechanism. The absorption of energy by the donor, results in excitation from the ground state S0, to an excited singlet state S1.figure.caption.16.

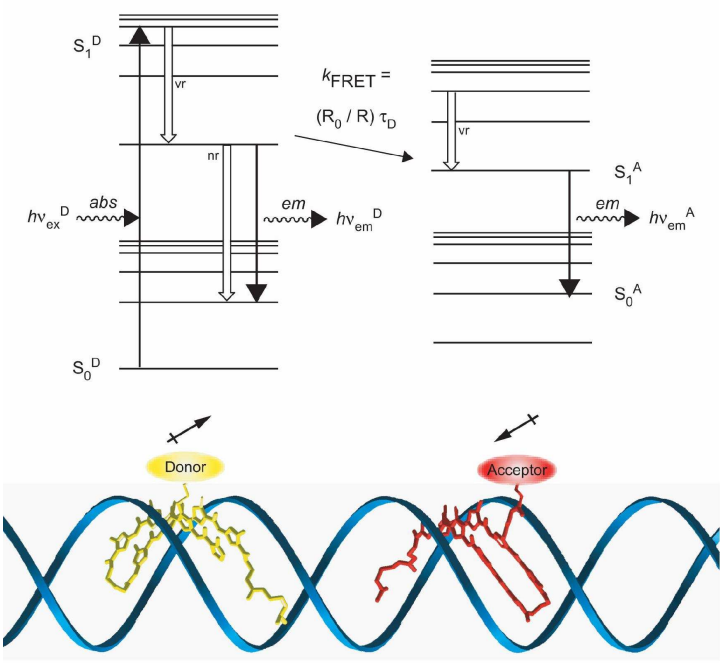


Figure 1.13: Schematic working principle of the FRET mechanism. The absorption of energy by the donor, results in excitation from the ground state S0, to an excited singlet state S1.

The first step involves absorption of energy by the donor molecule, resulting in excitation from the ground state, S0, to an excited singlet state, S1. Several excited states are available to the donor; however, vibrational relaxation to S1 D by internal conversion is rapid, ensuring that a majority of emission occurs from this state. Several fates are possible for the excited donor, including spontaneous emission and non-radiative processes. If a suitable acceptor fluorophore is nearby, then non-radiative energy transfer between the donor and acceptor occurs. This transfer involves a resonance between the singlet-singlet electronic transitions of the two fluorophores, generated by coupling of the emission transition dipole moment of the donor

and the absorption transition dipole moment of the acceptor. Thus, the efficiency of FRET and the range of distances over which it can be observed are determined by the spectral properties of a given donor/acceptor pair. FRET can be experimentally measured in a number of ways, using either time-resolved or steady-state techniques. The most commonly employed methods for quantifying FRET monitor either the reduction in the donor quantum yield in the presence of acceptor or the enhancement of acceptor emission in the presence of donor. Quantum mechanics dictates that the rate of energy transfer correlates with the inverse sixth power of the distance separating the fluorophores, R.

### 1.3.3 FRET use and applications

FRET is used in many fields of research to localize and study molecular ruler. Theodor Förster demonstrated that between two fluorescent molecules there is an energy transfer if they are within a precise radius of distance; hence, if the fluorescent molecules are in the Förster radius exciting the donor, the acceptor emission is recorded. An application of this kind of analysis is the Kjem's DNA box (Andersen *et al.*, 2009, Figure 1.143D DNA cube made with origami face and with controllable lid. The M13mp18 was folded to generate six interconnected sheets, which were subsequently arranged to form a 3D box; the edge of the box were than bridged with more staple strands, resulting in a cuboid structure. The lock–key system to open and close the lid of the box was obtained by the attachment of two sets of complementary DNA strands to the lid and an adjoining face to achieve the closed lid. The strands on the adjoining face had sticky-end extensions to provide the displacement of the complementary DNA on the lid by an externally added key strand, which opens the lid. This selective lid opening was confirmed by fluorescence resonance energy transfer between the fluorescent dyes attached to both of the faces (Andersen *et al.*, 2009).figure.caption.17). Since an acceptor emission frequency may be very different from that of the emitter, a typical FRET application implies the use of an acceptor to quench the donor emission. The quencher, has the role of quenching the fluorescence so that there is no emission when the molecules are in strict contact; on the contrary an increase in the distance produces an increase in the recorded fluorescence and can be taken as an indication of the change of conformation of an object.

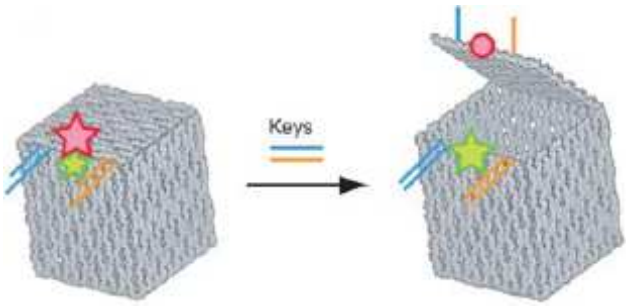


Figure 1.14: 3D DNA cube made with origami face and with controllable lid. The M13mp18 was folded to generate six interconnected sheets, which were subsequently arranged to form a 3D box; the edge of the box were than bridged with more staple strands, resulting in a cuboid structure. The lock–key system to open and close the lid of the box was obtained by the attachment of two sets of complementary DNA strands to the lid and an adjoining face to achieve the closed lid. The strands on the adjoining face had sticky-end extensions to provide the displacement of the complementary DNA on the lid by an externally added key strand, which opens the lid. This selective lid opening was confirmed by fluorescence resonance energy transfer between the fluorescent dyes attached to both of the faces (Andersen *et al.*, 2009).

### 1.3.4 Microscopy techniques

To allow the analysis of the real shape of the designed DNA structures, the use of microscopy techniques was needed. Transmission Electron Microscope (TEM) is used for an estimation of the shape and the dimensions of the objects but the sample has to be very thin, to allow the transmission of electrons as it is recommended for two dimensional DNA Origami and not for 3D structures. To gain more information about the 3-D structures, is used the Cryo-EM, where the sample is kept at low temperatures. This technique does not need any staining or fixation, the sample can be analyzed in its native conditions except the initial freezing step. To provide more detailed information on three-dimensional structures, Cryo-EM or TEM are combined with the small angle X ray scattering (SAXS). All the techniques based on electron microscopy have many disadvantages such as the need of the creation of a vacuum condition in the working chamber compromising the real conformation of the soft objects, the drying, staining or freezing steps and the investigation are destructive. The most informative microscopy technique is the Atomic Force Microscopy (AFM), where biolog-

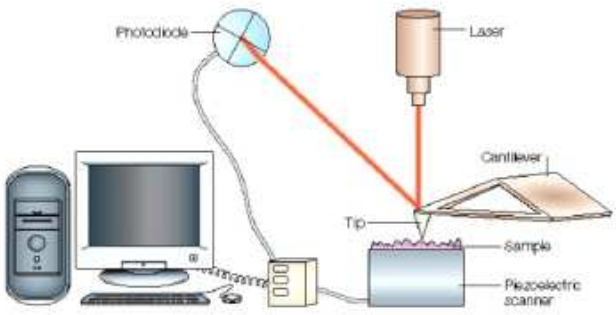


Figure 1.15: Schematics of AFM setup. The AFM consists of a cantilever with a sharp tip at its end that is used to scan the sample surface. When the tip is brought into proximity of a surface, forces between the tip and the sample lead to a deflection of the cantilever, measured using a laser spot reflected from the top surface of the cantilever into an array of photodiodes.

ical objects can be imaged in their appropriate environment, in example in a buffer or more generally, in liquid. In this way the reactivity of the sample and the eventually morphological changes induced by the interaction can be monitored in real time.

*Atomic Force Microscopy*

In 1986 Binning, Quate and Gerber demonstrated the possibilities to measure Van der Walls interactions and used this result to design a new scanning probe microscope, the atomic force microscope (AFM), one of the most used tools for imaging, measuring and manipulating matter at the nano-scale.
The working principle, evidenced in Figure 1.15Schematics of AFM setup. The AFM consists of a cantilever with a sharp tip at its end that is used to scan the sample surface. When the tip is brought into proximity of a surface, forces between the tip and the sample lead to a deflection of the cantilever, measured using a laser spot reflected from the top surface of the cantilever into an array of photodiodes.figure.caption.18 is that when the tip is in proximity of a sample surface, forces between the tip and the sample lead to a deflection of a cantilever, which acts like an ideal spring.

Usually the deflection of the cantilever is measured using a laser beam which is reflected by the cantilever into a four quadrant photodiode. The photodiode is adjusted until the reflected beam hit the centre of the quadrant photodiode and the signal is near zero. Any deviation from the rest position of the cantilever is translated into a positive or negative voltage on the photodiode output. Thanks to the particular geometry of atomic force microscopes, the typical sensitivity of this method is about 50mV per nm which allows the detection of very small cantilever deflection. To create a topographic map, the tip is raster-scanned in contact with the sample surface and the cantilever deflection is recorded and converted in actual height. The rapidity with which the deflection recovers the set point value after the tip has encounter a height step is regulated by a parameter which is usually named feedback gain. The higher the feedback gain the better the tip follows the sample profile. However if this setting is too high the system can be driven to resonance and the tip starts to tap the sample with high force which can result in tip and sample damages. The fine tuning of the feedback gain requires a very high sensitivity by the microscope user and is one of the key point in obtaining good AFM images. During a scan the tip moves in one direction and returns in the opposite direction generating two images (trace and retrace image) of the same scan line. When the parameter are set correctly, trace and retrace images are identical. When instead the tip interact and modify the sample trace and retrace could appear dramatically different. Piezo-actuators made of piezoelectric ceramics are typically used to control, among x and y, the z position with the desired accuracy. The use of piezo actuation combined with the high deflection sensitivity of AFM cantilever and the possibility of manufacture high resolution tips with radius of curvature of the order of 1nm allowed AFM imaging to obtain routinely resolution of 1 nm in the x/y plane and of 0.1 nm in z-axis. AFM can be operated in contact or non contact mode. When the tip is in contact with the sample with a constant scan force, AFM measures the repulsive forces between the tip and the sample.

Non contact or dynamic mode operation includes frequency modulation and the more common amplitude modulation. In frequency modulation, changes in the oscillation frequency provide information about tip-sample interaction. Frequency can be measured with phase locked loop techniques which can track with high speed and precision any frequency change and thus the

frequency modulation mode allows for the use of very stiff cantilevers. Stiff cantilevers provide stability very close to the surface and, as a result, this technique was the first AFM technique to provide true atomic resolution in ultra-high vacuum conditions (Giessibl, 1995). Also in dynamic mode is it possible to generate an error image, mapping either the frequency or the amplitude difference with the respective set point. Several other image modes are available in atomic force microscopy, among them phase imaging, current imaging, lateral force and friction imaging are the most common.

### 1.3.5 AFM imaging on DNA origami structures

AFM imaging permits to observe biological samples with high definition and with advantages if compared with other microscopy techniques such as transmission (TEM) or scanning electron microscopy (SEM). The absence of the vacuum need in fact is a great advantage for the imaging of three dimensional or non planar objects and the sample does not need preliminary preparation with noble metal coating, drying process or staining. The more important aspect is that biological samples can be imaged in their appropriate environment, allowing the possibility to analyze samples' behaviour in the most proper buffer, maintaining biological molecules active and alive during the imaging process. In these conditions the analysis of sample reactivity is made possible by exposing it to analytes and evaluating, in real time, the structural variations induced by the interaction. The AFM technique could be used even for force curves analysis to explore the physics characteristics, such as elasticity, deformability, molecule bond tension, cells membrane composition.
As a substrate for AFM imaging, muscovite mica is the most used due to the low roughness. For DNA-Origami imaging a Mg2+ buffer is required to permit to DNAs to firmly adhere on the negative mica surface; both the mica surface and the DNA are negatively charged so the salt buffer is necessary to screen these charges one from each other. To image soft biological samples the softest cantilevers should be used to minimize potentially destructive interaction with the sample surface, combined to use the non-contact mode that is more gentle than contact-mode. Scanning tips are available in various shapes and sizes and the geometry and composition play a critical role on AFM imaging of the sample (Taatjes *et al.*, 1999); indeed artefacts or convolutions may occur if the scanning tip is less sharp than the

profile of the object (Hoh and Hansma 1992). In fact when the scanning tip is sharper than the sample features, the real profile of the features is obtained. However sharper tips can damage more the biological samples. So it is important to choose the appropriate tip also taking in consideration the nature of sample (You, Lau *et al.* 2000).

# Chapter 2

# Materials and Methods

In this section, materials and methods for the production and the assembly of each component of the device are presented. If not specified, oligonucleotides are purchased from Sigma-Aldrich (Germany) and resuspended in water at 100$\mu$M concentration and stored at -20°C. All the solutions used were sterilized by autoclaving at 121°C for 21 minutes.

## 2.1 Nucleic acids fabrication

### 2.1.1 DNA based Origami *in silico* design

The program used for the design of the DNA origami was caDNAno square lattice package v.0.2.3. (Dietz *et al.*, 2009), chosen among the others (SARSE DNA-Origami package, Nano-Engineer-1). Below I summerize how to proceed for origami design using this program, showing the various types of diagrams that the program can draw to aid in design. When the desired prototype of the needed final shape has been determined, the design of a DNA origami proceeds in four main phases (manual design steps and passes of the program):

1. *Generation of the cylinder model*: by hand, a rough model is generated. It is comprised of circular blocks in which each block is taken to be one turn of DNA wide and one DNA helix plus half the inter helix gap in height. Such approximation overestimates the width of the structure by approximately the 180%.

2. *Generation of the folding path*: after the automatic generation of the

single strand in each row for a given shape there are many putative patterns. The preferred pattern must be chosen by the operator and then hand-designed.

3. *Generation of the first pass design*: automatically the program generates a few staple strands of arbitrary length, usually very long and unusable

4. *Break and modify the staple strands*: in this part of the design, one of the basic principles is that crossovers may be used to hold helices rigidly in a parallel orientation. Because the natural equilibrium length for a single turn of DNA appears to be close to 10.5 base pairs (Wang, 1979) and because DNA backbones are not symmetrically spaced around the helix designs of such two dimensional DNA nanostructures invariably incorporate features that should cause strain. The bases at the end of the helices are highly available for stacking against other DNA origami (Rothemund, 2006). To avoid stacking interactions between adjacent origami and the consequent aggregation, 4T tiles were added to staple strands sequences on the edges of the shape.

### 2.1.2 DNA-Origami in vitro production

The desired set of staple strands was mixed in a 10-fold excess with 1.6nM circular M13mp18 DNA (New England Bioulabs) in a 100$\mu$l volume of 1X Tris-Acetate-EDTA buffer (TAE, 200ml of 50x buffer solution: 48.4g Trizma, 11.42ml acetic acid, 20ml EDTA 0.5M, pH 8.0) added of 12.5mM magnesium acetate and annealed by cooling slowly from 95°C to 25°C in a PCR machine (Eppendorf) at a rate of 0.01°C/second ramp. Annealing products were stored at 4 °C.

#### Origami purification from staples excess and desalting

Purification from the staple strands excess was carried out with different methods, following manufactor instructions for the GenSpin Genomic DNA Purification Kit and the PCR product purification kit (Promega, Madison, Wisconsin). The Amicon Ultra 0.5ml 100kDa (Millipore, Massachussets) where used adjusting the protocol supplied by the constructor. Briefly, 2x TAEM solution was added in the same amount of the sample to reach the 1x TAEM concentration; capped Amicon ultra were centrifuged five times

for 1.5 minutes at 14000·g. Concentrated sample was eluted spinning the inverted filters in a clean vial at 2000·g for 2.5 minutes.

### 2.1.3 Production of long single stranded oligonucleotides

The single stranded DNAs (ssDNA) required for the target and the complementary probe strand were constructed using three different DNA molecules each. Oligonucleotides' sequences are reported from pag.92.

### 2.1.4 *In silico* design of long single stranded oligonucleotides

The sequences were drawn using the program BioEdit and were built using the rules of no self annealing, no loops in the singular sequence, no strong dimers and 50% GC. This general parametres were checked using the open source softwares Oligo Calc and IDT's Oligo Analyzer v.3.1. Exception was made for the target, where the high GC content was required due to the presence of the 20bp GC clamp to enrich the strenght of the complementarity between a partial sequence of the ssDNA probe. The approximate melting temperatures (Tm) were calculated with this rule, valid for sequences longer than 14 nucleotides:

$$\text{Tm} = 64.9°\text{C} + 41 \cdot [(\text{number of GC} - 16.4)/\text{sequence length})]$$

The annealing temperature (Ta) was calculated as follows:

$$\text{Ta} = \text{Tm} - 4°\text{C}.$$

### 2.1.5 Construction of the target and biosensing ssDNAs

Oligonucleotides were reacted with their partial complementary strand in equimolar proportion in a water 10$\mu$M solution containing 2x SSC (0.3 M NaCl, 0.03 M NaCitrate, pH 7,0). The solutions were boiled at 95°C for 3 minutes and then annealed at 70°C for 10 minutes in a thermocyclator and allowed to cool down at room temperature for at least two hours. The samples were run in 1xTAE on a gel electrophoresis with 4x low melting agarose gel (IBI-SHelton).

### 2.1.6 Enzymatic manipulations

*Ligation*

T4 Dna Ligase (Promega) catalyzes the formation of phosphodiester bonds between neighbouring 3'-hydroxil- and 5'-phosphate ends in double stranded DNAs. One unit of T4 DNA Ligase is the amount that joins more than 80% of 1ug RsaI digested Lambda DNA in 30$\mu$l 1x ligation buffer after incubation at 15°C to 25°C. The oligonucleotides (NAMES) were first annealed as previously reported and then ligated using 5U of enzyme each microgram of construct. The reaction was carried out in water solution, adding the 10x incubation buffer from the supplier to 1x concentration. Reactions were let occur at 15°C over night.

*Exonuclease digestion*

Lambda Exonuclease is an exodeoxyribonuclease which preferentially degrades the 5'-phosphorylated strand of double-stranded DNA and catalyzes the stepwise and processive hydrolysis of duplex DNA from 5'-phosphoryl termini liberating 5' mononucleotides. Lambda Exonuclease does not degrade 5'-hydroxyl termini. One unit of the enzyme catalyzes the production of 10nmol of acid-soluble product from double-stranded DNA containing a single 5' terminal phosphate in 30 min at 37°C. The digestion was made in a water solution using 10x incubation buffer supplied with the enzyme to 1x concentration and using 6U of enzyme each 2$\mu$g of dsDNA product with the shorter oligonucleotide modified with a phosporous 5' thermini. Reactions were performed in wather bath at 37°C over night. The digestion products were visualized by a 3% gel electrophoresis.

## 2.2 Nucleic acids visualization

### 2.2.1 Gel electrophoresis

DNA constructs and products were visualized preliminary by agarose gel electrophoresis. Electrophoresis was accomplished using 1xTAE as running buffer. Gels were prepared pouring a 2%, 1%, 0.7% or 0.5% (w/v, Pronadisa) solution in 1xTAE into a suitable gel case and let polymerize for 20-30 minutes. In all cases, gels were previously added of 0.5x Gel RedTM nucleic acid stain (Biotium, Hayward, CA) Running time varied from 60 minutes to 120 minutes, due to the voltage and DNA sizes. DNA ladders were used such as Marker VIII (Roche) and 1kb ladder (Promega). Loading buffer 6x (0.25% xylene cyanil, 0.23% bromophenol blue, 15% Ficoll 400 in water) was loaded with the nucleic acid structures in solution. The electrophoresis results were visualized and photographed under UV light.

### 2.2.2 FRET system

Fluorescence Resonance Energy Transfer (FRET) is a spectroscopic process by which a donor fluorophore transfers energy nonradiatively over long distances to an acceptor fluorophore; the efficiency of FRET and the range of distances over which it can be observed are determined by the spectral properties of the chosen given donor/acceptor pair. In this case the couple 6'-FAM/BHQ-1 was used with a typical Förster radius of 16nm and emitting green light if excited with blue wavelength. To monitor the conformation of the object, the internal and the external disk were functionalized with a FRET couple, substituting oligonucleotide DkD3 with the 6'-FAM labelled DkDFRET and CrI3 with the BHQ-1 labeled CrIFRET; oligonucleotides were purchased HPLC purified from MWG Operon, Ebersberg). The DNA origami were directly monitored with a CCD detector (model AP47p, Apogee) mounted on a fluorescence microscopy (Leitz Orthoplan). Measurements were performed putting 12ul of DNA-origami sample in a home made cell and photographed with personal computer remote control with the software package MaxIm DL after excitation of the sample with a blue led with (an exciting 470nm blue emission and a 517-540nm filter). Led was powered at 3.9V and photographs were taken after 1 second exposure.

### 2.2.3 Transimssion Electron Microscopy

DNA origami samples were adsorbed for 10 minutes onto carbon-coated nickel grids and visualized at 64000x and 102000x magnification with a Philips CM 10 transmission electron microscope operating at 120 kV. No staining or contrast agents were used in order to minimize the perturbations to the origami state.

### 2.2.4 Atomic Force Microscopy

Samples were dispersed on a freshly cleaved mica in saline buffer (125mM MgCl2, 400mM Tris-HCl, 10mM EDTA pH 8.0, 20mM NaCl) The large concentration of positive ions, mainly Mg++ has the functionality of screening the negative charges present at the mica surface and on the external structure of the dsDNA, allowing the adhesion of the origami on the mica surface. Samples were let sediment for at least 5 minutes and were never rinsed or dried. Images have been obtained using either a JPK nanowizard II, a VEECO Multimode with Nanoscope V control or an Asylum MFP3D. All the instruments where operated in liquid in tapping mode. We used Olympus tips OMCL-TR400PSA with force constant of 0.08N/m and resonance frequency, in air of 34kHz.

## 2.3 Nucleic acids operation

All the oligonucleotides sequences interactions were based on the hybridization and complementarity between bases of DNA. With the same principle probes were inserted on the upper face of the origami and, were needed, complemented with their target molecules. In this section the different systems probe-target, probe-targer-competitor are evaluated.

### 2.3.1 Probe-target recognition

Different combination of oligonucleotides for open and close the structure where used. At first two protruding oligonucleotides named Linker Sx and Linker Dx were substituted to DkS3 and DkD4 of the DNA-origami v1. With their sticky ends protruding on the upper face of the object, they were designed for the hybridization with the probe molecule. Different probes long 120 nt were evaluated, starting from completely random sequences to real samples.

### 2.3.2 Linear and hairpined targets

Each probe was designed to be complementary to a target molecule, hybridizing for 84 nt. Two conformation of targets where evaluated for each probe. The hairpin target is composed of the 84nt specific sequence and a 18nt sequence at both 3' and 5' termini made of guanine and cytosine (GC clamp) to guarantee a highly stable hairpined structure. Also linear targets were evaluated, obtained removing the GC clamp.

### 2.3.3 Probe-target mismatch

A target not perfectly complementary to the probe was *in silico* designed and in vitro evaluated. The hairpin target (target mismatch) was complementary to the probe for about 2/3 of the molecule, except for the internal part leaving a mismatch. An oligonucleotide named "competitor" was also designed perfectly complementary to the target molecule. The hybridization starts from the middle part of the target and triggers the complementation of all the molecule. This permits to the competitor to remove the target from the probe. The complementarity of the systems target-competitor and probe-target were previously verified by gel electrophoresis; also the effect

of the adding of the competitor to a stable solution of target and probes was evaluated.

### 2.3.4 Validation with real samples

All test plants were grown in sterilised soil under insect-free conditions. Viruses and phytoplasma strains used in the present study belong to IVV collection.

Original freeze-dried plant material stored at -20 °C of Tobacco Mosaic Virus (TMV- IFA9strain), Tomato Spotted Wilt Virus (TSWV- P105strain) and Iris Yellow Stunt Virus (IYSV- Cip6strain), were mechanically inoculated on *Nicotiana benthamiana*. Freeze-dried leaf tissue was homogenised (1/5 w/v) with 50mM phosphate buffer pH 7 containing 1mM Na-EDTA, 5mM Na-DIECA, 5mM Na-thioglycolate and 50 mg/ml activated charcoal. Inoculum, mortars and buffer were cooled on ice before and during inoculation.

FD isolate was graft propagated and maintained in periwinkle from the original source kindly supplied by E. Boudon-Padieu (Laboratoire de Phytoparasitologie, INRA, Dijon, France).

Total RNA from 0,1 g of symptomatic leaves of N. bentamiana (viruses) and periwinkle (phytoplasma) were extracted using RNeasy Plant Mini Kit (Qiagen, Hilden, Germany) according to the manufactures instruction.

After the extraction, 3 $\mu$l of RNA were added in 120 $\mu$l DNA-origami in solution and visualized as described in paragraph 2.3.4. Each fluorescence value reported is the average of at least 20 independent measurements.

# Chapter 3

# Results

This chapter is divided in six main sections.
First, I present the working principles of a new reusable DNA-based origami designed, built, operated and imaged by several qualitative and quantitative techniques.
Secondly, to ensure that the objects imaged by AFM were actually the DNA-disks and not artifacts of salt on mica surface and to understand the orientation of the disk, the initial version of the design was modified introducing an "IF" motif in the internal disk.
Then I present the results of the experimental work that has been carried out to develop the sensing mechanism of the DNA-origami, obtained by linking a probe on the DNA-Origami i.e. a single stranded molecule that is recognizable by a complementary target molecule.
I also evaluate the results of the addition of a third single stranded molecule that, displace the target from the probe and restore the initial state of the origami.
Finally, another modification to the first DNA origami design was made to have a clear response to ssDNA targets; the results of the switching of modified DNA-origami were used for the device validation with real samples such as viral RNAs.

## 3.1 The project rationale

In recent years, the DNA-Origami technique has lead to many preliminary applications. DNA-based platforms were used to create 3- and 2- dimensional objects (as nanoscale template for protein assembly and for gold nanoparticles) and to create patterns combining different subunits. The versatility of the DNA hybridization between complementary bases made real the possibility to obtain objects with endless shape possibilities as Rothemund and Dietz demonstrated.
The shape chosen for this work was a isodiametric disk composed by two main subunits: a rounded internal disk connected to an external ring in two, diametrically opposite points. To facilitate this movement some bases of the scaffold strand were leaved uncomplemented in the point of the bending of the flap, to reduce the amount of stretch and constrain. In order to control the DNA origami wings motion, in a more complete design two opposite oligonucleotides of the internal disk were substituted with longer oligomers with sticky ends protruding on the upper face of the disk, on the edges of the two opposite movable wings; this modification allowed the link, in the self-assembly step, of the "probe", a single stranded DNA molecule designed to be 120 nucleotides long with the ends complementary to the above mentioned sticky ends. The single stranded DNA, connected to two edges of the disk, is perpendicular to the axis of constrain. In presence of a hybridizing target molecule, the probe is expected to coil into a double helix that stretched the inner disk forcing the edges to move toward each other. The probe was designed to be perfectly or partially complementary to a hybridizing target molecule, hairpin shaped and named "target", as shown in Figure 3.1Schematic model of the DNA-Origami designed in this work. As represented, the Origami is made of two main subunits, an external stripe (crown) and an internal disk connected in two opposite points to the crown. The flexibility of the internal disk is guaranteed by a four non complemented nucleotide spacer (green lines). On the left: upper and lateral view of a closed DNA-Origami with a non complemented single stranded probe (red). On the right: upper and lateral view of an actuated DNA origami; the probe is complemented to the hairpin target molecule (blue).figure.caption.20. The hybridization between the target and the probe nucleic acids and the consequent double stranded (ds) DNA formation, originates a tensile force on the internal disk changing its conformation by moving the wing edges toward

each other.

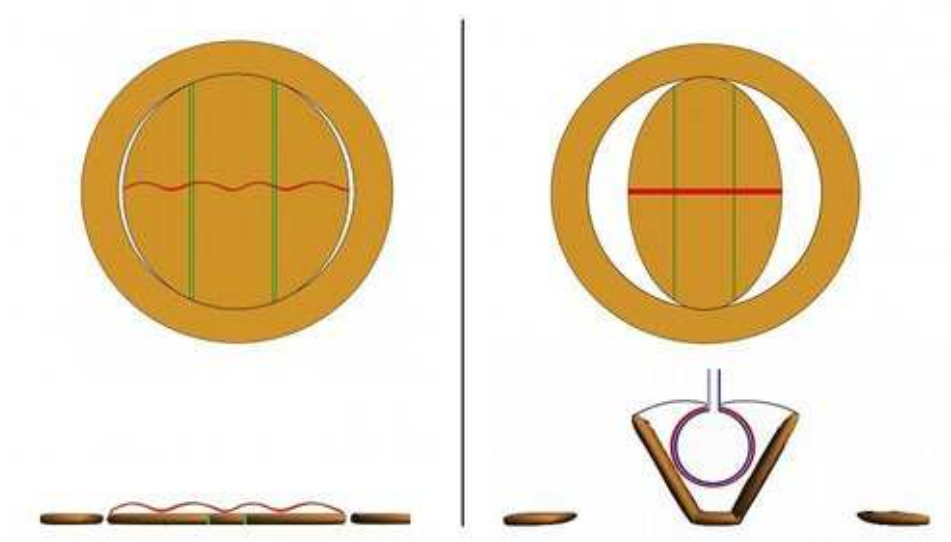

Figure 3.1: Schematic model of the DNA-Origami designed in this work. As represented, the Origami is made of two main subunits, an external stripe (crown) and an internal disk connected in two opposite points to the crown. The flexibility of the internal disk is guaranteed by a four non complemented nucleotide spacer (green lines). On the left: upper and lateral view of a closed DNA-Origami with a non complemented single stranded probe (red). On the right: upper and lateral view of an actuated DNA origami; the probe is complemented to the hairpin target molecule (blue).

To provide a further degree of freedom to the device, a way to make the wing movement reversible was envisaged. The use of probe/target pairs that were not fully complementary allowed a reversible design for the DNA origami actuation. This design implied a first hybridization step between the probe DNA on the DNA origami and a partly complementary target. This hybridization event is subsequently displaced by the addition of an excess of an additional oligonucleotide named “competitor”, that was designed to be perfectly complementary to the target; due to this charcteristic,the competitor is able to displace the target from the hybrid with its partially complementray probe, reverting the DNA Origami to its original state. The concept of the reversible switch is summarized in Figure 3.2Base sequence schematics for the probe/target and target/competitor actuation system. Illustration of the reversible system concept. a and b) The target (harpin) reacts with a probe (red) that complements only on its terminal

parts with the target, leaving a mismatch of 34 nucleotides in the middle of the molecules. This not complemented site remains available for a third DNA molecule involved in the reversible switching process, the competitor (pink). c) The 84 nts competitor is perfectly complementary to the target and, fueled by the free energy of base pair formation and starting from the 34 nucleotides mismatch, triggers the detach between target and probe. This hybridization event target/competitor turns off again the system due to the relaxation of the probe.figure.caption.21.

In figure Figure 3.3The basic principle of the reversible switching mechanism thet I planned. (a) the target (in blue) complements the probe (in red) on the two termini, producing a mismatch of 34 nucleotides. (b) when a competitor (in brown) is added in solution, it complements in its complete length the target removing it from the hybrid with the probe. The system is again in the starting conformation, with the probe as a single strand but with target and competitor in a double stranded conformation, that may eventually be washed away, allowing a further cycle.figure.caption.22 is reported a scheme on the mechanics involved during the opening/closure of the disk; in panel a, the origami switch is closed, the wings lay in the same plane of the external ring and the ssDNA probe is not hybridized. In panel b, the partially complementary target binds to the corresponding sequences of the probe, inducing the wing opening; in panel c, the fully complementary competitor binds to the target dehybridizing the probe: the wings, which are no longer subject to the the tensile force generated by the hybridization, relax to the rest conformation on the plane. Thus the addition of a third single stranded molecule that displaced the target from the probe restored the initial state of the origami.

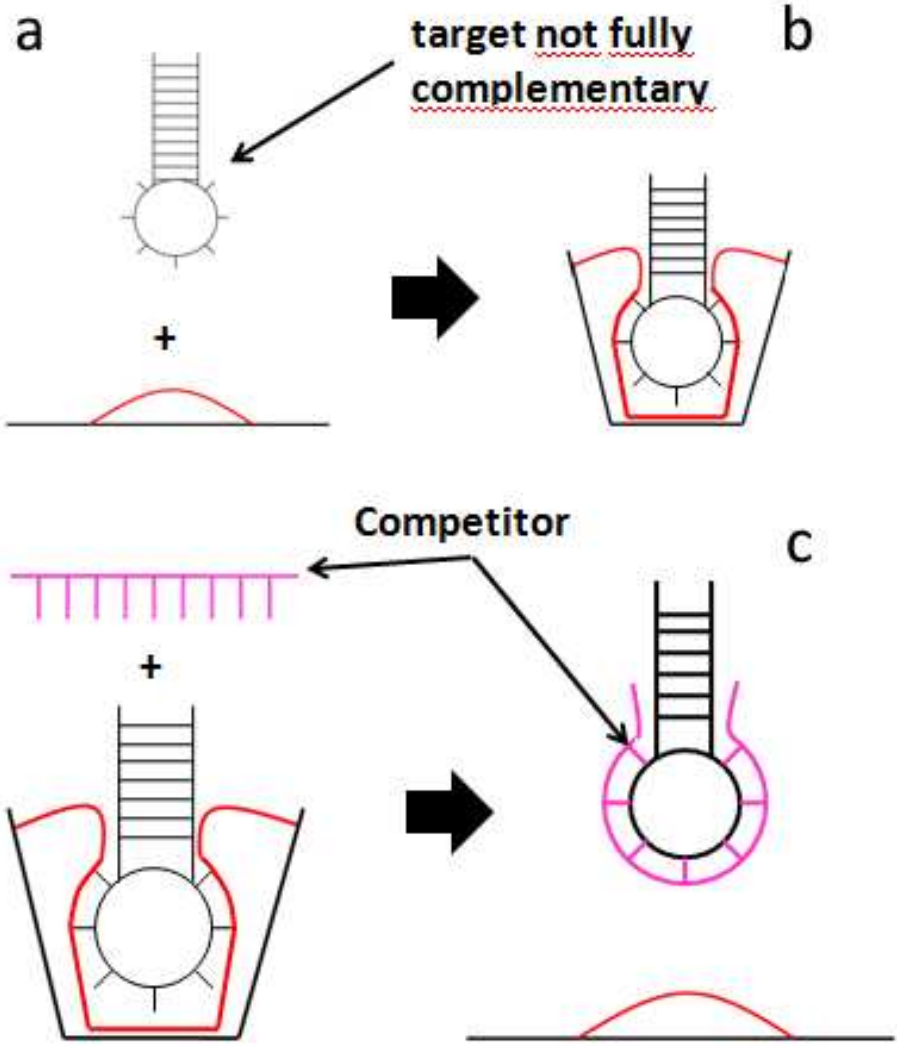


Figure 3.2: Base sequence schematics for the probe/target and target/competitor actuation system. Illustration of the reversible system concept. a and b) The target (harpin) reacts with a probe (red) that complements only on its terminal parts with the target, leaving a mismatch of 34 nucleotides in the middle of the molecules. This not complemented site remains available for a third DNA molecule involved in the reversible switching process, the competitor (pink). c) The 84 nts competitor is perfectly complementary to the target and, fueled by the free energy of base pair formation and starting from the 34 nucleotides mismatch, triggers the detach between target and probe. This hybridization event target/competitor turns off again the system due to the relaxation of the probe.

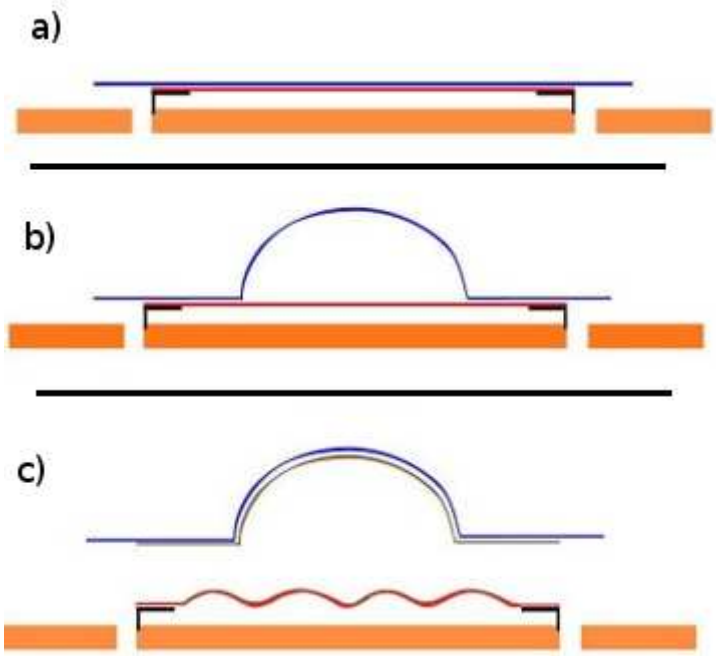


Figure 3.3: The basic principle of the reversible switching mechanism thet I planned. (a) the target (in blue) complements the probe (in red) on the two termini, producing a mismatch of 34 nucleotides. (b) when a competitor (in brown) is added in solution, it complements in its complete length the target removing it from the hybrid with the probe. The system is again in the starting conformation, with the probe as a single strand but with target and competitor in a double stranded conformation, that may eventually be washed away, allowing a further cycle.

## 3.2 *In silico* design of the DNA-origami

Structural DNA nanotechnology has been heavily dependent on the development of dedicated software tools for the design of unique helical junctions, to define unique sticky-ends for tile assembly, and for predicting the products of the self-assembly reaction of multiple DNA strands (Seeman, 1982, Pierce, Winfree). Recently, several dedicated 3D editors for computer-aided design of DNA structures have been developed (Birac *et al.*, 2006, Zhu *et al.*, 2009). However, many of these tools are not efficient for designing DNA origami structures that require the design of more than 200 unique DNA strands to be folded along a scaffold strand into a defined 3D shape (Rothemund, 2006). The recently developed semi-automated DNA origami software packages as SARSE (Andersen *et al.*, 2009) and caDNAno (Douglas *et al.*, 2009) use a 2D sequence editor in conjunction with several automated tools to facilitate the design process. For both programs the use was extended for designing DNA origami structures in 3D. Due to the completeness and versatility of the tools, the best choice was caDNAno. Among the software packages for the DNA origami *in silico* design, the possibility to precise control the turning of staples strands, made caDNAno(SQ) the most suitable for a working DNA-origami. Nevertheless, it was not user friendly: a lot of manual control of the structure was needed and it was difficult to design the right folding path and adjust the structure once definitely designed. The main difficulty was the impossibility to import pre-designed images to be converted in the folding path (as SARSE does) and to modify the path without starting again.

Different paths were evaluated before choosing the most appropriate. The one reported in Figure 3.4Folding path of the DNA-origami v.1. The scaffold strand (in blue) is folded with more than two hundreds of staple strands starting from the first row on the top. The unfolded nucleotides are indicated with a red X on the scaffold. As visible, the folding path resulting from caDNAno does not correspond to the real shape of the object and it is deformed on the x axis. The estimated dimensions of the object are 100nm in length and the same measure in width.figure.caption.23 was the folding path chosen among the others, due to the complete use of the 7249 nucleotides sequence of the scaffold strand and to the theoretical absence of distance between the ring and the central disk. By the AFM observations of Rothemund (2006), the helices are not close packed, revealing gaps be-

tween, tipically 1 or 2 nanometres wide; the position and length follow the pattern of crossovers in the underlying structure. Wherever two helices have a crossover, no gap is observed; a few nanometers away from a crossover, an inter-helix gap is observed. The interhelix gap appears to be an important aspect of DNA nanostructures constructed from parallel helices, and this approximation was suggested:: the length of the structure should be 2h+(h-1)g nm where h is the number of 2 nm wide helices and g is the inter-helix gap. Lengths measured by AFM are typically within 5% for the length and 10% for the width predicted by this formula. In the design of this project, the gaps are about every 16 nt (1.5 turns, approximately 1nm) so the estimated dimensions are:

length: 2h+(h-1)g = 2·34+(34-1)·1nm = 101nm ± 5,05nm
width: (39 blocks of 8nt)·0.34nm = 312·0.34nm = 106nm ± 10.6nm

To gain a preliminary qualitative information about what happened during the annealing process, the assembly results of the DNA origami were run on a standard agarose gel GelRed stained and imaged under UV light. The migration profile shown in Figure 3.5Standard agarose gel electrophoresis of the DNA-origami. The migration profile in lane 3, suggests an efficient formation of constructs, revealed by the sharp band besides the band corresponding to the excess of staple strands. If compared with M13mp18 (lane 2, arrow b), the annealing mixture migrates slower. Lane 1: 1kb DNA ladder.figure.caption.24, suggests an efficient formation of some constructs: in lane 3, besides the band corresponding to the excess of staple strands there is only a single sharp band (arrow a) in the DNA Origami sample, migrating slower than the M13mp18 viral genome (lane 2), used as control. This analysis revealed only that an object(s) of a higher molecular weight if compared to the control was formed during the process, but provided no informations about dimensions, shapes and correctness of the expected folding.

Because of the rough qualitative information of the agarose gel analysis, to understand the real shapes and dimensions, microscopy imaging techniques were required.

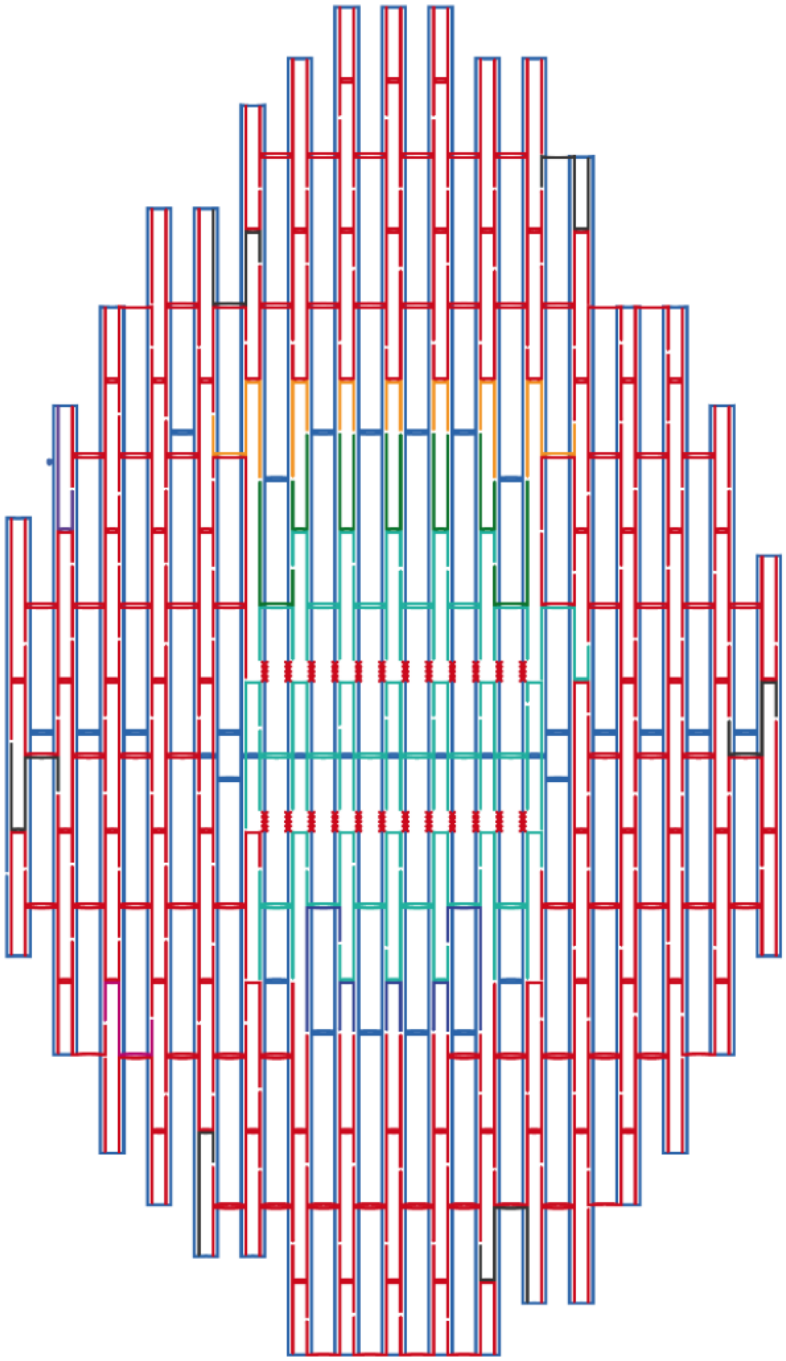

Figure 3.4: Folding path of the DNA-origami v.1. The scaffold strand (in blue) is folded with more than two hundreds of staple strands starting from the first row on the top. The unfolded nucleotides are indicated with a red X on the scaffold. As visible, the folding path resulting from caDNAno does not correspond to the real shape of the object and it is deformed on the x axis. The estimated dimensions of the object are 100nm in length and the same measure in width.

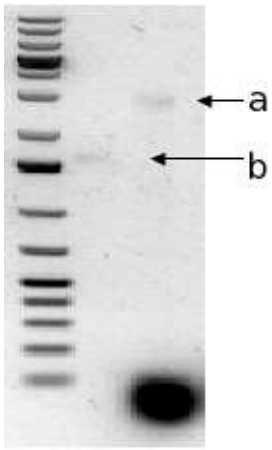


Figure 3.5: Standard agarose gel electrophoresis of the DNA-origami. The migration profile in lane 3, suggests an efficient formation of constructs, revealed by the sharp band besides the band corresponding to the excess of staple strands. If compared with M13mp18 (lane 2, arrow b), the annealing mixture migrates slower. Lane 1: 1kb DNA ladder.

*TEM imaging*

To gain more information about the shape, the sample was prepared for Transmission Electron Microscopy (TEM) dropping the solution containing the DNA origami on a carbon-coated grid and letting it dry. TEM imaging was performed with and without contrast agent. As clearly visible compairing Figure 3.6TEM images of closed DNA-origami visualized without the use of contrast agent. Images are clearer and not packed.figure.caption.25 and Figure 3.7TEM images of a close DNA-origami visualized using contrast agent. A weaker difference of density between the internal part and the external crown can be appreciated.figure.caption.26, the use of contrast agent makes the images darker and dirtier. As reported in Figure 3.6TEM images of closed DNA-origami visualized without the use of contrast agent. Images are clearer and not packed.figure.caption.25 the impurity problems were definitely imputed to the contrast agent.

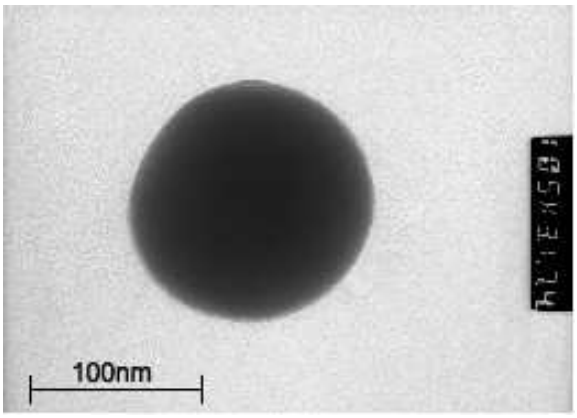


Figure 3.6: TEM images of closed DNA-origami visualized without the use of contrast agent. Images are clearer and not packed.

In some images is possible to appreciate a difference of density comparing the internal part to the external crown (Figure 3.7TEM images of a close DNA-origami visualized using contrast agent. A weaker difference of density between the internal part and the external crown can be appreciated.figure.caption.26).

This imaging technique provided us a measure of the real dimension of the object. No informations were given about the height of the object. The closed state of the DNA-based disk was perfectly characterized, and

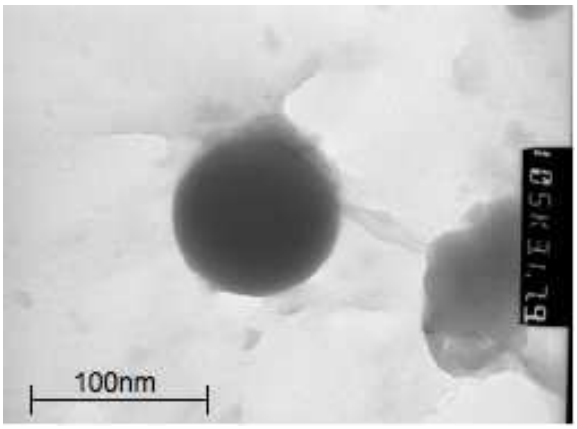


Figure 3.7: TEM images of a close DNA-origami visualized using contrast agent. A weaker difference of density between the internal part and the external crown can be appreciated.

described by the diameter of approximately 100nm. TEM imaging appears to confirm that the DNA origami folding occurred correctly, revealing the expected shape and dimensions. No information were provided about object heights and the resolution was not sufficient to investigate double helices; for these reasons investigations in liquid with AFM technique were performed.

*AFM imaging*

To further investigate the structural conformation of the origamis, atomic force microscopy (AFM) was used to characterize the samples. Up to 2000 DNA origami were evaluated and mainly origami with average diameter of 97 ± 6 nm and average height of 2.1±0.2 nm were observed, suggesting that there was no formation of double layers between different disks and confirming the results of TEM imaging (Figure 3.8Example of an AFM image of a well formed DNA-origami. The profile analysis (left) confirms the diametre of nearly 100nm and the expected height of 2nm (right).figure.caption.27) for what concernes shape and dimensions.

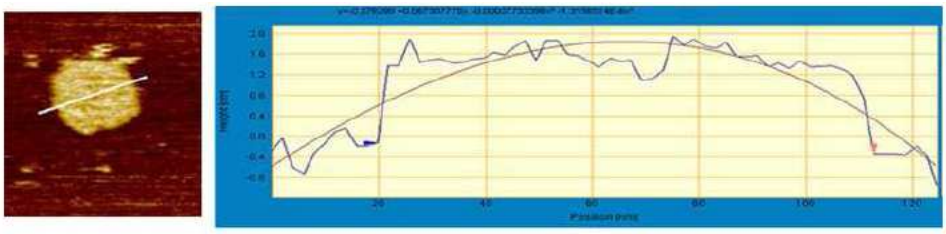

Figure 3.8: Example of an AFM image of a well formed DNA-origami. The profile analysis (left) confirms the diametre of nearly 100nm and the expected height of 2nm (right).

However, in the first design a significant portion of origami appeared to be connected on their side, in big clusters. As AFM imaging demonstrated, stacking interactions were a critical parameter and revealed to be quite strong; disks which had many blunt ends along the edges stacked so strongly that they formed big clusters (Figure 3.9Example of an AFM image of DNA-origami with blunt ends interactions, resulting in disks connected one to each other.figure.caption.28). This characteristic is highly undesirable: the presence of big clusters of many origami means the impossibility to impose direction of linkage or adhesion to a surface in a predetermined place, precluding the way to the precise delivery of the object in a featured place of a surface with a predetermined orientation. To prevent this aggregation the insertion of T-tails was required to prevent stacking and clustering between origami groups. After the introduction of this variation the clusters mainly disappeared (Figure 3.10Example of an AFM image of DNA-origami without blunt ends interactions, resulting in disks detached

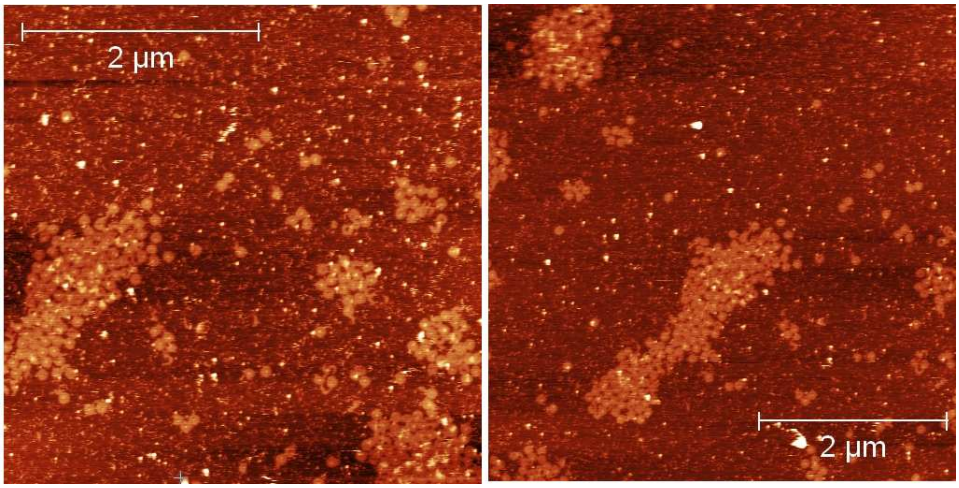


Figure 3.9: Example of an AFM image of DNA-origami with blunt ends interactions, resulting in disks connected one to each other.

one to each other.figure.caption.29), while some non frequent interaction between edges of couples of DNA origami remained.

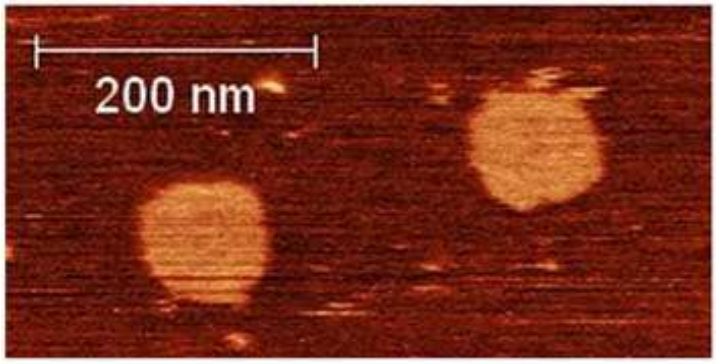


Figure 3.10: Example of an AFM image of DNA-origami without blunt ends interactions, resulting in disks detached one to each other.

AFM analysis permitted better understanding of the efficiency of the origami formation, information missed in TEM imaging due to the low number of origami adhered to the carbon coated grid and, as explained in the above paragraphs, not allowed in gel electrophoresis. An analysis on more than 2200 nanostructures revealed that 75±2% of the disks adopted the designed circular shape while 25±2% of the disks were incomplete, missing often the internal disk, the external ring, showing holes or, more general defects, as showns in Figure 3.11AFM image that shows some DNA origami

with defects and holes and, on the left, the correspondent profile of the holed structure. The distance between the blue and red markers is 37.17 nm, corresponding to the missing inner disk.figure.caption.30.

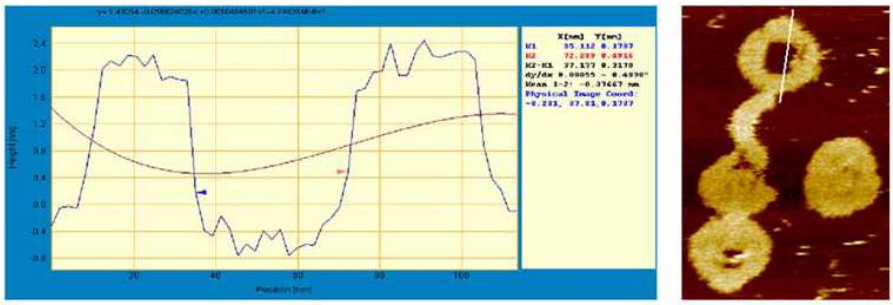

Figure 3.11: AFM image that shows some DNA origami with defects and holes and, on the left, the correspondent profile of the holed structure. The distance between the blue and red markers is 37.17 nm, corresponding to the missing inner disk.

The main defects can be imputable to a sub–optimal annealing process, evident especially in the weakness of the bridge in the two diametrical opposite connections between the internal disk and the crown compromising the presence of the inner disk. As represented, a little number structures appear to be just fragments of the crown. Of incidental interest, various defects can be justified by tip damage, especially when a structure was imaged more than once in an attempt to get images at high resolution. Some DNA-origami showed severe damages.
From the profile analysis of some incompletely formed origami it was found that the formed part had a height resulted to be of the right height (2nm) and the diameter of the joint disk is of nearly 37.2 nm, in complete accord with the *in silico* design.

## 3.3 The "IF" Origami

In addition to shape analysis, one of the main issues of the imaging is to determine the DNA-origami disk orientation when it is dispersed on a surface such as mica. The disk is designed to have two faces, on upper layer exposing the probe and a bottom layer, without functionalization for target recognition. Therefore, exposing a DNA origami to a target solution allowed the disk to adhere to the support, means that the origami can open or not depending on which surface is exposed after adhesion. In the DNA-origami v.1, the two faces of the origami in the initial design were indistinguishable. Therefore it was planned to insert an asymmetric shape in the disks to understand unequivocally the orientation. Origami v.1 was slightly modified in the central disk in order to obtain an hole F-shaped and a prominence I-shaped made of a second layer of DNA, obtaining an origami that was called the "IF origami" (Figure 3.12IF origami scheme. On the left is possible to see the correct orientation of the "IF origami", exposing the two letters to the observer. If the adhesion to mica occurs upside down, the F is not readable and in accord to the first version of the origami, the probe is not exposed to the solution.figure.caption.31).

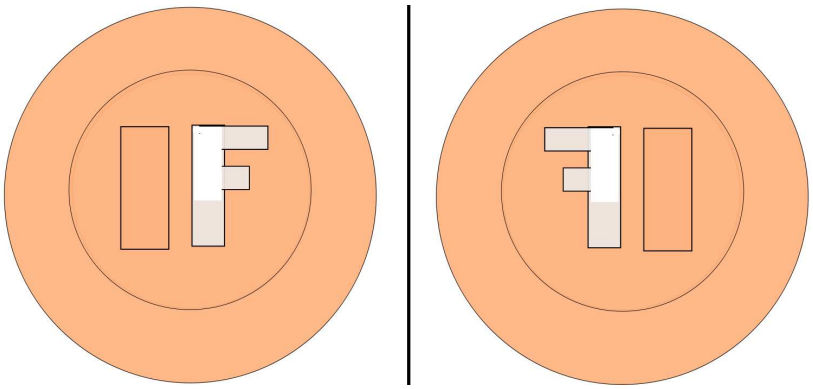

Figure 3.12: IF origami scheme. On the left is possible to see the correct orientation of the "IF origami", exposing the two letters to the observer. If the adhesion to mica occurs upside down, the F is not readable and in accord to the first version of the origami, the probe is not exposed to the solution.

The new folding path (Figure 3.13IF origami folding path. In this folding path is clearly visible the modification of the internal disk with a hole and an upper layer forming a "I". This design results expected to be a higher "I" near the long side of the "F" hole.figure.caption.32) was designed inserting

different crossovers on the edge of the internal disks, removing part of the scaffold strand to create the "F" hole and adding the removed M13mp18 nucleotides to a second layer, protruding from the internal disk near the F, originating the "I"; finally, the wings motion was blocked adding longer oligonucleotides linking the external crown to the internal disk. According to the design, when adhesion to mica occurs on the bottom of the IF origami the two letters have to be visible (and correspondently, the probe is exposed). On the contrary when the "F" is not readable for it's asymmetrical proprieties (the two images cannot be superimposed by rotation) and the position of the I, the origami is adhered on its top.

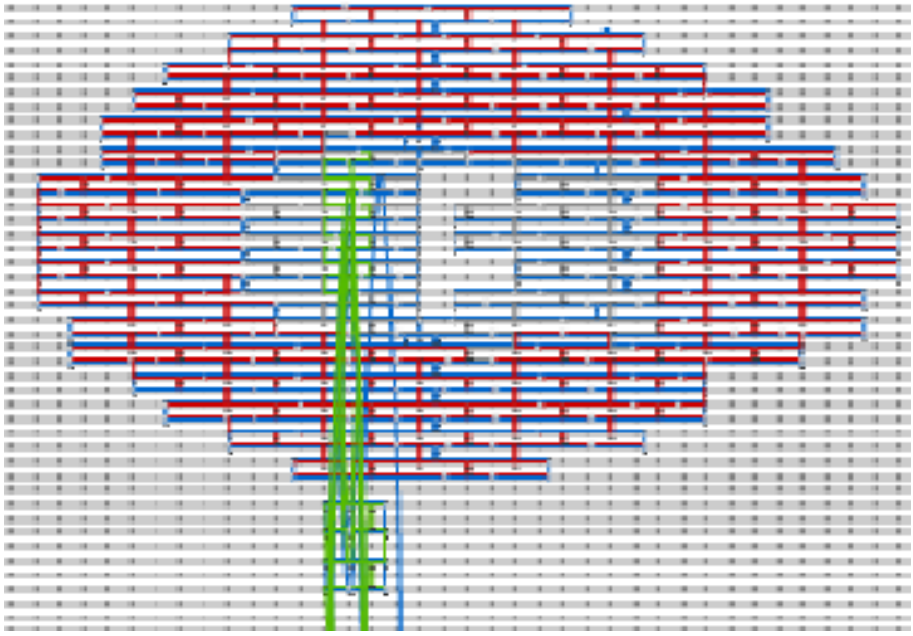

Figure 3.13: IF origami folding path. In this folding path is clearly visible the modification of the internal disk with a hole and an upper layer forming a "I". This design results expected to be a higher "I" near the long side of the "F" hole.

In liquid evaluation of the disks with AFM permitted the analysis of the dimensions of the new objects, confirmed the expected diameter of 100nm of the complete disk. The F hole in the design was estimated to be 20nm on the long side and 10nm on the short. However with a width of 4 nm (Figure 3.14IF origami 3D prototype. In this image are reported all the espected measures of the two letters inserted in and on the internal

disk.figure.caption.33) problems occurred in the imaging, likely due to the very small hole dimensions. In many images was never possible to see with high resolution the "F" hole. On the contrary the I was well characterized (Figure 3.15Two AFM images of the "IF" DNA origami.The higher part in the middle of the structure in both images is distinguishable but the "F" hole is not visible.figure.caption.34).

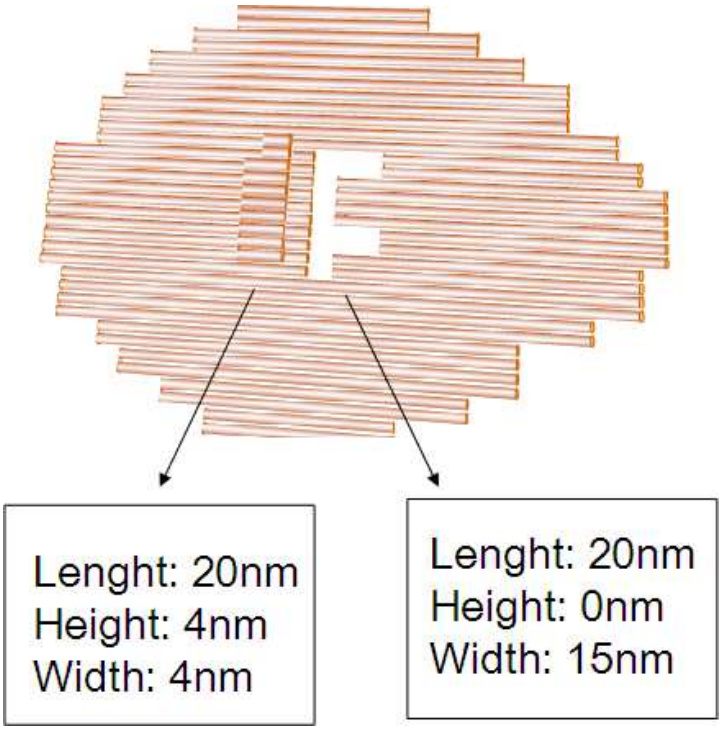


Figure 3.14: IF origami 3D prototype. In this image are reported all the espected measures of the two letters inserted in and on the internal disk.

The use of sharp tips, allowed to gain images with high resolution the higher layer of double helices of the I object and also the presence of the F hole (Figure 3.16a) AFM image of "F" origami and (b) a zoomed detail of the same image (50nm scale bar). (c) AFM image of an "F" origami in which the hole is visible (100nm scale bar) and (f and g) two profile lines with the dimensions of the hole in two directions: (f) is referred to (d); (g) is referred to (e). Note that the length of the hole is 19.8 nm and the width is 15.7 nm with a hole depth around at 1.5 nm (the blue and red markers in f and g), that compare well with the dimension calculated

from the *in silico* model.figure.caption.35) were appreciated. In this image the IF origami image presents a blurred "F" hole and, depending on the relief position, the DNA origami seems to be faced down. In this case, there was no sufficient resolution to clearly discriminate the two "F" holes, but it is possible to see two main holes, one perpendicular to the I, observation confirmed by the analysis of the profiles showing length and width of the object (Figure 3.16a) AFM image of "F" origami and (b) a zoomed detail of the same image (50nm scale bar). (c) AFM image of an "F" origami in which the hole is visible (100nm scale bar) and (f and g) two profile lines with the dimensions of the hole in two directions: (f) is referred to (d); (g) is referred to (e). Note that the length of the hole is 19.8 nm and the width is 15.7 nm with a hole depth around at 1.5 nm (the blue and red markers in f and g), that compare well with the dimension calculated from the *in silico* model.figure.caption.35, panels f and g).

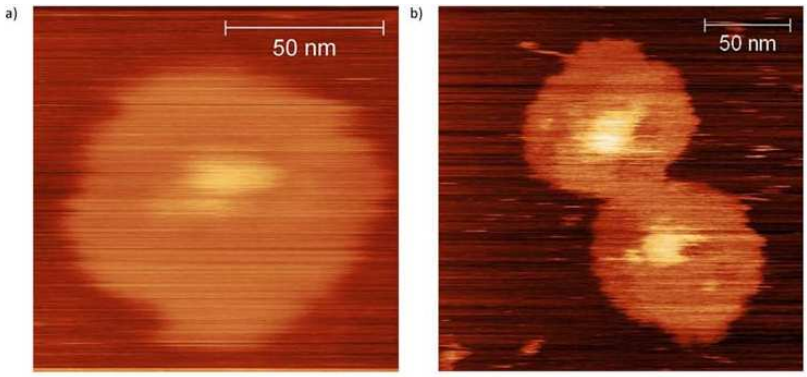


Figure 3.15: Two AFM images of the "IF" DNA origami.The higher part in the middle of the structure in both images is distinguishable but the "F" hole is not visible.

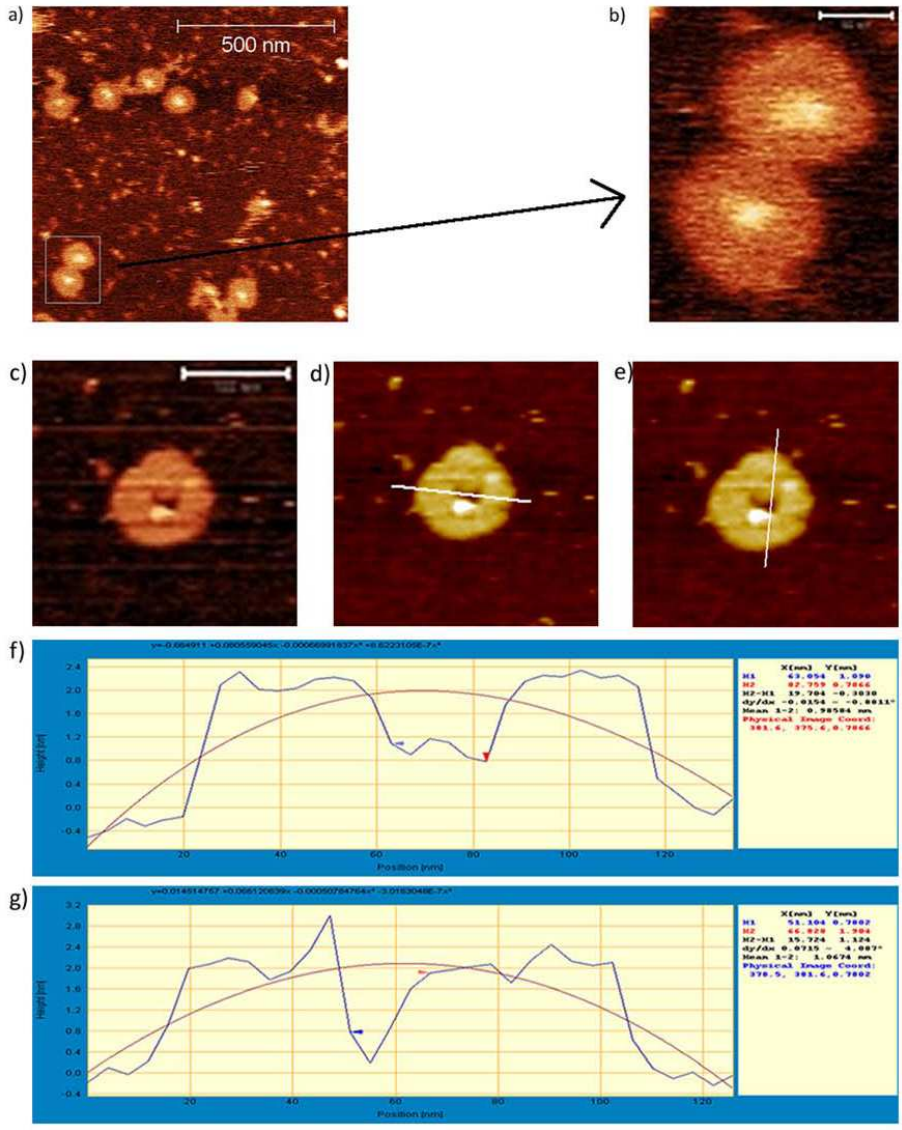


Figure 3.16: a) AFM image of "F" origami and (b) a zoomed detail of the same image (50nm scale bar). (c) AFM image of an "F" origami in which the hole is visible (100nm scale bar) and (f and g) two profile lines with the dimensions of the hole in two directions: (f) is referred to (d); (g) is referred to (e). Note that the length of the hole is 19.8 nm and the width is 15.7 nm with a hole depth around at 1.5 nm (the blue and red markers in f and g), that compare well with the dimension calculated from the *in silico* model.

## 3.4 The actuation

A major task of this project was to confer to the origami the ability to switch in response to the recognition of a probe linked by hybridization to the internal disk of the origami by target molecule in solution. To link the probe to the internal disk of the origami, two staples strands on the wings in opposite positions were substituted with other two oligonucleotides with protruding sticky-ends on the upper face of the object. This modification was need to link by hybridization the probe in the annealing phase of the objects' construction. In the following paragraphs I present the results on the production of long single stranded and double stranded nucleic acids and the demonstration of their capability of switching.

### 3.4.1 Production of long DNA strands

Long double stranded DNAs were in a first time obtained after a annealing step, enzimatic digestion and then purification by column. Due to the low reproducibility of the procedure, the number of intermediates and the time consuming steps, this oligonucleotides were ordered and purchased chemically synthesized.

## 3.5 Imaging the actuation

The actuation of the origami v.1 was imaged using several techniques: standard gel electrophoresis, Transmission Electron Microscopy and Atomic Force microscopy.

### 3.5.1 Gel electrophoresis and TEM

Addition of the target ssDNA molecule the DNA-origami sample was expected to produce a conformation variation in the internal disk spatial disposition (Figure 3.2Base sequence schematics for the probe/target and target/competitor actuation system. Illustration of the reversible system concept. a and b) The target (harpin) reacts with a probe (red) that complements only on its terminal parts with the target, leaving a mismatch of 34 nucleotides in the middle of the molecules. This not complemented site remains available for a third DNA molecule involved in the reversible switching process, the competitor (pink). c) The 84 nts competitor is perfectly complementary to the target and, fueled by the free energy of base pair formation and starting from the 34 nucleotides mismatch, triggers the detach between target and probe. This hybridization event target/competitor turns off again the system due to the relaxation of the probe.figure.caption.21). This variation was at first investigated with standard gel electrophoresis, giving no result. As demonstrated by Figure 3.17Migration profile of open DNA-origami. The closed (lane 1) and the presumedly opened objects (lane 2) present the same migration profile suggesting two hypothesis: the objects do not open or the screening via gel electrophoresis is not enough informative.figure.caption.36 the migration profile between the not actuated (lane 1) and the actuated object (lane 2) is the same and the variation of conformation is not sufficient to produce a variation in mobility the gel. To determine wether or not the objects were opened, also in this phase of the work, microscopy techniques were required to further investigate the dynamics.

Using TEM, a change in conformation of the object after target addiction was was visible but the size detected was 30 nm (Figure 3.18TEM images of open structures. Is visible in both images a change of conformation of the internal disk, as of the dimensions of the object that are nearly a half of the correspondent closed one.figure.caption.37) possibly due

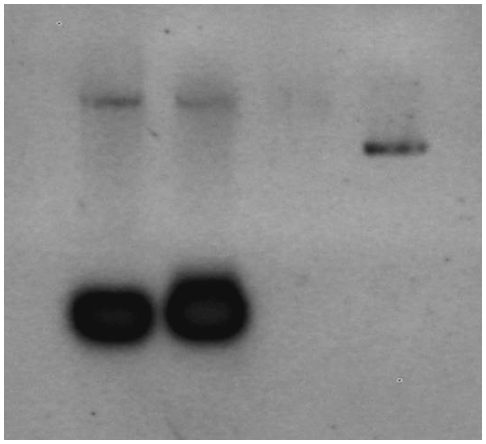

Figure 3.17: Migration profile of open DNA-origami. The closed (lane 1) and the presumedly opened objects (lane 2) present the same migration profile suggesting two hypothesis: the objects do not open or the screening via gel electrophoresis is not enough informative.

to rapid dehydratation of the samples when subjected to high vacuum. The other variation observed was the apparent formation of some holes in the centre of the origami structure; some points of attachment to the crown, presumebly the points of linkage between the two sub-units of the origami are detectable. This result was not completely convincing due to the very small diametre as compared with the closed DNA-origami to obtain a more detailed information the use of AFM resulted necessary.

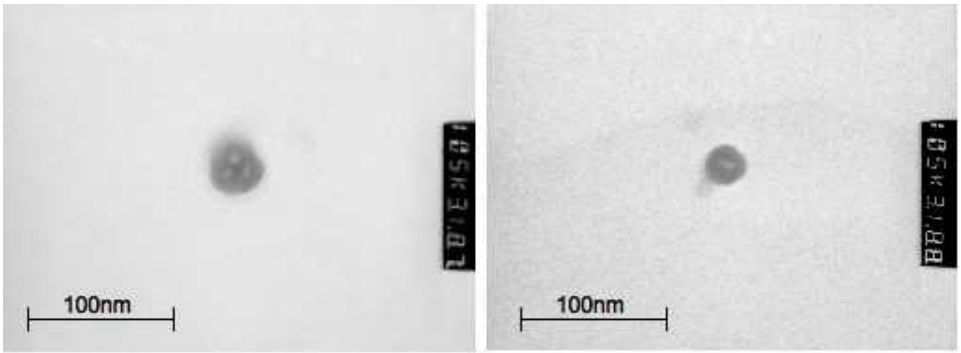


Figure 3.18: TEM images of open structures. Is visible in both images a change of conformation of the internal disk, as of the dimensions of the object that are nearly a half of the correspondent closed one.

### 3.5.2 AFM imaging of open objects

The efficiency of the actuation was investigated, collecting a number of AFM images and counting the number of reacted vs. non reacted origami. Origami actuation may be obtained by adding the target either: after the origami deposition on mica or in solution before the origami is dispersed on the surface. When the single stranded target is added directly in solution, it has higher probability to hybridize with the complementary target because in free solution both faces of the origami are exposed and available to hybridization to the target molecules. On the contrary if the origami is previously adhered to a surface such as mica, the probability for the object to lie face-up exposing the probe to the solution is reduced by about the 50%. For this reason, the probability to see DNA origami opened when previously adsorbed on mica is lower than imaging samples complemented in free solution. When the target was added to origami suspended in solution, a percentage of the structures extimated to be of 86±6%, reacted with the target with the consequent change of conformation of the DNA-based disk. When the origami was deposited on the substrate and then exposed to the target solution, 48±15% of the origami were opened. Therefore the actuation force is large enough to overcome the electrostatic and Van der Walls interaction with the substrate. Figure 3.19Effect of target addition on origami previously adhered on mica and observed by AFM imaging. The object presents a particular pattern of the internal disk, showing a drammatically change of conformation due to the actuation. (a) and (b) Representative AFM images of the DNA origami opened, with (c) a zoomed detail of the structure used for the profiles analysis. In (f) is shown the profile for the line in (d): the two apertures that are distant  34 nm, while in (g) is shown the profile for the line in (e): the length of the "vertical" axe of the aperture is  45 nm, that fits with the *in silico* design.figure.caption.38 shows images and profile analysis performed adding the target to origami directly adhered on the mica. The actuated origami structure appears as having a distinct and characteristic pattern in the middle of the internal disk: a two holes and a stripe of DNA in the middle of the internal disk, coinciding with the axis of constrain.

As confirmed from the profile study, the holes edges are  45nm distant in accord with the internal ring design and the complete width of the aperture in the middle is ∼34 nm. Similar structures are viewed when analyzing DNA

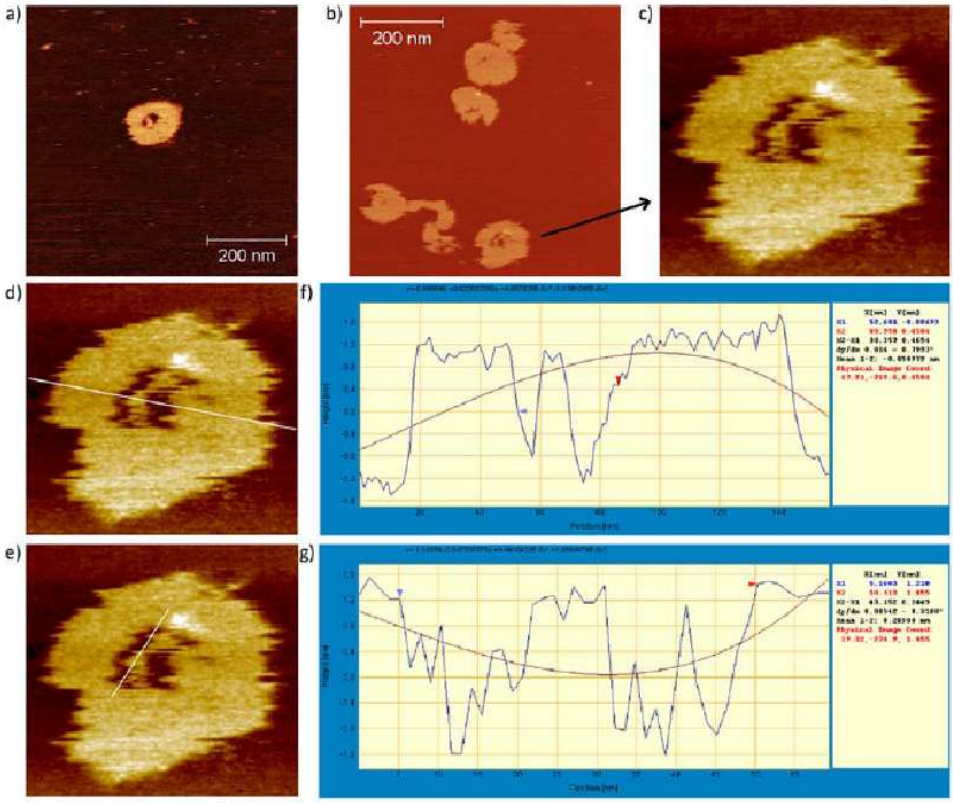


Figure 3.19: Effect of target addition on origami previously adhered on mica and observed by AFM imaging. The object presents a particular pattern of the internal disk, showing a drammatically change of conformation due to the actuation. (a) and (b) Representative AFM images of the DNA origami opened, with (c) a zoomed detail of the structure used for the profiles analysis. In (f) is shown the profile for the line in (d): the two apertures that are distant 34 nm, while in (g) is shown the profile for the line in (e): the length of the "vertical" axe of the aperture is 45 nm, that fits with the *in silico* design.

origami in which opening was induced in solution (Figure 3.20Representative AFM images of the sample with target added in solution. In (a) many open DNA origami, and in (b) an open DNA origami couple. In image (c) is possible to appreciate better the double helix features.figure.caption.39).

Figure 3.21High resolution AFM images of open DNA origami. Are clearly visible the double helix features; in the (b) and (c) images the same object rotated of 90°. In (c) is visible a rotation of the vertical axe (the green lines).figure.caption.40 shows an opened DNA origami in which the DNA double helix feature; in panel c the same image is rotated by

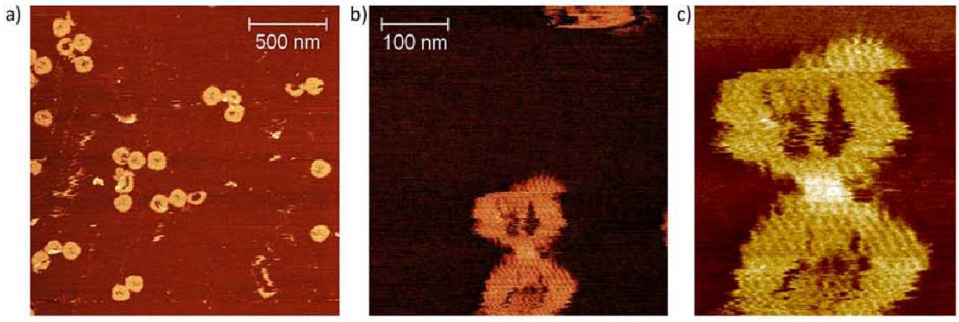


Figure 3.20: Representative AFM images of the sample with target added in solution. In (a) many open DNA origami, and in (b) an open DNA origami couple. In image (c) is possible to appreciate better the double helix features.

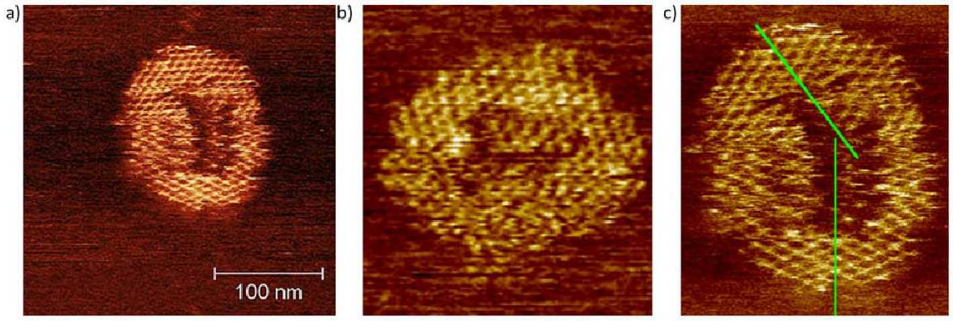


Figure 3.21: High resolution AFM images of open DNA origami. Are clearly visible the double helix features; in the (b) and (c) images the same object rotated of 90°. In (c) is visible a rotation of the vertical axe (the green lines).

90°to better show the characteristic honeycomb pattern obtained from DNA crossovers. From the profile shown in Figure 3.22AFM image of an open DNA origami and its profile graph: are clearly detectable the dimension of the double helix intervals: 1.2 nm the height and 15 nm every gap between crossovers.figure.caption.41, more information about the double helix pattern can be obtained. The red and blue markers in the profile highlight the distance between two gaps in the DNA "honeycomb" pattern and every gap represents the length of two crossovers. From the standard design distances, there is a crossover every 1.5 helical turns (16 bp), whereas a turn is 3.5 nm, we should have a crossover every 5.3 nm. From the profile examined in Figure 3.22AFM image of an open DNA origami and its profile graph: are clearly detectable the dimension of the double helix intervals: 1.2 nm the height and 15 nm every gap between crossovers.figure.caption.41, is possible

to evaluate every 15nm a hole and every 7.5 nm a crossover that is quite different from the 5.3 nm of the expected distances from the design.

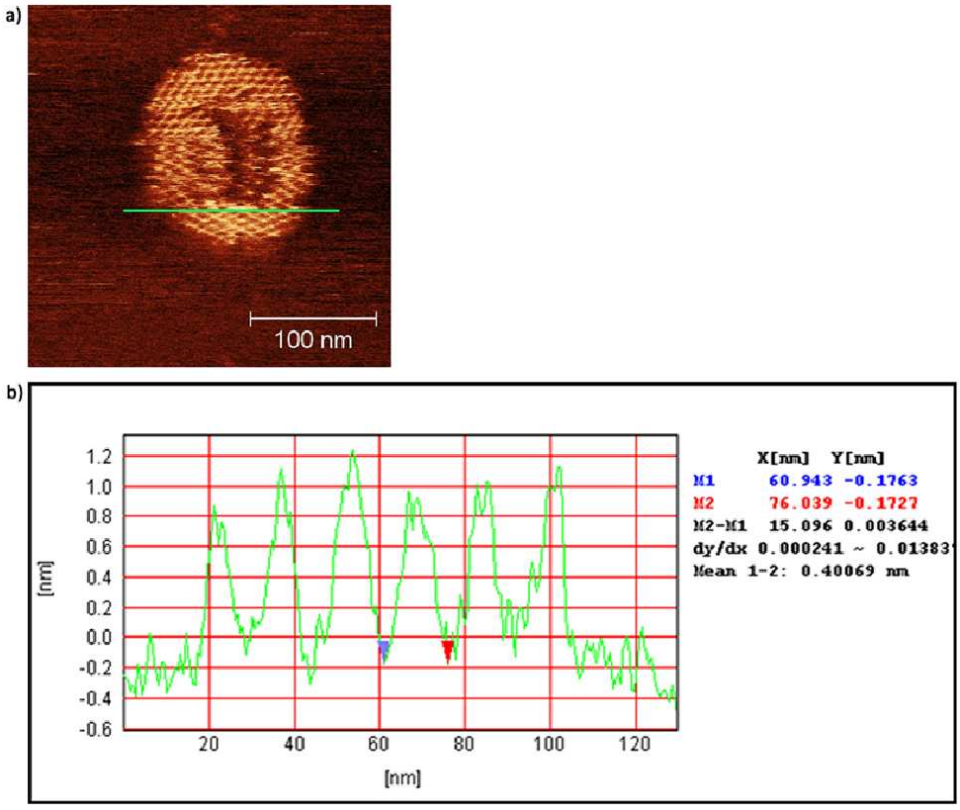


Figure 3.22: AFM image of an open DNA origami and its profile graph: are clearly detectable the dimension of the double helix intervals: 1.2 nm the height and 15 nm every gap between crossovers.

### 3.5.3 FRET assays

A fast and qualitative method to monitor the conformation changes of the DNA origami associated with wings motion that follows target addition, based on the insertion of a Förster resonance energy transfer (FRET) couple in the structure, was introduced in order to monitor the working capability of the system. The DNA origami was provided with a staple strand on the external edge of the internal disk labeled with a fluorophore (6'-FAM), and with an oligonucleotide on the internal edge of the external ring labeled with a quencher (BHQ-1), substituting two oligonucleotides of the origami v.1. In the absence of the target, a low intensity signal was

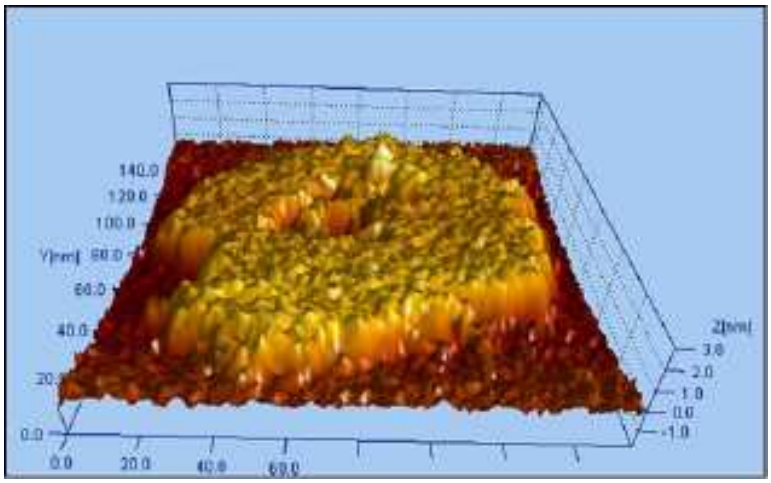


Figure 3.23: A 3D image obtained with SPIP tool of one single DNA origami opened in the middle.

expected, since fluorophore and quencher were located within the Förster radius (approximately 1nm). Conversely, when the wings were constrained following the addition of a probe hybridizing target, the consequent separation resulted in a distance between 6'-FAM and BHQ-1larger than 16 nm, with an expected significant increase of fluorescent signal intensity. As shown in Figure 3.24FRET detection of the origami opening. Fluorescence measurements of the closed disk before (column a) and after (column b) the addition of partially complementary target molecules. (c) emission values after the addition to the closed origami of a non complementary target used as a negative control. The low emission signal of columns a and c are comparable, demonstrating the specificity of the actuationfigure.caption.43, the hypothesis was confirmed by recording of a low signal intensity of the green emitted light revealing a low signal intensity in the non actuatued conformation and (Figure 3.24FRET detection of the origami opening. Fluorescence measurements of the closed disk before (column a) and after (column b) the addition of partially complementary target molecules. (c) emission values after the addition to the closed origami of a non complementary target used as a negative control. The low emission signal of columns a and c are comparable, demonstrating the specificity of the actuationfigure.caption.43 bar a) of a higher intensity signal after the target addition in solution (Figure 3.24FRET detection of the origami opening. Fluorescence measurements of the closed disk before (column a) and after (column b) the addition of

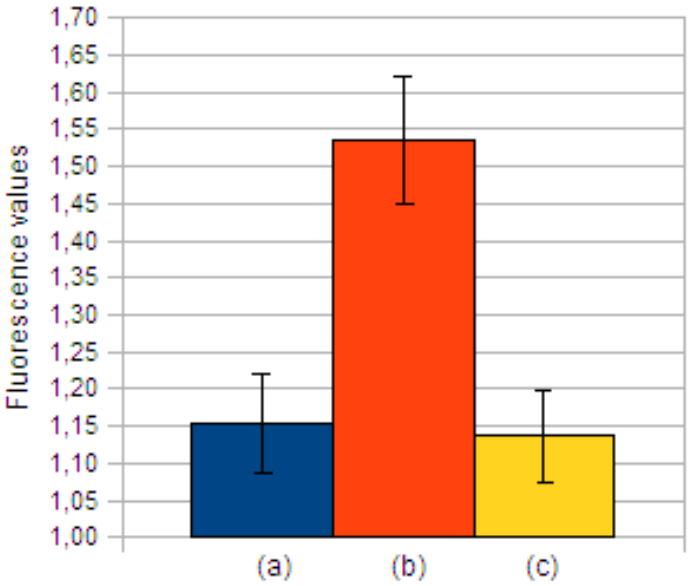


Figure 3.24: FRET detection of the origami opening. Fluorescence measurements of the closed disk before (column a) and after (column b) the addition of partially complementary target molecules. (c) emission values after the addition to the closed origami of a non complementary target used as a negative control. The low emission signal of columns a and c are comparable, demonstrating the specificity of the actuation

partially complementary target molecules. (c) emission values after the addition to the closed origami of a non complementary target used as a negative control. The low emission signal of columns a and c are comparable, demonstrating the specificity of the actuationfigure.caption.43 bar b). No variation in fluorescence intensity was recorded for the controls: when a non-target DNA was added to the origami suspension (bar c in Figure 3.24FRET detection of the origami opening. Fluorescence measurements of the closed disk before (column a) and after (column b) the addition of partially complementary target molecules. (c) emission values after the addition to the closed origami of a non complementary target used as a negative control. The low emission signal of columns a and c are comparable, demonstrating the specificity of the actuationfigure.caption.43) the emitted fluorescence was comparable with that of the initial state.

## 3.6 Revertability of the system

In this phase of the design, the opening system was slightly modified to become reversible so that the origami's nanovalve can be opened and closed more than once. To obtain this variation, a new target molecule was designed inserting a new degree of affinity between the two strands. The target was designed to be not complementary for the 100% of the length of its molecule, leaving in the middle an uncomplemented domain of 34 nucleotides. The new target, in analogy with the previously reported, has the complementary 3' and the 5' termini rich in C-G, creating the described C-G clamp of the hairpin structure. Further another 84 nucleotides single strand named "competitor" was designed, totally complementary to the target. Hybridization between target and competitor is expected to start from the uncomplemented 34 nucleotides; the high affinity between sequences, autonomously triggers the complete hybridization of the 84 nucleotides of the two species. With this mechanism, in absence of the competitor the target binds the probe changing the conformation of the origami, on the contrary when the competitor is added, it displaces the target from the probe and the conformation of the origami is comparable again to the initial state.

The efficiency of displacement and annealing in the case of mismatched strands was preliminarlyevaluated by gel electrophoresis. In Figure 3.25Preliminary gel electrophoresis of target/probe/competitor complementation. in lanes 1-8: molecular maker VIII, lane 2-3 ssDNAs, respectively the target (120nt) and the competitor (84nt). In lane 4 the band represents the annealing product of target and probe and in lane 7 annealing between target and competitor. In lane 5 and 6 two samples of the results of the addition of the competitor molecule in solution; the competitor displaces the target from the probe originating a main band comparable with lane 7.figure.caption.44 in lane 2 as negative control is reported the the target in the single stranded conformation; its hybridization with the probe permits to obtain a double stranded specie represented by a sharp higher band (lane 4). In lane 3 is represented the migration profile of the competitor, coherently migrating more than the probe due to the lower molecular weight. The addition of the competitor molecule to a solution containing only the target (lane 7) reveals a double stranded annealing product. In lanes 5 and 6 the addition of the competitor to a solution containing the partial double stranded specie probe-target mismatch, displaces the probe from the target. Is possible to see in

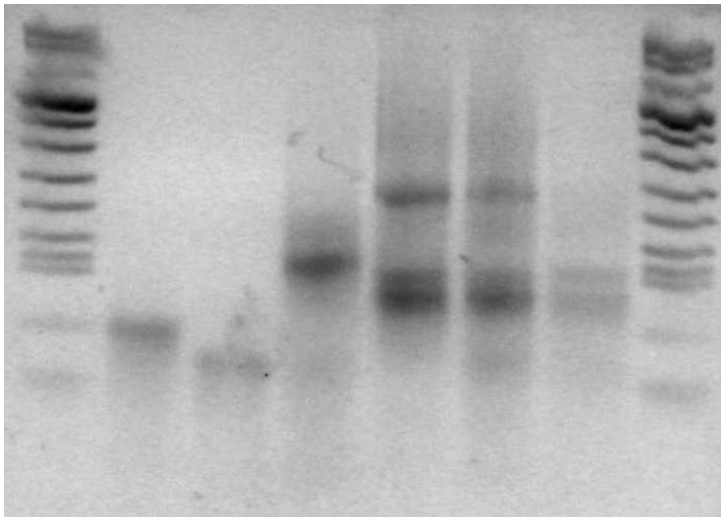

Figure 3.25: Preliminary gel electrophoresis of target/probe/competitor complementation. in lanes 1-8: molecular maker VIII, lane 2-3 ssDNAs, respectively the target (120nt) and the competitor (84nt). In lane 4 the band represents the annealing product of target and probe and in lane 7 annealing between target and competitor. In lane 5 and 6 two samples of the results of the addition of the competitor molecule in solution; the competitor displaces the target from the probe originating a main band comparable with lane 7.

fact a higher band representing a double stranded DNA product and a single stranded molecule comparable with the one of the target. Moreover the migration profile of the double strands probe-target and target-competitor after the displacement are clearly uncomparable, suggesting that strand displacement performs well.

The same experiments were performed allowing the annealing of the above mentioned combination in the origami solution and evaluating the effects of hybridization and displacement using fluorescence responses. Bar b in Figure 3.26FRET detection of the origami reversible opening. FRET measurements of the closed disk before (column a) and after (column b) the addition of partially complementary target molecules. a) with the origami in the closed state fluorophore and quencher are within a Förster radius distance and there is no emission. b) with the origami in the open state, the flourophore and the quencher are moved far away and green light is emitted. In column (c) are represented the emission values of a non complementary target used as a negative control. d) fluorescence values after the addition

of the competitor and (e) after the addition of a competitor non complementary to the target. The low emission signal of columns a, c and e are comparable, demonstrating the reversibility of the system.figure.caption.45 shows the increase in fluorescence intensity recorded after the addition of a target partially complementary to the origami probe. Moreover, following further addition of a competitor to the suspension of reacted origami, the fluorescence intensity returned, within the experimental error, to the initial value (column d), proving that the origami configuration was reverted. Parallel assays carried out with a competitor that was non-complementary to the target produced no changes in fluorescence.

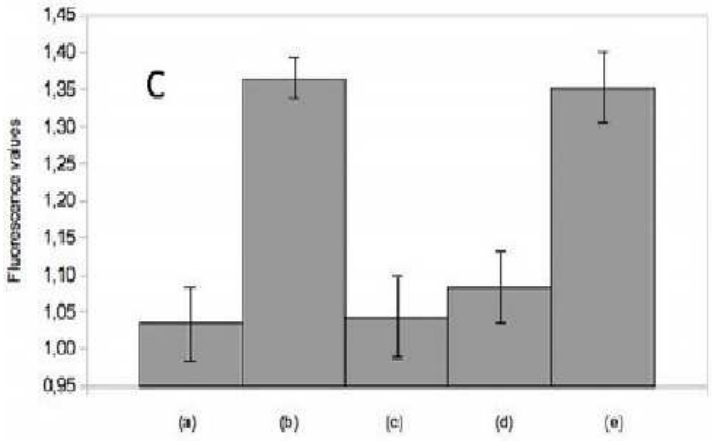


Figure 3.26: FRET detection of the origami reversible opening. FRET measurements of the closed disk before (column a) and after (column b) the addition of partially complementary target molecules. a) with the origami in the closed state fluorophore and quencher are within a Förster radius distance and there is no emission. b) with the origami in the open state, the flourophore and the quencher are moved far away and green light is emitted. In column (c) are represented the emission values of a non complementary target used as a negative control. d) fluorescence values after the addition of the competitor and (e) after the addition of a competitor non complementary to the target. The low emission signal of columns a, c and e are comparable, demonstrating the reversibility of the system.

To have more data, AFM imaging was performed and the opened or closed origami were checked. The comparison of the images showed a great similarity with the one taken for DNA origami v.1, as visible in Figure **??** made us believe that also a non completely complementary target in the middle of the sequence can activate the origami nanovalve as well as a perfectly complementary structure.

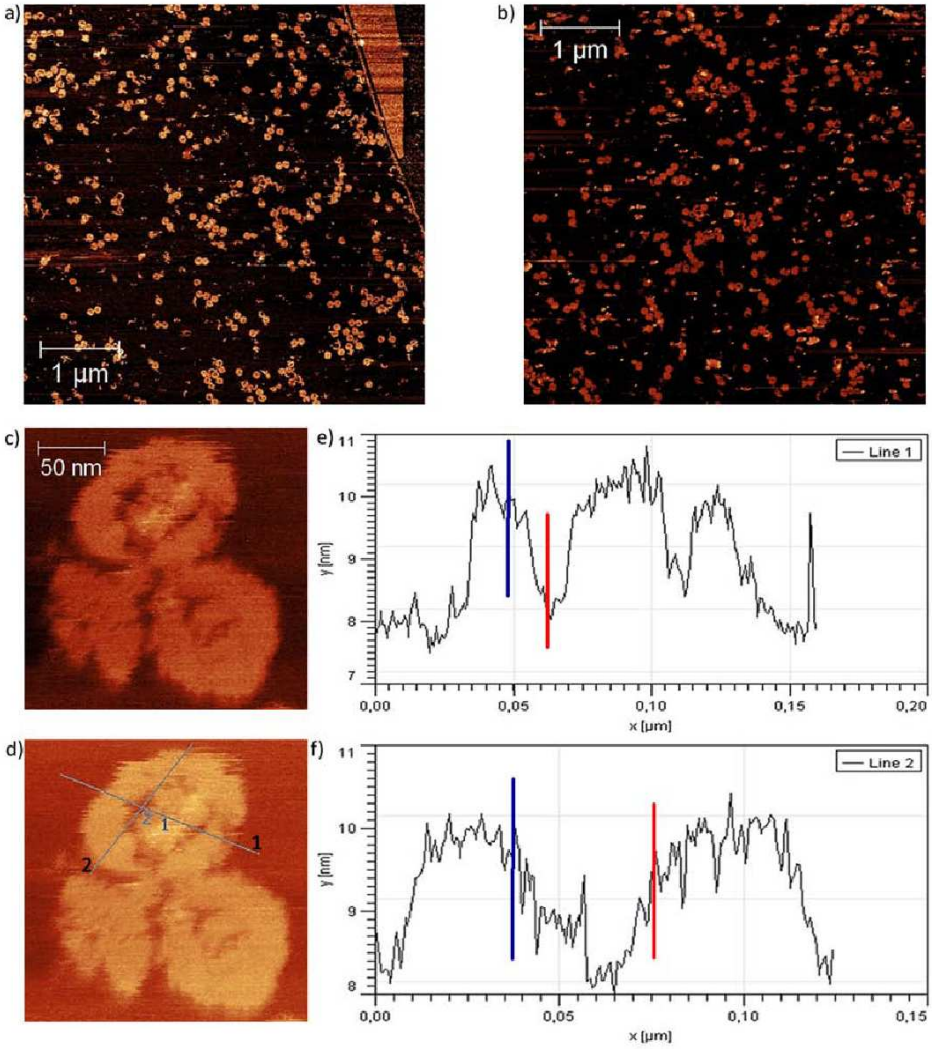


Figure 3.27: (a),(b) Two representative AFM images of the sample with the second type of target added directly on the mica, in which we can see DNA origami close and open. (c) A zoomed AFM image of two open structures. (e) and (f) Two profiles referred to the lines shown in (d). Note the height of the structure: 2 nm, and the length of the aperture in line 2: 38 nm, that is similar to the previous DNA origami imaged.

## 3.7 Actuation with linear targets

As preliminary work before improve the functionality of the origami with viral RNAs extracted from plants, were performed some experiments with the correspondent single stranded oligonucleotide target molecule. The nucleotides sequence was obtained by removing the GC clamp from the previously described targets and the sequence was ordered and chemically synthesized. In a first design, the probe linked on the DNA origami was complementary to a conserved portion of the RNA sequence of the Tobacco Mosaic Virus. The effects of the addition of the linear target are reported in the hystogram of Figure 3.28Validation of the origami version 1 with single stranded DNAs. In bar a, the closed DNA-origami in bar d the opened object and in bar e the negative control with a non target sequence; the data obtained are coherent with the data reported for the previous results. In column b is reported the fluorescence values of an object opened with a linear ss target DNA and in column c the negative control (non complementary linear target); the fluorescence values are not comparable with the one obtained with the clamp target.figure.caption.47. The same experiment was performed also with the hairpin-shaped targets, to have a comparison between the fluorescence values obtained.

As visible in bars b and d the fluorescence intensity emitted from the origami after the addition of a clamp target (bar b) or the correspondent linear target molecule (bar d) are not comparable; in the first case the results are comparable with the ones obtained in the previously reported experiments where coherently the environmental signal actuate the DNA-based object. In the case of the single stranded DNAs the fluorescence emitted is higher than all the negative controls (bars a, c, e) confirming the hypotesis that the object opens the wings also without the G–C clamp in the molecule of interest. Among this the signal is too low to be compared with the unambiguously increase of fluorescence of bar b so to enhance this preliminar result and to ensure the comparison between the actuation performed by single stranded and hairpined targets, a structural modification of the origami's v.1 was carried out. In Figure 3.29Folding path of the DNA-origami used for single stranded DNAs or RNAs detection.figure.caption.48 is reported a scheme of the modified origami v.1. In fact on the left of the internal disk, the edge was firmly connected with the external ring closing one of the two wings; on the other hand the axis of constrains (represented in green) was

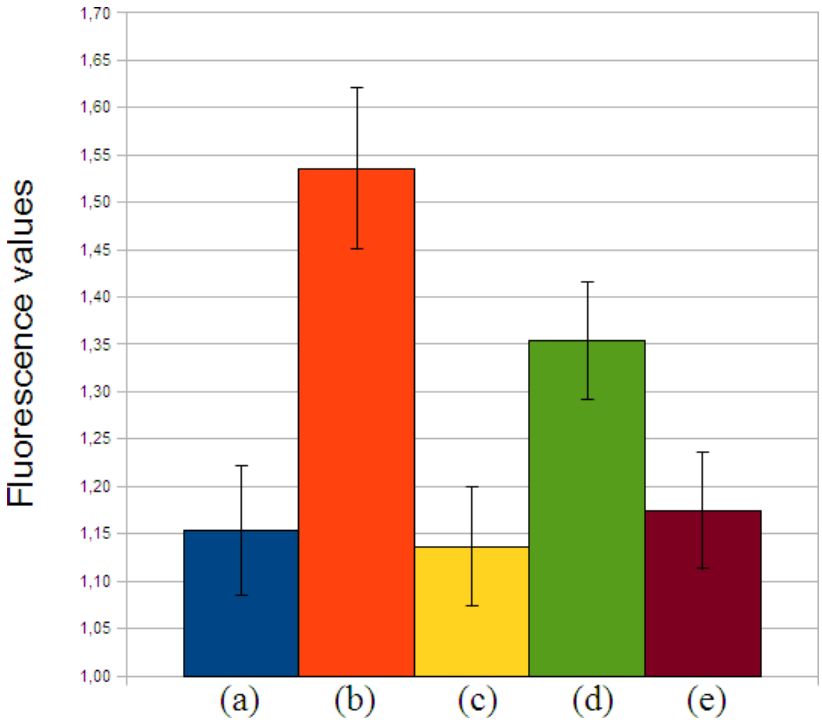


Figure 3.28: Validation of the origami version 1 with single stranded DNAs. In bar a, the closed DNA-origami in bar d the opened object and in bar e the negative control with a non target sequence; the data obtained are coherent with the data reported for the previous results. In column b is reported the fluorescence values of an object opened with a linear ss target DNA and in column c the negative control (non complementary linear target); the fluorescence values are not comparable with the one obtained with the clamp target.

sligthly moved on the left permitting a huge opening of the right wing towards the left one. This modification was apported with the aim of increase the distance between the fluorophore and the quencher after linear target complementation with the probe.

The same experiments of before were performed with the origami v.2 and results of the actuation are reported in Figure 3.30Validation of the origami version 2 with single stranded DNAs. In bar a, the closed DNA-origami, in bar b the object opened with a clamp target and in bar c the negative control with a non target sequence; the data obtained are comparable with the results reported for the origami version 1. In column d are reported the fluorescence values of an object opened with a linear ss target DNA and in column e the negative control (non complementary linear target);

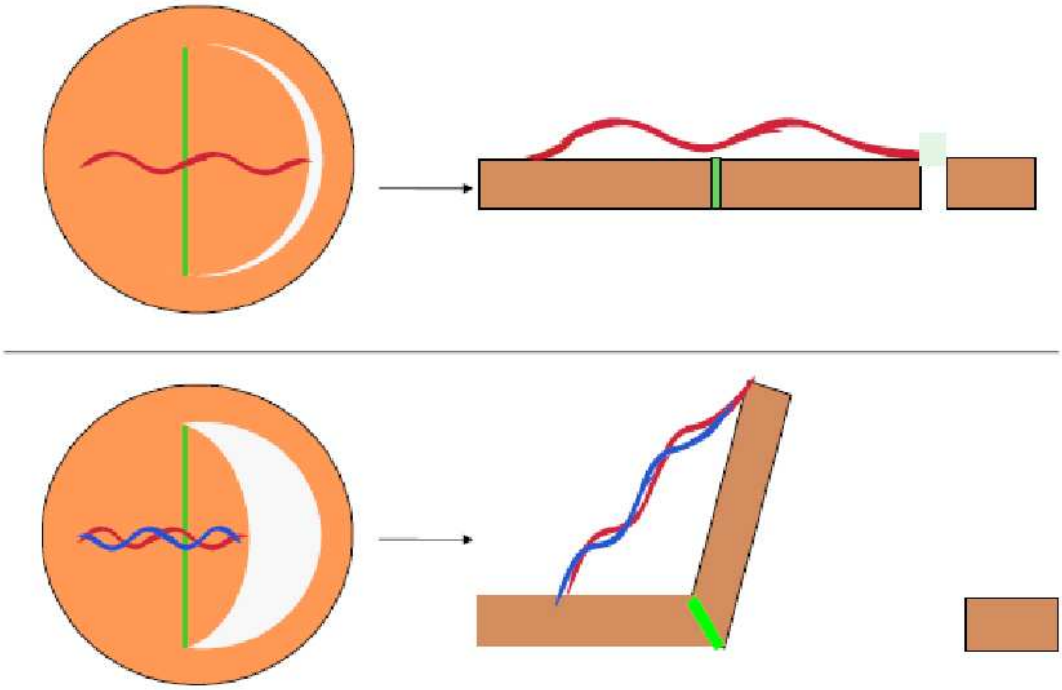

Figure 3.29: Folding path of the DNA-origami used for single stranded DNAs or RNAs detection.

the fluorescence values are now comparable with the one obtained with the clamp target.figure.caption.49

As visible now the fluorescence signal evaluated for the origami after the addition of the clamp TMV target (bar b) or the correspondent linear target oligonucleotide (bar d) are comparable and coherent with the previously obtained results of actuation with the clamped target. In both conformation of the targets the fluorescence emitted is higher than all the negative controls (bars a, c, e) confirming that the objects opens the right wing with or without the GC clamp in the molecule of interest. With this promising results where performed fluorescence evaluation also for the RNAs of TMV, other two plant viruses (IYSV, TSWV) and the Flavescence Doree (FD) phytoplasma.

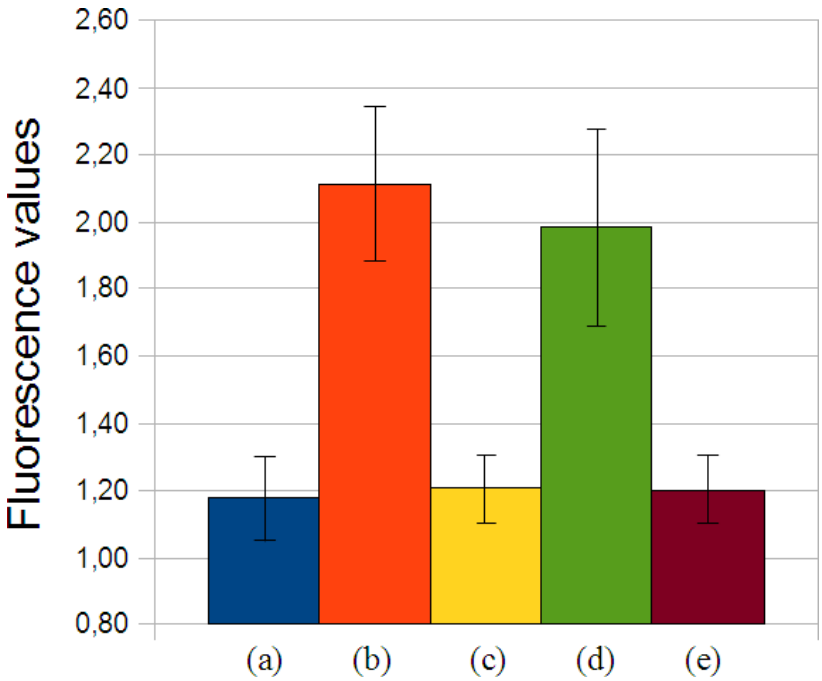


Figure 3.30: Validation of the origami version 2 with single stranded DNAs. In bar a, the closed DNA-origami, in bar b the object opened with a clamp target and in bar c the negative control with a non target sequence; the data obtained are comparable with the results reported for the origami version 1. In column d are reported the fluorescence values of an object opened with a linear ss target DNA and in column e the negative control (non complementary linear target); the fluorescence values are now comparable with the one obtained with the clamp target.

## 3.8 Validation with real RNAs samples

The DNA origami v.2 was validated using real RNAs samples extracted from infected plants. The plant pathogens evaluated were:

1. Tobacco Mosaic Virus
2. Iris Yellow Spot Virus
3. Tomato Spotted Wilt Virus
4. Flavescence Dorée phytoplasma

so resuming three tipes of viruses and a phytoplasma. In all the four cases, was evaluated the fluorescence

1. when the DNA–origami is closed (as negative control)
2. after the addition of the hairpined target
3. after the addition of a non complementary hairpined target (as negative control)
4. after the addition of the linear target
5. after the addition of a non complementary linear target (as negative control)
6. after the addition of the target RNAs
7. after the addition of a non complementary RNAs (as negative control)

The results of the addition of the targets in solution and the following fluorescence evaluation are reported in Figure 3.31Validation of the origami opening system with TMV RNAs' samples. Column (a) closed DNA-Origami, column (b) actauted DNA-Origami opened with a linear target, column (c) negative control with a non complementarity linear target (d) actauted DNA-Origami opened with a hairpin target, column (e) negative control with a non complementarity hairpin target, (f) DNA-origami actuated with a TMV's RNA sample (g) negative controls with non complementary RNAsfigure.caption.50, Figure 3.32Validation of the origami opening system with IYSV RNAs' samples. Column (a) closed DNA-Origami, column (b) actauted DNA-Origami

opened with a linear target, column (c) negative control with a non complementarity linear target (d) actauted DNA-Origami opened with a hairpin target, column (e) negative control with a non complementarity hairpin target, (f) DNA-origami actuated with a IYSV's RNA sample (g-h) negative controls with non complementary RNAsfigure.caption.51, Figure 3.33Validation of the origami opening system with TSWV RNAs' samples. Column (a) closed DNA-Origami, column (b) actauted DNA-Origami opened with a linear target, column (c) negative control with a non complementarity linear target (d) actauted DNA-Origami opened with a hairpin target, column (e) negative control with a non complementarity hairpin target, (f) DNA-origami actuated with a TMWVś RNA sample (g-h) negative controls with non complementary RNAsfigure.caption.52 and Figure 3.34Validation of the origami opening system with Flavescence Dorée phytoplasma RNAs' samples. Column (a) closed DNA-Origami, column (b) actauted DNA-Origami opened with a clamp target, column (c) negative control with a non complementarity clamp target (d) and a non complementary linear target, column (e) DNA–origami actuated with linear target, (f) negative controls with non complementary RNAs (g)DNA-origami actuated with a FDś RNA sample figure.caption.53.

In the absence of the target, with the wings laying in the same plane of the crown, a low fluorescence signal was detected, and as described before, the fluorophore and the quencher were located within the Förster radius of $\sim$1nm). Conversely, when a target hbridizes the probe, in all case the FRET separation resulted in a significant increase of fluorescent signal intensity. Low fluorescence intensity was recorded for the controls within statistical error: when non-target DNAs (both linear and hairpin shaped) were added to the origami solution the emitted fluorescence is comparable with the one of the initial state. The same results were obtained with the addition of non complementary real sample of RNAs.

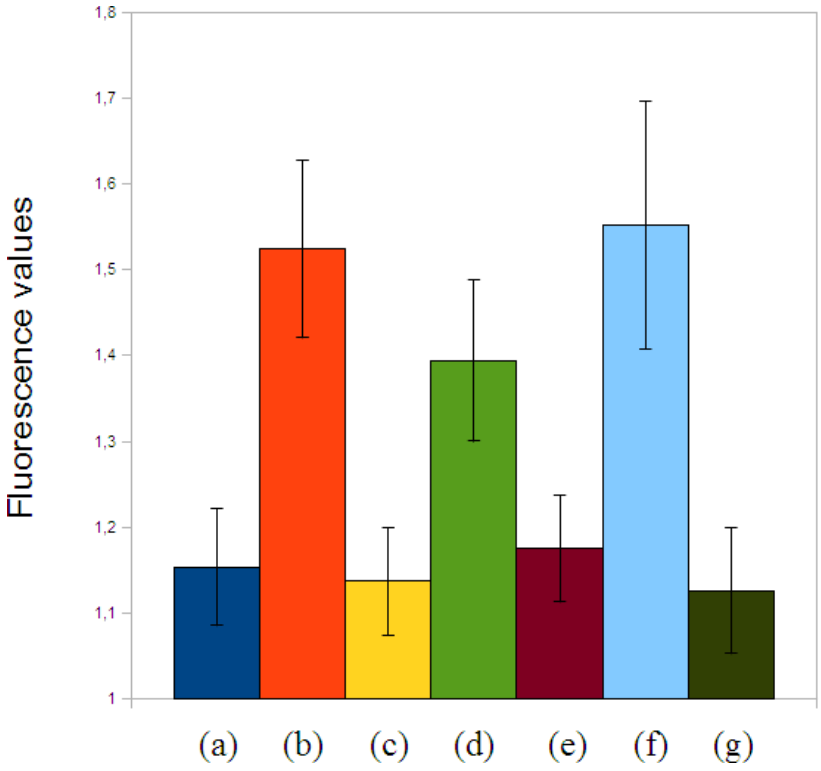


Figure 3.31: Validation of the origami opening system with TMV RNAs' samples. Column (a) closed DNA-Origami, column (b) actauted DNA-Origami opened with a linear target, column (c) negative control with a non complementarity linear target (d) actauted DNA-Origami opened with a hairpin target, column (e) negative control with a non complementarity hairpin target, (f) DNA-origami actuated with a TMV's RNA sample (g) negative controls with non complementary RNAs

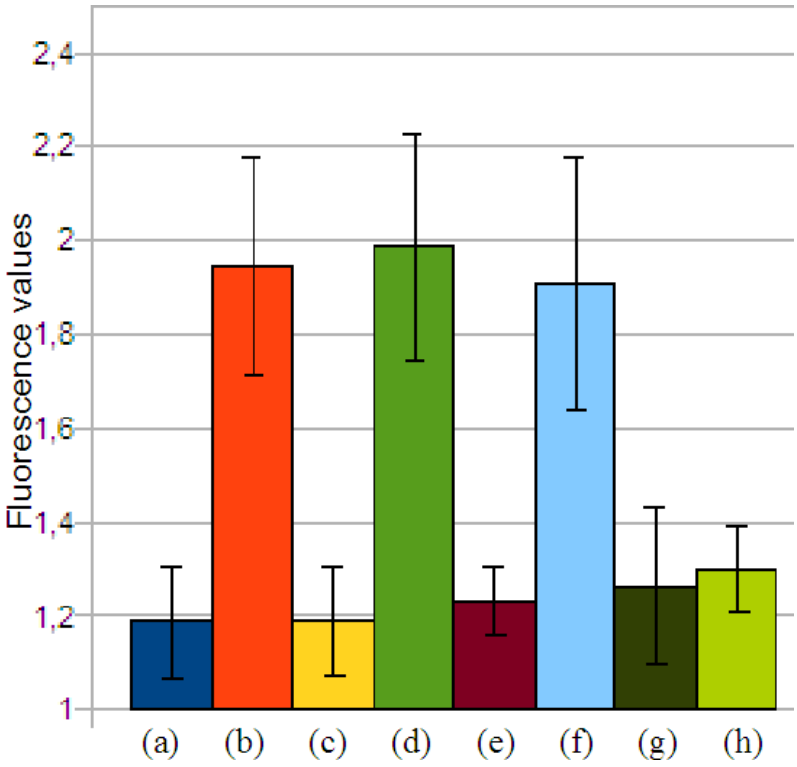


Figure 3.32: Validation of the origami opening system with IYSV RNAs' samples. Column (a) closed DNA-Origami, column (b) actauted DNA-Origami opened with a linear target, column (c) negative control with a non complementarity linear target (d) actauted DNA-Origami opened with a hairpin target, column (e) negative control with a non complementarity hairpin target, (f) DNA-origami actuated with a IYSV's RNA sample (g-h) negative controls with non complementary RNAs

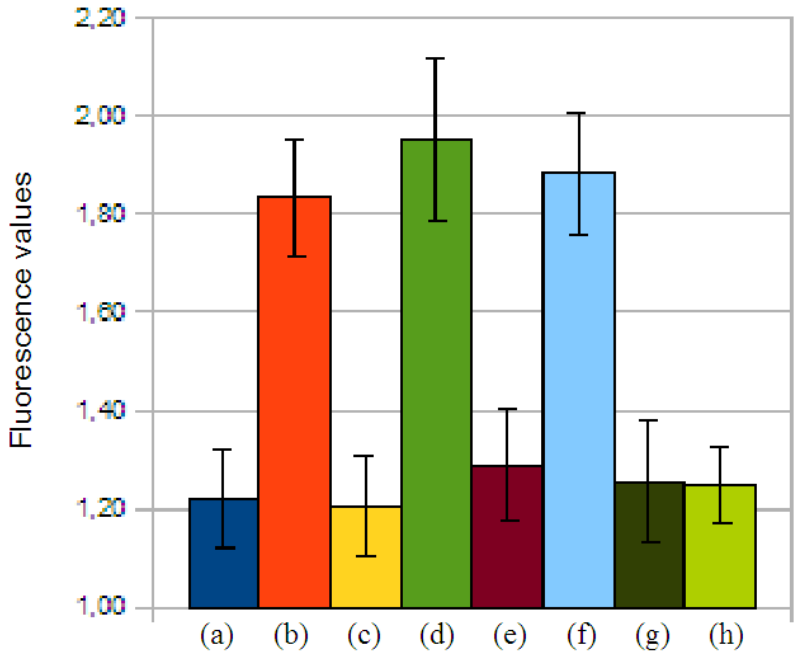


Figure 3.33: Validation of the origami opening system with TSWV RNAs' samples. Column (a) closed DNA-Origami, column (b) actauted DNA-Origami opened with a linear target, column (c) negative control with a non complementarity linear target (d) actauted DNA-Origami opened with a hairpin target, column (e) negative control with a non complementarity hairpin target, (f) DNA-origami actuated with a TMWVś RNA sample (g-h) negative controls with non complementary RNAs

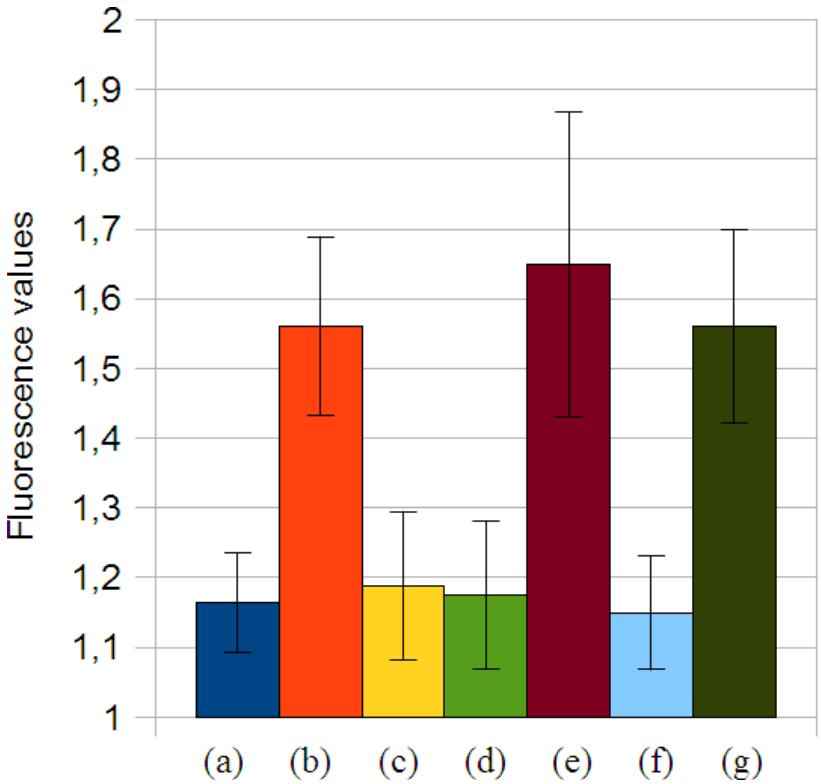


Figure 3.34: Validation of the origami opening system with Flavescence Dorée phytoplasma RNAs' samples. Column (a) closed DNA-Origami, column (b) actauted DNA-Origami opened with a clamp target, column (c) negative control with a non complementarity clamp target (d) and a non complementary linear target, column (e) DNA–origami actuated with linear target, (f) negative controls with non complementary RNAs (g)DNA-origami actuated with a FDś RNA sample

# Chapter 4

# Discussion

Traditionally, the presence of most pathogens such as bacteria, fungi and protozoa is determined directly, usually after the growth in a pure culture. The method has many limitations; it only works for organisms that can be grown in vitro, it is a time consuming procedure (in the order of days), it lacks specificity (most bacteria are identical in shape) if not followed by often laborious identification assays. These limitations are more significant in the detection of viruses which cannot be grown axenically. Several indirect methods have therefore been developed. Laboratory techniques such as immunology-based methods rely on immunological based antibodies interaction for the detection of bacterial cells, spores, viruses and toxins. Although the immunological-based detection is not as specific and sensitive as nucleic acid-based detection, it is convenient for the easy sample preparation and has the advantage of detecting both contaminating organisms and their metabolic products such as toxins. The most common examples of immunological techniques include the enzyme-linked immunosorbent assay (ELISA), flow injection immuno-assay, enzyme-linked fluorescent assay (ELFA), immunochromatography, immunomagnetic separation, immuno-precipitation assay and western-blot test. These techniques have limitations such as the inability to detect microorganisms in real-time, low sensitivity and possible low affinity of the antibody to pathogen belonging to diversified populations or other analyte being measured with potential interference from contaminants. A method less prone to produce false positives than immunological methods is the Polymerase Chain Reaction (PCR), a technique that can detect theoretically a single copy of a target DNA sequence. In addition to sensitivity, PCR has distinct advantages over culture and other standard

methods for the detection of microbial pathogens, i.e. specificity and accuracy. Limitations of the PCR technique includes false negative results and the need of enzymes to carry out the amplification and the time required to perform the assay, that causes a delayed response. Conventional molecular diagnostic techniques are widely used to identify pathogens with high reproducibility and sensitivity but most of these techniques cannot be utilized directly in the field because they require sample pre-process instrumentation, and require trained personnel. Additionally, the high costs and short shelve half-life of some reagents, such as enzymes, limits the detection of most conventional molecules of interest. Despite their performance or their wide application, current technologies, like ELISA and PCR, require extensive sample preparation and have long readout times, which delays prompt response. A further major advancement in the detection technology has been the introduction of biosensing.

Generally, biosensing is based on two main components: bioreceptors and and transducers (Velasco-Garcia, 2009). The principle of detection involves the specific recognition of the analyte to the complementary bioreceptor, in many cases immobilized on the suitable support. The interaction results in a variation of one or more physico-chemical properties, and the change is detected and measured by the transducer. The usual aim is to produce an electronic signal which is proportional in intensity to the concentration of the target(s) molecule(s).

The bioreceptor is a biological molecule such as an antibody, an enzyme, a nucleic acid, a protein or a more complex biological system e.g., cell or tissue that utilizes a biochemical mechanism for recognition. The first objective of the recognition system is to provide the sensor with a high sensitivity for the analyte to be measured. Recent technical developments suggest that faster, sensitive and more economical diagnostic assays can be developed taking advantage of the unique electrical, magnetic, luminescent, and catalytic properties of nanomaterials,. The nanotechnology-based systems have the potential to become the core of assays to be performed in media like blood and milk, without sample preparation, providing fast results in simple and user-friendly formats (Kaittanis et al., 2010). With this aim, the use of nanotechnology based bioreceptors could provide superior sensibility and reduce the time of diagnosis. Many nanostructures were used as in-vitro nanodiagnostic tools e.g. liposomes (small vesicles consisting of concentric lipid

bilayers surrounding aqueous compartments), carbon nanotubes (sheets of graphite rolled into a closed tube), dendrimers (hyperbranched uniform 3-D structures), gold and polystyrene nanoparticles and quantum dots (Qds, for diagnostic applications of bioimaging and labeling). Signal transduction can be achieved in optical (including fluorescence and surface plasmon resonance) or electrochemical manner.
This project attempted to create a novel device on which signal transduction and target recognition can be performed directly on a single platform without the mediation of other biological molecules than the ones to be detected. In this work, the device is projected to perform the detection without the action of an operator nor the addition of reagents other than the solution to be tested.
The interest in biosensing methods that perform a recordable output signal (electric, electrochemical, fluorescent) for detection is high, as it is the decrease of the costs for equipment amenable to integration in portable instruments: however, approaches that conjugate low costs and high sensitivity are, nowadays, still technically challenging. Size reduction is another major task in biosensor development, as it is the pre-requisite for portability. In this context the use of a bottom up approach for the construction of the biosensors has been an innovation of fundamental importance.

## 4.1 The bottom-up approach

The use of molecular self-assembly to fabricate objects with nanometer precision has been called the bottom-up approach . DNA molecular structures and intermolecular interactions are useful to the design and construct complex 2- and 3- dimensional objects, using chemically synthesized DNA double-crossover molecules. Intermolecular interactions between structural sub-units or, more generally other DNAs in solution, are designed to have some sticky ends that hybridize in a controlled manner according to Watson and Crick base pairing rules, enabling us to create specific periodic patterns at the nanometer scale. Among the other methods based on DNA hybridization proprieties the DNA origami technique allows the folding of long, single-stranded DNA sequences into arbitrary structures by a set of designed oligonucleotides. The method has revealed a great strength and efficiency for programmed self-assembly of molecular nanostructures and the

production of precise addressable nanostructures with wide-reaching application potential within the field of nanoscience.
Rothemund (2004) has reported that the viral M13mp18 polynucleotide can be folded to obtain arbitrary well formed 2- and 3- dimensional shapes mainly used for the precise and controlled addressment of nanoparticles and biomolecules on surfaces. This recent origami technique has found noteworthy applications in the study and the control of the shape of DNA-based object and in preliminary approaches to sensing. Dietz et al., (2009) recently designed, synthesized and characterized a DNA-Origami 3-D box with a cavity demonstrating that the lid of the structure can be opened after an external signal in the environment and therefore that DNA origami structures can be designed to have dynamic changes induced by the interaction with the environment. In spite of the programmability of the box lid, its opening was only partially controllable and tunable and the change of the position of the lid was monitorable qualitatively via fluorescence or atomic force microscopy but to gain satisfing information on the 3-D structural variations, more complex techniques were required e.g. cryogenic trasmission electron microscopy and X- ray scattering.
Here, I advance the idea of a novel biosensing strategy where the molecular detection is performed on the surface of a disk shaped DNA origami and demonstrate its autonomous movement by different techniques such as FRET, TEM, and high resolution AFM in liquid. The changing of conformation of the object occurs after the target recognition and this nanomechanical event can be monitored and evaluated directly with AFM imaging due to the changing of the structure conformation or by fluorescence signal evaluation.
The highly selective recognition mechanism between complementary DNA sequences is at the basis of the actuation in this work. The hybridization of the oligonucleotides and the strand displacement process were used in the project as signal activators and de-activators. In fact, because of their extremely simplicity with which are synthesized, functionalized and manipulated, not only nucleic acids were used as constructive material in the DNAbased platform but also as the key of actuation: the target RNAs molecules of plant pathogens that in the project maintain their biological meaning and are the object of analysis.
The project developed in this PhD thesis focuses on a prototype that could

lead to develop a portable, simple, highly sensitive and cheap detector for diagnostic purposes based on the change of the object conformation after the detection of an environmental signal: the DNA origami is a platform divided in two main parts, named the internal disk and the external ring. The internal disk is constructed to act as a switch, and the recognition of the target DNAs is the switching impulse. This fact implies that each DNA origami can detect different targets in relation to the probe hybridized on the surface of the DNA-based platform and different probes can be tested independently. Second, the system gives easily detectable, low noise signals that are dependent on a relatively small threshold number of interacting molecules. These characteristics made this system an interesting technology for the implementation of DNA based logics and hybrid computing.
The DNA origami was at first *in silico* designed and two software packages were compared and choose. The individuation of the scaffold strand to be used in the *in silico* evaluation is a critical step due to the need of use a sequence available at low costs with high reproducibility; however, several aspects had to be optimized starting from the scaffold sequence. The first point is that, as the other DNA origami in literature, the availability of single-stranded scaffold strands is limited to M13mp18 or to a small number of other sequences derived from the M13 genome and obtained by time consuming preliminary phases such as the enzymatic digestion and ligation. If longer scaffold alternatives could be identified with high precision and reproducibility, object larger than the one presented in this work can be obtained without the need to anneal different subunits. The use of a longer scaffold strand to make available the construction of bigger structures that can have more complex features and perform more more complex task without the needs of a hybridation step between the sub-units during production.
Another important point is the development of automated and more complete software packages for the design process. Computational tools for predicting complex 3-D structure of DNA origami designs before initiating expensive oligonucleotide synthesis are currently lacking, especially when complex objects that incorporate curved and twisted elements have to be designed. Sequence details are neglected at present, and users may specify geometric and mechanical parameters for the double-helical DNA domains; moreover, software packages do not model interhelical electrostatic repulsion and stacking interactions. In an iterative manner of design and analysis

should lower the barrier to the design of sophisticated DNA origami shapes. Among the 3-D origami, an advance toward more complete and user friendly software can be appreciable also for 2-D structures with complex features on the surface such as the IF origami; the choice of design parameters is one of the most time-consuming steps and requires a substantial understanding of DNA behaviour and folding. Future advances in DNA-based nanostructures and their design will require a mature understanding of the kinetics and thermodynamics of self-assembly within and between DNA building-blocks.

The structural information on the shape of designed DNA was gained with microscopy techniques such as TEM for a first screening of the annealed structures and then with liquid phase AFM. AFM imaging directly revealed the formation of isolated DNA origami nanostructures of the expected diameter and height, coherently with the *in silico* models. No double layers were evidenced so no interaction forces were revealed between DNA origami surfaces. From the images on the contrary, stacking interactions were evident between external edges; in fact with the first rough design of the disk, many clusters of objects were clearly visible. A lot of origami nanostructures appeared to be connected on their side, conceivably, due to interactions forces between the edges. After the modification of the fist design inserting 4T tails on the oligonucleotide terminus protruding from the origami, the interactions between disks evidently decreased and just a portion of the origami appeared to be connected in couples.

In small percentage the disks appeared incomplete, missing often the internal disk, part of the external ring or both. There broken structures can be imputated mainly to the performance of the annealing process; the frequent absence of the internal disk suggested that in some cases the link between the disk and the crown is too weak to maintain a well formed structure. The lack of small parts of the structure can also be accounted to tip damages during the imaging. A weakness in the DNA-origami method is the absence of quantitative tools for the analysis of defects occurrence in complex DNA-based nanostructures. Test structures should be designed to evaluate folding errors during the annealing steps to produce wrong geometries and, in addition, more work is needed to investigate the kinetic aspects of self-assembly, such as the concentration of staple strands compared to the scaffold.

## 4.2 The actuation

One of the major challenges for the use of nanodevices is their ability to perform actuation and motion at the nanoscale. These movements are usually based on conformational changes, which are triggered by changes the ionic composition of the medium or by the hybridization event between complementary single strands of nucleic acids. The conformational changes are transitions between single stranded DNA and duplex DNA or between unusual and conventional DNA conformations. The first example of DNA nanomechanical device demonstrated was based on the BZ transition of DNA (Mao et al., 1999); the device consisted of two nucleic acids molecules connected by a well designed sequence that could be converted from normal right-handed DNA (known as B-DNA) to a left-handed conformation, known as Z-DNA (Mao et al., 1999). The problem with this device is that it is activated by a small ionic molecule, and with all devices sharing the same stimulus, an ordered collection of those DNA-based molecules would not produce a diversity of responses.

A different approach towards nanoscale motion was taken by Niemeyer's group (Niemeyer et al., 2001). In their device, DNA supercoiling was induced by the presence of magnesium ion and this principle was utilized to produce nanoscale movements and variation in the DNA-network connectivity that could be characterized using AFM.

A different operational principle for DNA devices was introduced by Yurke and colleagues (2000); they developed a protocol for a sequence-control device with tweezers-like motion. A so-called set strand containing a non-pairing sticky ends, hybridizes to a DNApaired structural framework and sets a conformation; another strand that is complementary to the set strand is then added, binding to both pairing and non-pairing portions, and removes it from the structure, leaving only the framework. The conformation of the DNA device can be flipped back and forth by adding different set strands followed by their complements. A variety of different devices can be controlled by a diverse group of set strands. A variation of the tweezers was termed DNAscissors were tweezer structures are joined by short carbon linkers (Mitchell et al., 2002). A more complex device was constructed by Seeman and co-workers based on multiple crossover motifs (Yan et al., 2002) and using branch migration; a DNA structure can be switched between a four-stranded DNA structure that can be partly removed and replaced to

DNA sections without crossovers.
Resuming, this DNA nanoactuators have been built from DNA molecules which switch between two stable conformational states, depending on controllable parametres such as the presence of complementary strands or the ionic composition of the medium.
The DNA origami used in this thesis, worked as actuator in the application as a DNA switch including, into the DNA device, a functional nucleic acid (the probe) acting as a switchable element between two states. It was found out that the DNA origami conformation can be changed after exposure to an environmental signal such as a complementary DNA target sequence. The probe was linked to the surface by hybridization to two oligonucleotides protruding from the origami surface; for operation, a complementary target molecule long 120 bases was designed and synthesized. Production of target and probe was initially accomplished by enzymatic manipulation but for fastness, simplicity and higher reproducibility, such oligonucleotides were chemically synthesized in their full length. At its first use, the DNA disk was tested with a target with a GC clamp of 18 nucleotides to ensure a stable hairpin shape. DNA origami was visualized as a planar, homogeneous and compact disc when closed, while with the addition of such a molecule, the it shows two evident long openings separated by a DNA bridge in the middle when switched. This structural information was obtained only by AFM imaging; the visualization by TEM resulted ambiguous and not coherent with the expected disk shape and dimensions. The operation of the origami actuator was tested both with the origami in solution and with the origami deposited on a solid mica surface. The statistical analysis on the actuation efficiency in the two experimental configurations provided comparable data. Since, in order to successfully hybridize with the target, the origami should lie on the substrate surface face-up, the two data are consistent; the small difference between the observed (48%) and the expected (one half of 86%) means, although within a statistical error, may be explained with a orientation preference when the origami were deposited on mica, as it has been reported before for other origami (Rothemund, 2006).
Moreover, the observations indicated that the actuation force was large enough to overcome the electrostatic and van der Waals interactions between the DNA origami actuator and the substrate, as well as the stacking between the external edges of the internal disk and the internal edges of

the ring in which no Ttails or loops were inserted to prevent interaction forces, demonstrating the applicability of our strategy for integration of DNA origami actuators with solid state detectors and electronics. The force exerted depends on the formation of the probe/target hybrid pair that is constrained by the G-C clamp designed in the target hairpin.
Another problem considered during this thesis was the determination of the DNA origami orientation upon origami dispersion on a solid surface. For this purpose I modified the DNAOrigami, linking the external edges of the internal disk to the internal edges of the crown and added an asymmetric IF structure placed on the internal disk of the origami.
This feature was designed to have the letter I higher than the other parts of the disk and the F designed to be a hole, and with the aim of obtaining an indication on whether each origami was face-up or face-down. However, the IF structure did not help to unequivocally understand the orientation, due to the too small dimensions of the F features, not suitable for routine visualization by AFM. The resolution was mainly limited by the tip sharpness and by the imaging noise; in the best experimental conditions only few images showing clearly enough the IF design were taken. The topography resolution achievable in AFM was better when the scanning was high-relief rather than the low-relief.
To integrate a further degree of flexibility in our nanodevice, I presented a design that makes the conformation change of the DNA origami actuator reversible, by using probe/target pairs that were not fully complementary. This design implied a first hybridization step between the probe DNA on the DNA origami and a partly complementary target for forward actuation which brings the two diametrically opposed edges of the internal disk close to each other, forming two clearly distinguishable semicircular gaps in the origami center (the wings). The hybridization event between the probe and the target left an uncomplemented sequence of 34 nucleotides in the middle of the newly formed partially double stranded species. This single stranded site is the starting point of the reverse actuation, performed by displacement the probe/target hybrid by adding an excess amount of an additional oligonucleotide named the competitor. The competitor is a single stranded DNA perfectly complementary to the target and 84 nucleotides long. The perfect complementarity of target and competitor ensured target displacement from the probe and caused reversal of the origami to its origi-

nal configuration; the wings, which are no longer subject to the tensile force generated by the hybridization, relax to the initial conformation so that the internal disk is on the same plane of the external ring. Because of the unsuccessful screening via standard gel electrophoresis, beside AFM imaging, a fast and qualitative method based on insertion of a Forster resonance energy transfer (FRET) couple in the structure was introduced to monitor the conformation changes of the DNA origami associated with the structure motion following the target addition. The DNA origami was assembled with a staple strand on the external edge of the internal disk labeled with a fluorophore (6-FAM), and with an oligonucleotide on the internal edge of the external ring labeled with a quencher molecule (BHQ-1). In the absence of the target, in the relaxed initial position, a low intensity signal was detected since fluorophore and quencher were located within the Forster radius (?1 nm). A fluorescence intensity comparable with the one of the closed origami was recorded when a non-target DNA was added to the origami suspension. Conversely, when the edges of the internal disk were constrained following the addition of a probe hybridizing target, the consequent FRET couple separation resulted enough large to significantly increase the fluorescent signal intensity. Moreover, following further addition of the competitor to the suspension of reacted origami, the fluorescence intensity returned to the initial value within the experimental error, demonstrating that the origami configuration was reverted. Parallel assays carried out with a competitor that was non-complementary to the target produced no changes in fluorescence.
Nanotechnology is expected to be a key technology for the development of lab on a chip, where miniaturized devices and mechanically movable parts are assembled on a single chip to efficiently perform required tasks. Through the present work an alternative to traditional devices is proposed, due to the moving nucleic acids-based artificial structures, consequent to a biological signal and operating in wet conditions. The motion is provided directly on the surface of the DNA-based origami, without the need of intermediate operations performed by skilled personnel. In contrast, most artificial molecular machines reported so far are less sophisticated and cannot achieve complicated motions.

## 4.3 Validation with linear targets and real samples

The same experiments on the actuation were performed using linear targets, removing the GC clamp of the hairpin molecule of interest. The use of the DNAorigami v.1 gave no satisfying results; the fluorescence values detected for the linear targets were higher than the negative controls suggesting that actuation was performed but not efficiently as occurred for the hairpin targets. To improve efficiency the design was revised *in silico*. The left wing was blocked on the external ring by substituting some oligonucleotides and the axis of constrain was slightly moved to the left toward the blocked part. This modification was performed with the aim of increasing the distance between the fluorescent and the quencher molecules; actually with such a modification, the fluorescence recorded with linear targets and clamp targets was comparable.

The system was then tested with real samples, such as RNAs from plant pathogens. Two kind of pathogens were evaluated : the Flavescence Doree phytoplasma and three different viruses: TMV, IYSV and TSWV. The list includes important plant disease agents, which are included in quarantine lists in Europe and whose detection in the field at the beginning of the growing season is crucial to prevent epidemics. TMV (genus Tobamovirus) is the model system for plant RNA viruses. Its accumulation as viral particle and free RNA is very high during the replication cycle in the plant, therefore it is a good starting point for setting up a new detection method. Moreover, TMV is still a problem in cultivars (like local tomato crops) that do not carry a specific resistance gene (Knapp and Lewandowski, 2001).

TSWV (genus Tospovirus) is representative of a group of viruses with a great economic impact for agriculture worldwide. TSWV is now one of the major threats to tomato and pepper crops, given the rapid and widespread occurrence of resistance-breaking strains (Adam and Kegler,1994; Aramburu and Marti, 2003). IYSV (genus Tospovirus) has been only recently shown to be a concern for onion crops in Italy, and is on the lists of the potential threats for our agriculture, and the currently available screening methods are not well suited for the IYSV strains present in Italy (Gent et al., 2006; Cosmi et al., 2003). Candidatus Phytoplasma vitis, the phytoplasma associated with Flavescence doree (FD), is a quarantine pathogen of grapevine that causes severe economic loss. The detection of such as pathogens with the DNA origami v.2 revealed that the fluorescence intensity recorded with syntethic

oligonucleotides for those pathogens was comparable with the recorded from real RNA sample.
For what concerns the diagnostic approach, the DNA-origami v.2 can be efficiently actuated both with clamped and linear targets and was validated with real samples of plant pathogens RNAs extracted from plants. Although I applied the biosensor only to detect nucleic acids, but the detection principle and the mechanism of the actuation can be applied to other interactions occurring between different molecules and in different environments.

## 4.4 Future applications

*Plasmon Resonance*

Surface plasmon resonance (SPR), a phenomenon involving the conducting electron oscillations induced by the interaction of light with a metallic film, as gold or silver on a transparent medium. As incident light interacts with the metal interface at angles larger than a critical one, the reflected light displays a characteristic increase, due to resonant energy transfer from the incoming photons to surface plasmons. The wavelength or angle at which resonance occurs depends on the refractive index of the analyte and the changes in local refractive index at or near the metal surface. Hence SPR can be used to study the specificity, affinity and kinetics of biomolecular interactions and to measure the concentration levels of analytes in complex samples. One of the most widely used metals is gold that enables the resonance shift due to refractive index changing thereby increasing the separation between resonance wavelengths and consequently increasing sensitivity. In this context the DNA-based device described in this work can be used as a convenient platform on which noble metal nanoparticles (e.g. AuNPs) of various sizes can be addressed with high precision and selectivity. Placing a NP on the external edge of the internal disk and another NP on the internal edge of the external ring, variation in plasmon resonance can be used to monitor the progress of actuation after the recognition between complementary nucleic acids molecules. SPR in this way is used to monitor biomolecular reactions such as DNA hybridization with the set-up presented in this thesis, or other molecules changing the probe hybridized on the origami surface. Another application of the DNA-Origami platform to SPR is the possibility to monitor the shift of the resonance after the actuation with targets non perfectly complementary to the probe; it is interesting to know how the double stranded conformation affects the opening of the DNA-origami. A set of targets can be designed and synthesized to have different degrees of hybridization with the probe. In this way part of the probe is expected to be coiled and, on the bases of the length of the mismatch within the two oligonucleotides, tunability of the wavelength of the excitation light of plasmonic nanostructure can be achieved.

*Integration in complex devices*

The construction of machines and actuators is one of the goals of nanotechnology. Self-assembly of nucleic acids allows the introduction of heteroelements such as nanoparticles (as described in the previous paragraph) and other biological molecules (e.g. proteins) increasing the DNA-origami functional potential, especially when precise control of the placement and orientation are required. Due to the synthetic characteristic of the oligonucleotides, the sequences can be conveniently synthesized and functionalized with attachment groups (e.g. biotins, ammines, thiols) on the basis of operator needs. In example, for the integration of proteins, oligonucleotides were coupled in a unique position before purification of the conjugate (Chen et al., 2011). Referring to the same principle, thiolated oligonucleotides can be synthesized and integrated in DNA-Origami platforms to address in controlled manner gold nanoparticles (Ding et al., 2010) or in the same way to link the nucleic acids nanostructures to gold surfaces with bonds stronger than the simple electrostatic interaction.
Functionalization of part of the origami's oligonucleotides in a pre-determined position enables the integration of DNA-based nanostructures on inorganic surfaces. Many lithographically patterned deposition of organic compounds, including DNA nanostructures (Sarveswaran, et al. 2006) demonstrated that highly selective adsorption is possible, but the molecules were smaller than the lithographic features. DNA origami structures such as the triangles of Rothemund (2006) are just large enough (127 nm) to overcome litographic limits and a general method for the placement and orientation of individual DNA origami on lithographically patterned surfaces was developed in recent years (Kershner et al., 2009). In another strategy (Gerdon et al., 2009) top-down fabrication and bottom-up self-assembly were combined to achieve deterministic position control of DNA origami structures over millimeter length scales on a wafer. Using these methods, it was demonstrated that the delivery of a single DNA-origami structure onto litographically patterned surfaces can be controlled.
Additional work and studies have to be carried out for precise addressment of complex DNA-origami nanostructures on surfaces, in example and allow the individuation of a defined number of molecules in a pattern on a surface coupled to DNA origami actuators.

In the context of the nanovalve prototype reported in this thesis, many origami disks can be addressed on a inorganic surface to form an array to allow multiple analysis experiments on different targets using specific DNA-based probes. Another important task that can be achieved in this context is the precise orientation of the disk: addressing its down surface with protruding thiolated oligonucleotides potentially interacting with a patterned gold surface should be an important advance to orient the upper face to the solution containing the target mixture.

*Integration of functional nucleic acids*

As previously described, the DNA-Origami surface can be addressed in many ways, and the probe on the upper face of the internal disk can be substituted with other functional nucleic acids. For example, the probe can be substituted with an aptamer molecule or a DNAzyme, single stranded nucleic acids able to recognize specific substances present in the environment; the recognition event could permit the change of conformational change of the aptamer or of the DNAzyme allowing the indirect variation of the origami structure. In this way, beside nucleic acids, other biological molecules can be investigated such as, in example proteins or toxins, increasing the potential of the specific actuation on DNA-based objects. Another ambitious goal in the context of sensing, is that the DNA-based platform may be conveniently placed on a hynorganic surface to create arrays of sensing spots on which can be recognized different target with different probes, completely independently one from each other in the case of a lab-on a chip integration of the actuation process. In this context, the project here presented is mainly inserted in the context of the development of innovative analytical techniques and methods with potential applications in the biological and medical fields, with the aim of collecting detailed informations reaching the single molecule detection.

# Chapter 5

# Conclusions

A fascinating target for research in nanotechnology is to gain the ability to precisely move molecules and nanosized objects under precise control. Directional, revertible motion on a well defined path in dependence of a single molecule recognition event could open visionary scenarios of development of nanofactories, i.e. minute assemblies of ordered molecules that can move coordinately to efficiently produce new chemicals or perform functions mimicking a live organism.
Here I presented an autonomous, revertible nanoactuator in which the perception of an environmental signal is associated to the change of conformation of a DNA-origami. The advancement presented n this thesis is the transduction of a nucleic acid recognition signal into a signal consisting of a macromolecular structure change, that is a step forward toward the construction of biological and synthetic systems able to perform a controlled answer only when a given reaction occurs. The development of such a device overcomes the constraint of many detection devices, such as the need to combine several single components to be assembled in intermediate setups, and then implemented.
The development of complex nano-sized objects capable of actuation upon single molecule interaction may represent a progress in the project of integrated, intelligent, rapid and high throughput analysis devices working with low volume sample/reagent due to the strict and direct molecular contact occurring between the units involved in the reaction. In addition, the reversibility of the actuation and the effectiveness of the mechanism presented with the origami in solution and deposited on a surface expands the potential range of applications. This DNA origami with reversible actua-

tion combines the characteristics of structure stability and high information density, and can be used as platform for addressing, moving and modifying nanomaterials or can be assembled into patterns with required directionality to guide matter or energy transfer when integrated with electrically active components.

Due to its fabbrication principle, this DNA-origami is well suited for integration with DNAzymes or DNA aptamers into more complex molecular machines in which the origami may switch between alternative position to address the point where a molecule attached to a functional nucleic acid has to be brought by the motor. Another option could be the use as a fluidic nanovalve, with solution se possible separation of a reservoir from the environmental solution, mediated by the DNA-origami that acts like a membrane. The selective autonomous change of conformation of the nanovalve can be applied to selectively open a nanopore, transducing the signal of the presence of a molecular target into the opening of a channel that can result in the release of drugs in controlled manner.

There is much research into targeted drug delivery to the appropriate part of the organisms with controlled release of the medical substances over an extended period of time because this approach ensures the reduction of unwanted collateral effects. The implication of the autonomous nanoactuator principle is that responsive DNA-origami could be programmed to deliver their toxic cargoes in a specific fashion, thereby maximizing efficacy while minimizing side effects. Therefore the DNA origami actuator developed in this work has potential for both in vitro and in vivo applications. With added functionalities, the DNA Origami nanoactuator seems to be a promising technology for the future nanomaterial science.

# Acknowledgments

Vorrei innanzitutto ringraziare il mio supervisore, il professor Giuseppe Firrao, per avermi avermi dato la possibilità di svolgere questa tesi e per gli stimolanti argomenti che mi sono stati proposti. Un particolare ringraziamento anche a Marco Lazzarino e Luca Piantanida per l'entusiastica collaborazione durante questi anni.

Vorrei ringraziare Emanuela, Federica, Emanuele e Manola, all'inizio conosciuti come brillanti colleghi ma che ora sono tra gli amici più cari che ho.

Un enorme grazie a Luisa, Max, Gabriele, Dario, Eleonora, Stefania e Simone, amici che oramai mi accompagnano nel bene e nel male da tanto tempo e che con il loro contagioso entusiasmo mi supportano e che con la loro pazienza mi sopportano.

Infine, e soprattutto, voglio ringraziare mia sorella Eliana, mia mamma Gabriella e mio papà Domenico perchè senza di loro, il loro sostegno, la loro forza, la loro fiducia nei miei confronti e il loro incondizionato amore, probabilmente non avrei fatto nulla di tutto questo e non sarei quella che sono...grazie papà che, in ogni caso, sei con noi tutti i giorni.

# List of oligonucleotides

All the substitutions are intended referred to the DNA origami v.1.

Yellow: Oligonucleotides on the internal right edge of the external ring
Grey: External oligonucleotide of the external edges of the ring
Blue: Oligonucleotides on the left edge of the internal disk
Dark Green: Oligonucleotides on the right edge of the internal disk
Light blue: Oligonucleotides of the internal disk
Red: Oligonucleotides of the ring

| Sequence | Length | Description | Color |
|---|---|---|---|
| AGGAACGCCATCAAAAATAATGTGTAGATGGGCGCATGCCATTCAG | 46 | CrI1 | |
| GATGAACGGTATCAGCTCATTTTTTAACCAAT | 32 | CrI2 | |
| CCTGAGTAATGACAAGAGAATC | 22 | CrI3 | |
| CATCCAATAAATAAATGCAATG | 22 | CrI4 | |
| TAAAGTACGGTAGTAGCATTAA | 22 | CrI5 | |
| CGCGTTTTAATTCGAGCTTCAAAATATGCAAC | 32 | CrI6 | |
| GTAAGAGCAATACTGCGGAATCGAGCCCGAAAGACTTCAAATAT | 44 | CrI7 | |
| TTGTTCCAGTTTGGAACAAGAGTCCACTATTAAAGTAAATCAA | 43 | Cr1 | |
| AAAGCCGGCGACGCGTAACCACCACACTACTATGGT | 36 | Cr2 | |
| AGAAAGGACGTCTATCAATTTAGAGCTTGACGGGG | 35 | Cr3 | |
| AAGAATAGCTGTTTGATGGTGGTTTTTTCACCA | 33 | Cr4 | |
| CTGGCAAGTGCTTTCCTCGTTAGAGAGCTAAA | 32 | Cr5 | |
| GGCGGGCGGGAGCAAAATCCCTTAAACGTGGACTCCA | 37 | Cr6 | |
| TGCTTTGAGACAGGAACGGTACGCGTTGTAGC | 32 | Cr7 | |
| TATAACGTGTAGCGGTCACGCTGACGTGGCG | 31 | Cr8 | |
| GTGAGACAGAGGCGGTTTGCGTAATACGAGCC | 32 | Cr9 | |
| CTGATTGCCAGCAGGCGAAAATCCCCGAGATAGGGTTGAGTG | 42 | Cr10 | |
| GCCTGGCAGCTGCATTAATGAATGGGTGCCT | 31 | Cr11 | |
| TGTTTTTATAATCAGTGAGGC | 21 | Cr12 | |
| TGAGAAGGCCGCTACAGGGCGCGCCGCCGCGCTTAATGCTTTT | 39 | Cr13 | |
| CAGGAGGCCATCACTTGCCTGAGTAAACTATC | 32 | Cr14 | |
| CAGAGCGGATCAGGGTGGTTTTTCCCGAAATC | 32 | Cr15 | |
| GCCCGCTTTCCAGTCGTTGCGTTGCGCTCACTAGGTCGACT | 41 | Cr16 | |
| CACCGAGTAAAAGAGTCTGTCCGCTCATGGAAATACCTATTTACA | 45 | Cr17 | |
| AATACTTAATATTACCGCCAGCCCCAGTAATA | 32 | Cr18 | |
| AGTAATAACGATTAAAGGGATTTTACGAGCACG | 33 | Cr19 | |
| GGAAGCACTGTGTGAAATTGTTATACGTGGC | 31 | Cr20 | |
| AAGCCTGCGGCCAACGCGCGGGGGGGCAACAG | 32 | Cr21 | |
| AATGAGTGCTCGAATTCGTAATCATTAGTCTTT | 33 | Cr22 | |
| ACATTAAGGAAACCTGTCGTGCCCCTGAGAGAGT | 34 | Cr23 | |
| AGGAAAAACATCACGCAAATTAACCCAGAATCC | 33 | Cr24 | |
| GGCCTTGCGATAGAACCCTTCTGACAATCAAT | 32 | Cr25 | |
| CAAAACTCAGAAGTTCCACACAACTTGGGCGC | 32 | Cr26 | |
| CTAGAGGGGGTTTTCCCAGTCACGGGGATGTG | 32 | Cr27 | |
| GTGCCAAGCTTGCATGCCTGC | 21 | Cr28 | |
| ATCGTCTGAAATGGATTACATTTTGACGCTCA | 32 | Cr29 | |
| TTGGCAGACATCGAGAACAAGCAAAGATATAG | 32 | Cr30 | |
| AAAGGGACCAAGAACGGGTATTACGCGAGGC | 31 | Cr31 | |
| CAACAGATGGTAATATCCAGAACCTTTGATT | 31 | Cr32 | |
| ACAGACAAAACCACCAGCAGAAGAGCTTTCCGG | 33 | Cr33 | |

| | | |
|---|---|---|
| ATGGCTATGGTCATAGCTGTTTCTAAAGTGTA | 32 | Cr34 |
| AATGCGCCCCTAAAACATCGCCAAGGCAAAGCGC | 34 | Cr35 |
| TAACGCCAATCCCCGGGTACCGAGAGCTAACTC | 33 | Cr36 |
| CCGCACTTTCACCAGTCACACGAATTGCAAC | 31 | Cr37 |
| AATCGGCTGGGAGGTTTTGGAAACCGGTCCACTCCAGCCATAAAACAG | 48 | Cr38 |
| AGGTGAGGCCTGAAAGCGTAAGAATCCGCTCA | 32 | Cr39 |
| CTGCAAGAACTGTTGGGAAGGGCGGGATAGG | 31 | Cr40 |
| TATTACGCCAGCTGGCGAAAGGACGTTGTAAAACGACGGCCATTTT | 42 | Cr41 |
| ATTACCGCGCCAATTTGCCAGTTTTT | 22 | Cr42 |
| AAGGCTTATACCAACGCTAACGAGCCCAATCCA | 33 | Cr43 |
| GTTTTAGCTTTGCACCCAGCTACA | 24 | Cr44 |
| GACTTGCGTCTTTCCTTATCATTCATTCTGGC | 32 | Cr45 |
| CACCGCTACGACAGTATCGGCCT | 23 | Cr46 |
| CGGAAACCTTAAAAATACCGAACGTATTTTTGA | 33 | Cr47 |
| CATTCCGTAACCGTGCATCTGCCAGTTTGAGGGGACGTCTGGTGC | 45 | Cr48 |
| GCTGCGCGCGATTAAGTTGATAGGAACTGGG | 31 | Cr49 |
| TGAATCTTCCGGTATTCTAAGAAAACCAAGTA | 32 | Cr50 |
| TCACGTTGTCGCGTCTGGCCTTCCTTAAATTT | 32 | Cr51 |
| CCGTCGGATTCTCCGTGGGAACAAACGCAACATTAA | 36 | Cr52 |
| TACAAAATAAACAGGGAAG | 19 | Cr53 |
| TTATTTATCGTCTTTCCAGAGCCTCAATAGCAA | 33 | Cr54 |
| AATAAGATAGCAGCCTTTACAGAATAACCCACAAGAATTGAGTT | 44 | Cr55 |
| TCCCATCCCAAGATTAGTTGCTATGAACCTCCC | 33 | Cr56 |
| ATGTGAGTTGTAAACGTTAATATCCGGTTGAT | 32 | Cr57 |
| CGCATTAGTCAGAGGGTAATTGAGATAGCTAT | 32 | Cr58 |
| ACGTCAAAAATGAAAAAACGATTTTTTGTTTAATTTTATCC | 41 | Cr59 |
| TTGTTAAAATCGTAAAACTAGCATTGAGAGTC | 32 | Cr60 |
| TTGTATAAGCAAATATTTAAACGAGTAACAAC | 32 | Cr61 |
| GAACAAAGACGGGAGAATTAACTG | 24 | Cr62 |
| CAGAGAGGAGAATAACATAAAAACAGCCATA | 31 | Cr63 |
| ATGTACCTTTGTTAAAATTCGCATGTAGCCAG | 32 | Cr64 |
| AATCAGAGAGAGATCTACAAAGGCGGAGACAG | 32 | Cr65 |
| CTTACCGAAACAAAGTTACCAGAATGTTAGCA | 32 | Cr66 |
| AAGCCCAATAATAAGAGCAAGCAATAATAACGGAATACCCAA | 42 | Cr67 |
| TGGAGCAATGTAGGTAAAGATTCAGAACCCTCA | 33 | Cr68 |
| CTATTTTTAAAGCCCCAAAAACAGGAAGA | 29 | Cr69 |
| ATAAATTAATGCCGGATCAACCGTTCTAGCTGTTTT | 32 | Cr70 |
| ATAGCCGAGCCCTTTTTAAGAAAAACACCCT | 31 | Cr71 |
| GGAAACGAAACAATGAAATAGCACGCTAATAT | 32 | Cr72 |
| AGAAAGGCCTATCAGGTCATTGCCGTCAATCAT | 33 | Cr73 |
| TCAAATCCCTTTATTTCAACGCAAAGCAATAA | 32 | Cr74 |
| AACGTAGAGAAACGCAAAGACACCATTCAACC | 32 | Cr75 |
| AAGAACTGGCATGATTAAGACTTGTCACAATCAATAGAAAAT | 42 | Cr76 |
| TATATTTTCATACAGGCAAGGCACAATTCTA | 31 | Cr77 |
| GGGAGAAGACCATCAATATGATATGAGGGTAG | 32 | Cr78 |
| ATTATGACCCTGTAATCGGTTGTACCAAAAAC | 32 | Cr79 |
| TATAAAAAAATACATACATAAAGAGTAAGCAG | 32 | Cr80 |
| AGTTTATTTCCTTATTACGCAGTAGGAAACCGA | 33 | Cr81 |
| GCAAAATTAGGATAAAAATTTTTAAAAGGGTG | 32 | Cr82 |
| AGCCTCATTCATTTGGGGCGCGATCCCAATTC | 32 | Cr83 |
| GATTGAGGTTAAAGGTGAATTATCCGGAAACG | 32 | Cr84 |
| TCATATGGTTTACCAGCGCCAGCCATTTGGGAATTAGATCACCAG | 45 | Cr85 |
| CTAATAGTGTCTGGAAGTTTCATTTAGCTCAA | 32 | Cr86 |
| GCTATATTGAGCATAAAGCTAAATACTTTTGC | 32 | Cr87 |
| CGCAAATGGTCAATAAACCATTAGATACATTTTTTT | 32 | Cr88 |
| ATTATTCAGAGGGAAGGTAAATATGTGGCAACA | 33 | Cr89 |
| GACTTGAAAGACAAAAGGGCGACACGGAATA | 31 | Cr90 |
| AGTTGATGCTGAAAAGGTGGCATAAGAATTA | 31 | Cr91 |
| TGCGAACGGCTTAGAGCTTAATTGTCAGGATT | 32 | Cr92 |
| TAGCACCATGTAGCGCGTTTTCATTTTGCCAT | 32 | Cr93 |

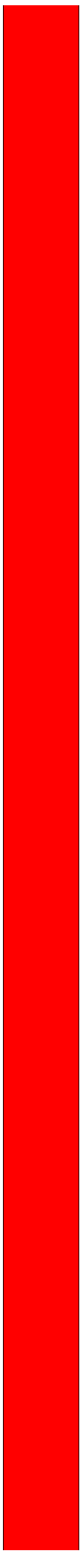

| | | | |
|---|---|---|---|
| GCAAAAGCCA | 10 | Cr94 | |
| CATGTTTTAAGCGAACCAGACCGGAAAAAGATT | 33 | Cr95 | |
| TAAGAGGTCATTTTTGCGGATGAGTAGATTTAGTTTGCCTGTTTA | 45 | Cr96 | |
| GCACCGTAATCAGTAGGAAACCATCGATAGCATGACGGAA | 40 | Cr97 | |
| CGTCAGACTTACCATTAGCAAGGCACCGTCACC | 33 | Cr98 | |
| TCCAACAGGCTGAATATAATGCTGCCATATAAC | 33 | Cr99 | |
| AGAGAGTCTATTATAGTCAGAAGTTTAAACAG | 32 | Cr100 | |
| CTTTTCATTCAGAGCCACCACCCTGAAAGCGC | 32 | Cr101 | |
| AAGAGGATCATAAATATTCATTGACGCCAAAA | 32 | Cr102 | |
| AAAATCAGGTCTTTACCCTGAACCTTTAATTGCTCCTTTTGATTTT | 42 | Cr103 | |
| GCCTCCCTCAGAGCCGCCACCAAGCGTCATACATGGCTTTTGTTTT | 42 | Cr104 | |
| GCCACCCAATCAAAATCACCGGAGCCTTTAG | 31 | Cr105 | |
| CCACCAGAAGCCCCCTTATTAGCGCGGCATTTTCGGTCAT | 40 | Cr106 | |
| ACCACCACCAGAGCCGCAAACAAAT | 25 | Cr107 | |
| TAGACTGGATAGCGTCCAACACTATCATAACCGGGAAGAA | 40 | Cr108 | |
| CAAATGCCAAAGCGGATTGCATCAAGCAAAC | 31 | Cr109 | |
| AACGAGAATGACCATAAATCA | 21 | Cr110 | |
| AGTCTCTGGTCAGTGCCTTGAGTAGTGCCGTC | 32 | Cr111 | |
| AAATCCTCAGTTAATGCCCCCTGTAGCGGGGT | 32 | Cr112 | |
| CAGACGAGTAATAGTAAAATGTT | 23 | Cr113 | |
| GGAATTAAACGGAACAACATTATAATAAGGC | 31 | Cr114 | |
| ATGATACAGGAGTGTACTGGT | 21 | Cr115 | |
| TTAACGGGAATTTACCGTTCCAGTCTCAGAACC | 33 | Cr116 | |
| CGTATAAACATTAAAGCCAGAATGCAGAGCCG | 32 | Cr117 | |
| GGAACCTATTGGCCTTGATATTCACCGCCAGC | 32 | Cr118 | |
| AAACATGAAGGCTGAGACTCCTCAAGCCACCA | 32 | Cr119 | |
| CGATTTTAGCGAGAGGCTAACCTTGCTTAGGTCAGACGATTATTCTG | 47 | Cr120 | |
| GCTCATTATTCAACTTTAATCATTCTGACCTTC | 33 | Cr121 | |
| AAATCTACCGAGTAGTAAATTGGGCCGGATATT | 33 | Cr122 | |
| TACAGGTAGAAAGATTCTAATGCAGATACATAAATCCCCCT | 41 | Cr123 | |
| GAGAGGGTCCGTACTCAGGAGGTTCTGTAGCATTCCACAGACAGCTTTT | 45 | Cr124 | |
| TTTGCTCAGAACCGCCACCCTCACTGAGTTT | 31 | Cr125 | |
| GGTTTAATTACCAGTCAGGACGTTCTCGTTTAC | 33 | Cr126 | |
| ACCAGAAGTTAATAAAACGAACTCGAGGCATA | 32 | Cr127 | |
| TTGCCCTGAGCTGCTCATTCAGTGCTTAGCCGGA | 34 | Cr128 | |
| CGGAATAGGTGTATCATGATATAAGTATAGCCAATAAGTT | 40 | Cr129 | |
| CACCCTCAGTACCAGGCGGATAAACAGTGCC | 31 | Cr130 | |
| ACCCTCAGAGAGAAGGATTAGGATCCTATTTC | 32 | Cr131 | |
| CCCTCATTGCAAGCCCAATAGGAAGGGATTTT | 32 | Cr132 | |
| TAGGCTGGGTGAATTACCTTTAAGAAGTATATG | 33 | Cr133 | |
| ATCAAGAGACAGATGAACGGTGTCAAGCGCGA | 32 | Cr134 | |
| CATTACCTAAGGGAACCGAACTGATCATCGCC | 32 | Cr135 | |
| CGTCACCATTTCCAGACGTTAGTATAAAGGAAT | 33 | Cr136 | |
| TGAAAGAGGTAATCTTGACAAGAACTTGAGAT | 32 | Cr137 | |
| TCAATCACAAATCAACGTAACAAACGAGAAAC | 32 | Cr138 | |
| ACGAGGGACCTGCTCCATGTTA | 22 | Cr139 | |
| CCTCATAGTTAGCGTAACGAT | 21 | Cr140 | |
| TGTCGTCGTACAAACTACAACGCTAGTACCGC | 32 | Cr141 | |
| TTCTGTATCCCATGTACCGTAACAGAACCGCC | 32 | Cr142 | |
| GCTAAACAGTTTCAGCGGAGTGAGGTTTATCA | 32 | Cr143 | |
| GATTATACACAGACCAGGCGGATATTCAGGCA | 32 | Cr144 | |
| AACAAAGACACTAAAACACTCATTTGAGGAC | 31 | Cr145 | |
| TGATAAAGCACCAACCTAAAACGTCCATTAAA | 32 | Cr146 | |
| TGCGAATAAAGGCTCCAAAAGGACGACAATGACA | 34 | Cr147 | |
| AAAGAATTACAACGGAGATTTGTACCAACTT | 31 | Cr148 | |
| CCACTACGAAGTTGTGTCGAAATCCGCCGCAGACGG | 36 | Cr149 | |
| TGAAAATCTCCAAAAAAATAATTTTTTCACGTCTAAAGTTT | 41 | Cr150 | |
| GCTTGCTTTTTCTTAAACAGCTTGTATTCGGTCGCTGAGGCTTGCAGG | 48 | Cr151 | |
| CAGAGGCTCTTTGACCCCCCAACAACTTTAGC | 32 | Cr152 | |
| TAAAGACTACAGCATCGGAACGAGGGCCGCTT | 32 | Cr153 | |

| | | |
|---|---|---|
| CGGGTAAAATACGTAATGTTTT | 18 | Cr154 |
| AGTTGCGCGCCTTTAATTGTATCGAATAGAAAGGAACAACAATGAATT | 48 | Cr155 |
| AGCAGCGAAAGTTTTCATGAGGAAGTTAAAGAGGCA | 36 | Cr156 |
| ACAACCATCGCCCACGCATAACCGATAATACCGAT | 35 | Cr157 |
| TTGCGGGATCGTCACCCTC | 19 | Cr158 |
| TGCAGCAAGCGGTCCACGCTGGTTTGCCCCCTTCACC | 37 | Loop |
| ACGTCAAAGGGCGAAAAACAGGGAAGAAAGCGAAACTAGGGCG | 43 | CrSH1 |
| GCAAATCGCCGTTTTTATTTTCATCGTAGGAATCTTTT | 34 | CrSH2 |
| CTTTCATGCGGATTGACCGTAATGATCGGTGCGGGCCTCTTCGC | 44 | CrSH3 |
| TCACCAATCGACAGAATCAAGTTTACCAGAGCCACCACCGGAACCTTTT | 45 | CrSH4 |
| TTCAGAAGGAATACCACATTCAACATCAGTTGAGATTTATTTT | 39 | CrSH5 |
| GAGTTAAAGGTAGCAACGGGTGAATCGAGCTA | 32 | CrSH6 |
| TATAAAGTACCGACAAAAGGTAAAGTAGGCATTTT | 35 | DkS1 |
| TACCAGTATAATAATAAGAGAA | 22 | DkS2 |
| TGGTTTGAAATATACAAATTCT | 22 | DkS3 |
| GTTATATAACTCCTAAATTTAA | 22 | DkS4 |
| ATGCTGATACCTTTTTAACCTCCGGCTTAGGTTGG | 35 | DkS5 |
| AAGTCCTGAACAAGAATTTATCAACAATAGAT | 32 | Dk1 |
| TAATTTACGAGCCATGTTCAGCTA | 24 | Dk2 |
| CGCCTGCAACCAGGAAGATCGAGTATATGTAAAGCCTTAAAT | 42 | Dk3 |
| AGTGCCACGCTGCAAACCCTCAAT | 24 | Dk4 |
| CAGACGACATGCAGAACGCGCCTGAAATAATA | 32 | Dk5 |
| GACAATAAACAAAACAACGCCAAC | 24 | Dk6 |
| AAAGGAATTGAGGATTTAGAAGTA | 24 | Dk7 |
| CGAGCCAGAGCCAACGCTCAACAGTAGTATCAT | 33 | Dk8 |
| CAAACAGGCAAATCAACAGTTGCAATATCTGGTCAGTTTAACAC | 44 | Dk9 |
| ATTGAGAATGTAATTTAGGCAGAATTCTGTC | 31 | Dk10 |
| ATCGCCATATTTGAATCATAATTA | 24 | Dk11 |
| TAAATCCTTTGCAATTATCATCAT | 24 | Dk12 |
| ATTAATTAGATAATACATTTGAGGAAGGTTATCTAAAATGCTGAACC | 47 | Dk13 |
| ATGCGTTACCGACCGTGTGATAATAATTTCATCTTCTGAATATGTAA | 47 | Dk14 |
| TTATCAGAATTCGACAACTCGTATTTAGACTTTA | 34 | Dk15 |
| TTAAATAACTAGAAAAAGCCTGTTTAGGGCTTA | 33 | Dk16 |
| GAATAAACACCGGAGAAAACTTTT | 24 | Dk17 |
| ATATAATCCTGAAATAAAGAAATT | 24 | Dk18 |
| ATTATACTCCACCAGAAGGAGCGGCCGAACGTT | 33 | Dk19 |
| TTTCAGGTTGATGGCAATTCATCAATTCCTGA | 32 | Dk20 |
| GACAAAGAACGCTTTATCAAAATC | 24 | Dk21 |
| ATACAGTAACAGGGCGAATTATTC | 24 | Dk22 |
| ACATCGGGTTGCACGTAAAACAGATTGTTTGG | 32 | Dk23 |
| GAGAGACTGCAAATCCAATCGCAATCAAATATATTTTAGTATAAGGCG | 48 | Dk24 |
| TACCTGAGTTAACGTCAGATGAATGCGTAGAT | 32 | Dk25 |
| TAGCGATAGCTTAGATAGAATCCTTGAAAACA | 32 | Dk26 |
| GTCAATAGTGAAAATCGTCGCTAT | 24 | Dk27 |
| AACAAACATCAAAAACAGTACATA | 24 | Dk28 |
| ATTAATTTACAAAATCGCGCAGATACCTTTT | 31 | Dk29 |
| ATATATGTGAGCAAAAGAAGATGATGAATTTCAAT | 35 | Dk30 |
| ATTGACAGTAATTAATTTTCCCTTTAAGACGCTGAGAAGAATAGGTCT | 48 | Dk31 |
| GAGGTTGAGGCCTGTATGAATTTTGCAAAAGAAATCA | 37 | Dk32 |
| AGTTTTGCCAGAGGGGCGATAAAAACCAAAATAAGAACTG | 40 | Dk33 |
| TCAAATATAGAGCCAGCAGCAAATGAAAAATCTAA | 35 | DkD1 |
| AGCATCACCTTATCTTTAGGAGCACTAACAAC | 32 | DkD2 |
| TAATAGATTAGAGCCGTCAATTTAAAAGTTTGAGTAACATTA | 42 | DkD3 |
| TCATTTTGCGGAACAAAGAAATCTGAATAATGGAAGGGTTAG | 42 | DkD4 |
| AACCTACCATATCAAAATTATAGAAACAATAACGGATTCGCC | 42 | DkD5 |
| TGATTGCTTTGAATACCAAGTACATTTAACAA | 32 | DkD6 |
| TTTCATTTGAATTACCTTTTTTAATGGGAAAACAAA | 36 | DkD7 |

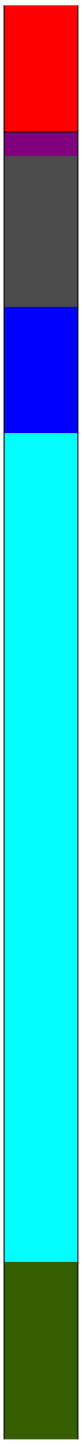

Probe
5'-CGATCCGACCTTCCTCCCTCCTCCTCTTCCCTTGGGTCGAAC
ATTGCTCGTCGTCACTGGGTCCTGCTCATATTGGGTTTACAGCTC
ACATAGGTAGACTTTAGCTTCCCGGGCTCGCAG-3'

Target
5'-GGGCGGGGCGGGGGCGCGAAAGTCTACCTATGTGAGCTGTA
AACCCAATATGAGCAGGACCCAGTGACGACGAGCAATGTTCGACCCA
AGGGAAGAGGAGGACGCGCCCCCGCCCCGCCC-3'

Target mismatch
5'-GGGCGGGGCGGGGGCGCGAAAGTCTACCTATGTGAGCTGTAAA
TTTGGCCGAGTTCAAGTTACTGACGACAAGTTCCTGTTCGACCCAAGG
GAAGAGGAGGACGCGCCCCCGCCCCCCC-3'

Competitor
5'-TCCTCCTCTTCCCTTGGGTCGAACAGGAACTTGTCGTCAGTAAC
TTGAACTCGGCCAAATTTACAGCTCACATAGGTAGACTTT-3'

*To link a probe to the origami substitute*

DkD4 with LinkerDx:
5'-GGGAGGAAGGTCGGATCGCTACCATCGGAACAAAGAAATCTGAAT
AATGGAAGGGTTAG- 3'

DkS3 with Linker Sx
5'- TGGTTTGAAATATACAAATCATGCTGCGAGCCCGGGAAGCT - 3'

*For the FRET visualization substitute*
DkD3 with DkFRET
5'- 6-FAM- TAGAGCCGTCAATTTAAAAGTTTGAGTAACATTA -3'

CrI3 with CrFRET
5'- CCTGAGTAATGACAAGAGA – BHQ1 -3'

# Chapter 6

# Bibliography

Alivisatos, A.P., Johnsson, K.P., Peng, X., Wilson, T.E., Loweth, C.J., Bruches, M.P., Schultz, P.G. (1996). Organization of 'nanocrystal molecules' using DNA. *Nature* 382: 609-611

Andersen, E. S., M. Dong, *et al.* (2008). DNA origami design of dolphin-shaped structures with flexible tails. *ACS Nano* 2(6): 1213–1218.

Andersen, E. S., M. Dong, et al. (2009). Self-assembly of a nanoscale DNA box with a controllable lid. *Nature* 459(7243): 73–76.

Ashkin, A. (1970) Acceleration and Trapping of Particles by Radiation Pressure, *Physical Reviews Letter*, 24: 156–159.

Balzani, V., Credi, A., Venturi, M. (2008) Molecular Devices and Machines. Concepts and Perspectives for the Nanoworld. *VCH-Wiley, Weinheim*

G. Binning, C. F. Quate, Ch. Gerber. (1986) Atomic force microscope. *Physical Review Letters* 56 (9): 930.

Birac, J. J., Sherman, W. B., Kopatsch, J., Constantinou, P. E., Seeman, N. C.(2006) Architecture with GIDEON, a Program for Design in Structural DNA Nanotechnology. *Journal of Molecular Graphic Model*, 25: 470–480

Borri, P., Schneider, S., Langbein, W., Bimberg, D. (2006). Ultrafast

carrier dynamics in InGaAs quantum dot materials and devices. *Journal of optics A–Pure and applies optics* 8 (4): 33-46

Brown, W. H (1996) *Chimica Organica*. EdiSes.

Buhleier, E., Wehner, W., Vogtle, F. (1978). Cascade and "Nonskid-chain like" syntheses of molecular cavity topologies. *Synthesis* 2: 155–158.

Castro, C. E. (2011) A primer to scaffold DNA origami. Nature Methods 8, 221229 (2011)

Chen, Y. X., Triola, G., Waldmann, H. (2011) Bioorthogonal chemistry for site-specific labeling and surface immobilization of proteins. *Accounts of Chemical Research* 44: 762773.

Clark, L. C., Jr. and C. 1962. Electrode systems for continuous monitoring in cardiovascular surgery. *Annual N Y Acad Sci*102: 29–45.

Cluzel, P., Lebrun, A., Christoph, H., Lavery, R., Viovy, J.L., Chatenay, D., Caron, F. (1996) DNA: An extensible molecule. *Science* 271 (5250): 792–794.

Denkewalter, R.G., Kolc, J.F., Lukasavage, W.J. (1981). Macromolecular highly branched homogeneous compound based on lysine units. *US Patents* 4: 289–872.

Dietz, H., Douglas, S.M., Shih, W.M. (2009) Folding DNA into twisted and curved nanoscale shapes. *Science* 325: 725–729.

Ding, B., Deng, Z., Yan, H., Cabrini, S., Zuckermann, R.N., Bokor, J. (2010). Gold nanoparticle self-similar chain structure organized by DNA origami. *Journal of the American Chemical Society* 132: 3248–3249.

Dirks, R.M., Pierce, N.A., (2004). Triggered amplification by hybridization chain reaction. *Protocols National Academy Science USA* 101: 15275–15278.

Douglas, S. M., J. J. Chou, et al. (2007). DNA-nanotube-induced alignment of membrane proteins for NMR structure determination. *Protocols National Academy Science USA* 104(16): 6644–6648.

Douglas, S. M., H. Dietz, et al. (2009). Self-assembly of DNA into nanoscale three-dimensional shapes. *Nature* 459(7245): 414–418.

Förster, T, (1946). Energiewanderung und Fluoreszenz. *Naturwissenschaften*, 6: 166–175.

Förster, T. (1948). Ueber Darstellung konstlicher Leuchtsteine. *Annalen der Physik*, 2: 55–75.

Förster, T. (1951). Fluoreszenz Organischer Verbindungen. *Vandenhoeck & Ruprecht*, Göttingen.

Förster, T. 1953. Transfer mechanisms of electronic excitation. *Discussions of the Faraday Society* 1959, 27: 7–17.

Fu, T., Seeman, N.C. (1993). DNA double-crossover molecules. *Biochemistry* 32: 3211–3220.

Giessibl., F.J. (1995) Atomic Resolution of the Silicon (111)-(7X7) Surface by Atomic Force Microscopy. *Science* 6(267): 68–71.

Green, S.J., Lubrich, D., Turberfield, A.J. (2006). DNA hairpins: fuel for autonomous DNA devices. *Biophysical journal* 91: 2966–2975.

Gu, H., J. Chao, et al. (2009). Dynamic patterning programmed by DNA tiles captured on a DNA origami substrate. *Nature Nanotechnology* 4(4): 245–248.

Hoh J.H., Hansma, P.K. (1992) Atomic Force Microscopy for High-Resolution Imaging in Cell Biology. *Trends in Cell Biology* 2: 208–213.

Huang, Y., Duan, X.F., Cui, Y., Lauhon, L.J., Kim, K.H., Lieber, C.M. 2001. Logic gates and computation from assembled nanowire building blocks. *Science* 294: 1313-1317.

James, D.K., Tour, J.M. (2005). Molecular wires. *Topics in current chemistry* 257: 33-62.

Jia, C.-J., Schuth, F. (2011). Colloidal metal nanoparticles as a component of designed catalyst. *Physical Chemistry Chemical Physics*, 13: 2457–2487

Kaittanis, C., Santra, S.M., Perez, J.M. (2010) Emerging nanotechnology-based strategies for the identification of microbial pathogenesis. *Advanced Drug Delivery Reviews* 62: 408–423.

Ke, Y., S. M. Douglas, et al. (2009). Multilayer DNA origami packed on a square lattice. *Journal of the American Chemical Society* 131(43): 15903–15908.

Ke, Y., S. Lindsay, et al. (2008). Self-assembled water-soluble nucleic acid probe tiles for label-free RNA hybridization assays. *Science* 319(5860): 180–183.

Kershner, R. J., L. D. Bozano, et al. (2009). Placement and orientation of individual DNA shapes on lithographically patterned surfaces. *Nature Nanotechnology* 4(9): 557–561.

Klinov, D., Atlasov, K., Kotlyar, A., Dwir, B., Kapon, E. 2007. DNA nanopositioning and alignment by electron-beam-induced surface chemical Patterning. *Nanoletters* 7 (12): 3583–3587.

Ko, S. H. (2010) Synergistic self-assembly of RNA and DNA molecules. *Nature Chem.* 2: 1050–1055.

Koch, S.J., Shundrovsky, A., Jantzen, B.C., Wang, M.D., 2002. Probing protein-DNA interactions by unzipping a single DNA double helix. *Biophys-*

*ical Journal* 83(2): 1098–1105.

Kricka, L.J., 2002. Stains, labels and detection strategies for nucleic acids assays. *Annals of Clinical Biochemistry* 39: 114–129.

Kibbe, W.A. (2007) OligoCalc: an online oligonucleotide properties calculator. *Nucleic Acids Research* 35 (webserver issue).

LaBean, T.H, Li, H. (2007).Constructing novel materials with DNA. *Nanotoday* 2: 26–36

Li. Y., Tseng, Y.D. Kwon, S.Y., d'Espaux, L., Bunch, J.S, McEuen, P.L., Luo, D. (2004). Controlled assembly of dendrimer-like DNA. *Nature Materials* 3: 38 - 42.

Li, Y., Cu, Y.T.H., Luo, D. (2005). Multiplexed detection of pathogen DNA with DNA-based fluorescence nanobarcodes. *Nature Biotechnology* 23: 885–889.

Liphardt, J., Onoa, B., Smith, S.B., Tinoco, I., Bustamante, C., 2001. Reversible unfolding of single RNA molecules by mechanical force. *Science* 292(5517): 733–737.

Liu, D., Wang, M., Deng, Z., Walulu, R., Mao, C. (2004). Tensegrity: Constructing of rigid DNA triangles with flexible four-arm DNA junction. *Journal of the American chemical society* 126 (8): 2324–2325.

Lund, K., Liu, Y., Lindsay, S., Yan, H. (2005). Self–assembly a molecular pegboard. *Journal of the American Chemical Society* 127: 17606–17607.

Luo, D. (2003). The road from biology to materials. *Materials today* 6: 38–43.

Mao, C. (2004). The Emergence of Complexity: Lessons from DNA. *PLoS Biology* 2 (12): 2036–2038

Magde, D., Webb, W.W., Elson, E. (1972) Fluctuations in a Reacting System Measurement by Fluorescence Correlation Spectroscopy. *Physical Review Letters* 29: 705–708.

McKinney, S.A., Tan, E., Wilson, T.J., Nahas, M.K., Declais, A.C., Clegg, R.M., Lilley, D.M.J., Ha, T., 2004. Single-molecule studies of DNA and RNA four-way junctions. *Biochemical Society Transactions* 32: 41–45.

Mirkin, C.H., Letsinger, R.L., Mucic, R.C., Storhoff, J.J. (1996). A DNA-based method for rationally assembling nanoparticles into macroscopic materials. Nature 382. 607 609

Moretti M., E. Di Fabrizio, S. Cabrini, R. Musetti, F. De Angelis, G. Firrao. (2008) An ON/OFF biosensor based on blockade of ionic current passing through a solid state Nanopore. *Biosensors and Bioelectronics*

Murphy, M.C., Rasnik, I., Cheng, W., Lohman, T.M., Ha, T.J., 2004. Probing single stranded DNA conformational flexibility using fluorescence spectroscopy. *Biophysical Journal* 86(4), 2530–2537.

NanoEngineer-1 http://www.nanoengineer-1.com/ (2008).

Newkome, G.R., Yao, Z., Baker, G.R., Gupta, V.K. (1985). Cascade molecules: a new approach to micelles. *Journal of organic chemistry* 50 (11): 2003–2004.

Niemeyer, C. M., Adler, M., Lenhert, S., Gao, S., Fuchs, H. and Chi, L. (2001). Nucleic Acid Supercoiling as a Means for Ionic Switching of DNANanoparticle Networks. *ChemBioChem* 2: 260264.

Pierce N.A. NUPACK. http://nupack.org/

Rief, M., Gautel, M., Oesterhelt, F., Fernandez, J.M., Gaub, H.E., 1997. Reversible unfolding of individual titin immunoglobulin domains by AFM. *Science* 276(5315): 1109–1112.

Rigler, R., Mets, U., Widengren, J., Kask, P., 1993. Fluorescencecorrelation spectroscopy with high count rate and low-background analysis of translatonal diffusion. *European Biophysics Journal with Biophysics Letters* 22(3): 169–175.

Rothemund, P.W.K. (2006) Folding DNA to create nanoscale shapes and patterns. *Nature* 44: 297–302.

Sarveswaran, K., Hu, W., Huber, P. W., Bernstein, G. H., Lieberman, M. (2006). Deposition of DNA rafts on cationic SAMs on silicon [100]. *Langmuir* 22: 11279–11283.

Seeman, N.C. (1982) Nucleic acid junctions and lattices. *Journal of Theoretical Biology* 99: 237–247.

Seeman, N.C. (1983). Design of immobile nucleic acid junctions. *Biophysical journal* 44: 201–210.

Seeman, N.C. (1999). DNA engineering and its application to nanotechnology. *Trends in biotechnology* 17: 437–443.

Seeman, N.C. (2003). DNA in a material world. *Nature* 421: 427–431.

Seol, Y., Skinner, G.M., Visscher, K., 2004. Elastic properties of a single-stranded charged homopolymeric ribonucleotide. *Physical Review Letters* 93(11).

Shih, W. M., J. D. Quispe, et al. (2004). A 1.7–kilobase single-stranded DNA that folds into a nanoscale octahedron. *Nature* 427(6975): 618–621.

Smith, S.B., Cui, Y.J., Bustamante, C., 1996. Overstretching B-DNA: The elastic response of individual double-stranded and single-stranded DNA molecules. *Science* 271(5250): 795–799.

Stryer L. (1978) Fluorescence energy transfer as a spectroscopic ruler.*Annual Review of Biochemistry.* 47: 819–846

Taatjes, D. J., Quinn, A. S., Lewis, M. R. and Bovill, E. G. (1999) Quality assessment of atomic force microscopy probes by scanning electron microscopy: Correlation of tip structure with rendered images. *Microscopy Research and Technique* 44(5): 312–326.

Tans, S.J., Dekker, C. (2000). Molecular transistors Potential modulations along carbon nanotubes. *Nature* 404: 834–835.

Terranova, M. L., Sessa, V., Rossi, M. (2006). The world of carbon nanotubes: an overview of CVD growth methodologies. *Chemical vapour deposition* 12: 315–325

Thompson, J.F. And Milos, P.M. (2011) The properties and applications of single-molecule DNA sequencing. *Genome Biology* 12 (2).

Tomalia, D.A., Baker, H., Dewald, J., Hall, M., Kallos, G., Martin, S., Roeck, J., Ryder, J., Smith, P. (1985). A new class of polymers starbust-dendritic molecules. *Polymer journal* 17: 117–132.

Turner, A.P. (2000). Biosensors sense and sensitivity. *Science* 290: 1315–1317.

Velasco-Garcia, M.N. (2009) Optical biosensors for probing at the cellular level: a review of recent progress and future prospects. *Seminars in Cell and Developmental Biology* 20: 27–33.

Voigt, N. V., T. Torring, Rotaru, V., Jacobsen, M.F., Ravnsbek, J.B., Subramani, R., Mamdouh, W., Kjems, J., Mokhir, A., Besenbacher, F., Gothelf, K.V. (2010). Single-molecule chemical reactions on DNA origami. *Nature Nanotechnology* 5(3): 200-203.

Walter, N.G. (2008). Single Molecule Detection, Analysis, and Manipulation. *Encyclopedia of Analytical Chemistry* 1–10.

Wang, J.C. (1979) Helical repeat of DNA in solution. *Protocols National*

*Academy Science USA* 76: 200–203.

Williams, P.M., Fowler, S.B., Best, R.B., Toca-Herrera, J.L., Scott, K.A., Steward, A., Clarke, J., 2003. Hidden complexity in the mechanical properties of titin. *Nature* 422(6930), 446–449.

Winfree, E. DNA design toolbox. http://www.dna.caltech.edu/DNAdesign/

Winfree, E., Liu, F., Wenzler, L., Seeman, N. (1998) Design and self-assembly of two-dimensional DNA crystals. *Nature* 394: 539–544.

Woodside, M.T., Behnke-Parks, W.M., Larizadeh, K., Travers, K., Herschlag, D., Block, S.M., 2006. Nanomechanical measurements of the sequence dependent folding landscapes of single nucleic acid hairpins. *Proceedings of the National Academy of Sciences of the United States of America* 103(16): 6190–6195.

Yan, H., Zhang, X. P., Shen, Z. Y., Seeman N. C. (2002) *Nature* 415: 62–65.

You, H.X., Lau, J.M., Zhang, S., Yu, L. (2000). Atomic force microscopy imaging of living cells: a preliminary study of the disruptive effect of the cantilever tip on cell morphology. *Ultramicroscopy* 82: 297–305.

Yurke, B., Turberfield, A. J., Mills, A. P. Jr, Simmel, F. C., Newmann, J. L. (2000) A DNA-fuelled molecular machine made of DNA. *Nature* 406: 605608.

Zhong, M., Rashes, M.S., Marky, L.A., Kallenbach, N.R. (1992). T-T base mismatches enhance drug binding at the branch site in a 4-arm DNA junction. *Biochemistry* 31 (34): 8064–8071.

Zhu, J., Wei, B., Yuan, Y., Mi, Y. UNIQUIMER 3D, a software system for structural DNA nanotechnology design, analysis and evaluation. *Nucleic Acids Research* (2009)

# List of Figures